MIND YOUR STEP

Cortical dynamics during the human reactive balance response

Mitchel Stokkermans

Mind your step

Cortical dynamics during the human reactive balance response

Mitchel Stokkermans

Mind your step

Cortical dynamics during the human reactive balance response

Proefschrift

ter verkrijging van de graad van doctor
aan de Radboud Universiteit Nijmegen
op gezag van de rector magnificus prof. dr. J.H.J.M van Krieken,
volgens besluit van het college voor promoties
in het openbaar te verdedigen op vrijdag 8 september 2023
om 10:30 uur precies.

door

Mitchel Stokkermans

geboren op 3 augustus 1990 te Tilburg

Contents

Chapter 1

General introduction

*Postural balance control is one of the most important functions, yet we lack a full understanding of the involved cortical mechanisms. It is of great interest to study the cortical mechanisms underlying impaired balance control (Read **box 1** for the clinical relevance of studying balance control), however, currently little is understood of how the healthy human brain facilitates balance control.*

Neural control in standing balance of healthy humans

To maintain an upright stable posture during quiet stance or in response to external perturbations, we continuously have to keep our center of mass (CoM) within the boundaries of our base of support (BoS). The CoM is the projection of the gravitational center of our body and is centered slightly above the hips when maintaining an upright posture (see figure 1). Our BoS is determined by the area from the edges of our feet including the distance between our feet. The position of our CoM relative to our BoS may change through external balance perturbations or by intentionally leaning towards a given direction (as illustrated in figure 1B). When standing upright, our CoM is relatively far from our toes, however, by slowly leaning forward (or when being pushed forward), the CoM will travel closer to the toes, which will then represent our BoS in the forward direction. Depending on how close the CoM will travel to the BoS, we may experience this posture as quite challenging to maintain compared to the upright stance. In the case our CoM extends beyond the BoS (figure 1C), we are likely to fall unless we make a corrective balance response and extend our BoS beyond our CoM.

Our central nervous system has different strategies to maintain postural stability in response to situations that threaten our stability. Sometimes balance perturbations are low in magnitude making it possible to maintain balance without requiring a step. This response is also known as the feet-in-place response. Yet, in other cases the relation between the CoM and BoS is disturbed to an extent where maintenance of the feet-in-place posture is no longer possible. Luckily, our central nervous system then has additional tactics such as reaching or stepping responses to prevent us from falling. This raises the question, how does our central nervous system decide when a feet-in-place corrective balance response does not suffice?

Traditionally, it was thought that balance was regulated subcortically, however, recent studies suggest cortical involvement during postural balance control. The impaired balance response in people that suffered from stroke hints towards cortical involvement during balance control ((1–9). In addition, dual tasking during balance tasks causes worse cognitive task performance and slower reaction times in healthy humans (10–14), indicating that balance tasks require cognitive resources and that

the cortex may play a role in balance control (for extensive reviews see (15,16). Interestingly, cognitive interference with the execution of the balance response is limited to a relatively late interval (250 ms following perturbation onset) during the balance response, suggesting a rather late involvement of the cortex (13,17).
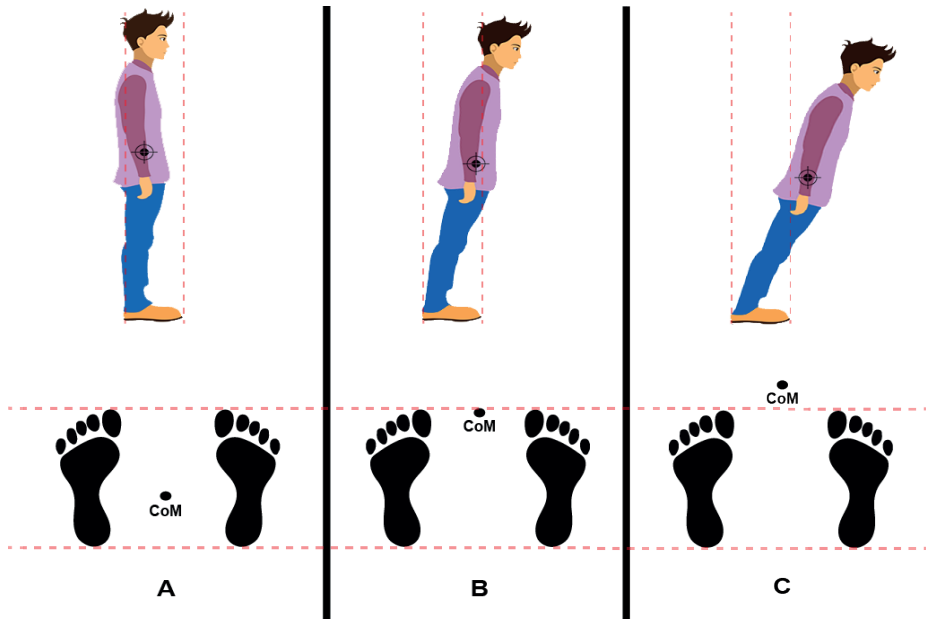
*Figure 1. Schematic representation of CoM dynamics relative to the BoS. **A**, upright standing posture. **B**, right a forward leaning posture. The black target in each figure represents the CoM position of that leaning posture. Vertical dashed lines represent the BoS projection from the floor. Below, the feet are presented with the forward and backward BoS plotted as dashed red lines. The position of the CoM in the figure below matches the posture as illustrated above.*

The initial balance response is not initiated by the cortex, however, the cortex is more likely involved during the late phase of the postural balance response by fine-tuning the postural response. The balance response may be divided in three different response latency loops: i) short, ii) medium, and iii) long response latency loop, which each characterizes the involvement of certain levels of our central nervous system during the balance response (16,18). In the short response latency loop, skeletal muscles are primarily activated through spinal mono- and oligosynaptic circuits (19); see short latency response figure 2). Yet, these short latency responses are non-functional to the reactive balance recovery response and involvement of higher brain regions are required to facilitate a functional balance response (16).

The functional balance response requires involvement from the brainstem and cortex. It is proposed that during the medium latency response loop of the reactive balance recovery response, an automatic postural response is initiated by brainstem regions (for an extensive review see (16,20). During the long latency phase of the reactive balance recovery response, the cortex is suggested to play a role through transcortical response loops (blue and green pathways in figure 2). During this long latency phase, the cortex facilitates sensorimotor processes and fine-tunes the postural response initiated by the short & medium latency loops (16,20). Yet, little is known about the exact cortical role during postural balance control and when the cortex starts to play a crucial role in the reactive balance response.
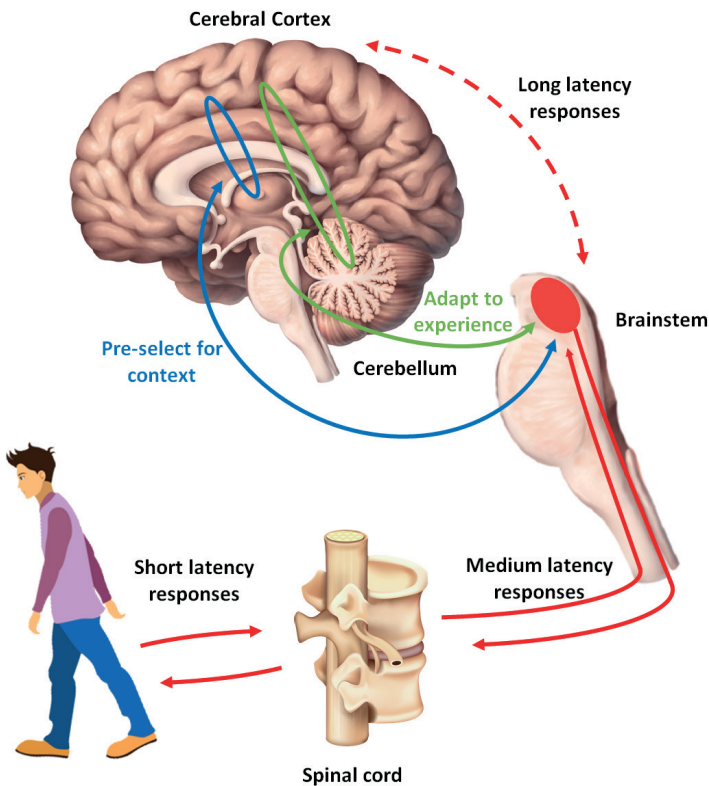
Figure 2. Schematic representation of (sub)cortical pathways involved in the postural control. *Adapted from Jacobs & Horak 2009. The short latency response loop is indicated with the red line through the spinal cord. The red arrows indicate the short & medium latency response loops which involve the spinal cord and the brainstem. The long latency response loop is indicated with the dashed line and involves the transcortical loop through the motor cortex (blue arrow) and the cerebellar-cortical loop (green arrows).*

1

Box 1. Clinical relevance of studying balance control

Impairments in postural stability are a major risk factor for falls (21,22). Prevalence of falls due to worse balance control is increased in elderly (23–25) and clinical populations with balance impairments such as people that suffer from stroke (1–9) and Parkinson's disease (26). Poor balance control and the consequent risk of falling not only increases the probability of physical injuries, but also leads to high healthcare costs as a result of increased care that these patients require due to falling and their lack of mobility (27).

Stroke

Impaired balance control is often seen in people post stroke (1–9). Stroke is an acute vascular incident in the brain that results from hemorrhage or infarction of arteries (28). Depending on the location and severity of a cerebral vascular incident, people post stroke often show paresis of the upper and/lower limbs on one side of the body. In addition, people post stroke often show an increase of postural sway during quiet stance (29). Moreover, balance responses to perturbations are delayed and discoordinated in people post stroke, contributing to an increased fall risk (30).

Parkinson's Disease

Parkinson's disease is a neurodegenerative disease that affects the dopaminergic neurons in the basal ganglia (for an extensive review on the affected neurocircuitry see (31). People with Parkinson's disease develop motor symptoms (32) as well as non-motor symptoms (33). In early onset of the disease, symptoms evolve unilaterally. However, as the disease progresses, symptoms will occur bilaterally. In later stages of the disease, people show freezing of gait and postural instability (34), which contribute to an increased risk of falling in all but mostly the backward direction (35–38). The exact cause of this impaired balance response in the backward direction is not yet understood. Interestingly, the backward balance response is notorious for being resistant to levodopa medication (39).

Despite the vast literature on these neurodegenerative diseases, little is known about the neural underpinnings of balance impairments. A better understanding of the cortical role during human postural control in the healthy brain may help better understand the balance impairments observed in these clinical populations. Moreover, this knowledge may contribute to specific methods in rehabilitation.

Studying balance control in the lab

A common method to study balance control is by imposing unpredictable external perturbations. In an experimental setup, sudden changes in the CoM relative to the BoS can be delivered by perturbations of the support surface. In this thesis, postural balance is disturbed by the use of the Radboud Falls Simulator (40,41); figure 3A & 3B). This sophisticated simulator allows researchers to deliver controlled external balance perturbations at a wide range of intensities and directions. Moreover, the falls simulator is equipped with force platforms that are embedded in the floor of the movable platform, allowing step onset (i.e. the moment the stepping leg is raised from the floor to facilitate a step) determination. (The red arrows in figure 3C & 3D indicate weight distribution of the participant on each force plate).

In addition, whole-body movements are recorded to investigate postural dynamics during balance recovery. To determine the trajectory of certain body parts, specific landmarks of the body (i.e. specific bones and joints) are marked on the skin with reflective markers (see markers on the participants body in figure 3A and 3B). Infrared cameras (visible on the ceiling in figures 3A & 3B) can record the position and trajectories of these reflective markers in the measurement volume during balance tasks. In addition, special 3-D motion capturing software (Vicon Motion Systems, United Kingdom) aids with the computation of CoM movements, using multiple body segments determined by the markers attached to the body (figure 3C & 3D).

Electroencephalography

Electroencephalography (EEG) is a relatively old non-invasive technique (First conducted in 1929 by a German psychiatrist Hans Berger) in the field of neuroscience, which measures the electrical brain activity from the scalp (42). Multiple hundred thousand to millions of neighboring neurons must fire simultaneously to cause a change of several microvolts in local field potential measurable from the scalp. The application of EEG involves a cap with small electrodes that tightly fit on the scalp of the head (figure 4). Disconnection or movements of these electrodes over the skin makes EEG very sensitive to artifacts. In addition, EEG has a very low spatial resolution, meaning that it is hard to identify the exact brain region contributing to a signal. Yet, EEG has a millisecond temporal accuracy (depending on the sampling rate), making EEG an interesting method to determine exact onset of cortical activity.
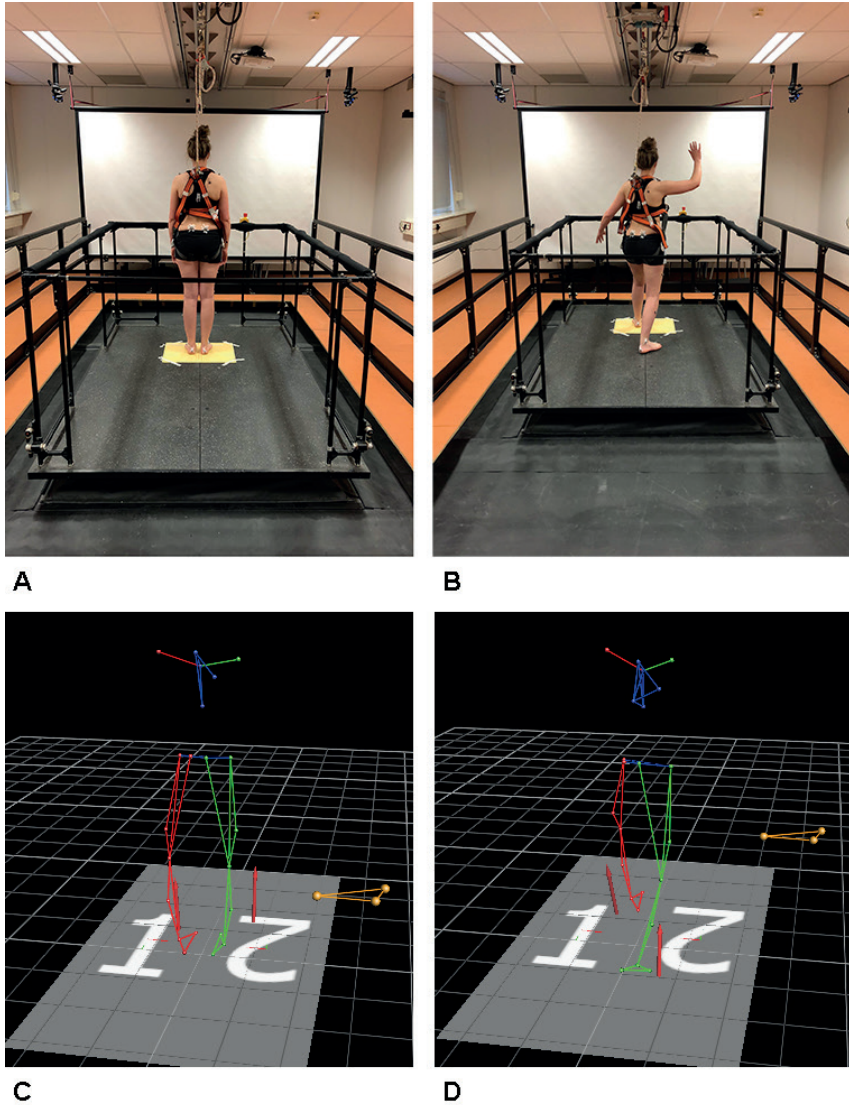
Figure 3. Lab equipment for balance control studies. A, a participant is standing on the Radboud falls simulator while maintaining a quiet standing posture. **B**, the participant is being perturbed in the backward direction, resulting in a backward step. **C,** reflective marker reconstruction of a participant standing on the platform while maintaining a quiet standing posture. This reconstruction would result from the posture in figure A. **D**, Reflective marker reconstruction of the participant while being perturbed in the backward direction, resulting in a backward step. This reconstruction would result from the posture in figure B. Figures **C** & **D** are generated in Vicon Nexus software 2.7.1. The orange dots visible in figures C & D are a reference for the platform position in the Vicon software.

Figure 4. EEG cap. *Equipment for measuring electrical brain activity from the scalp. This cap has 128 electrodes embedded to measure EEG at high density from the scalp.*

Advances in complex analyses contribute to better data quality and understanding of EEG results during balance paradigms. Traditional experimental paradigms isolated specific cognitive tasks while restricting head movements (this reduced artifact occurrence) to quantify cortical activity under specific conditions. Although these fundamental studies were important to reliably quantify cognitive electrophysiological markers, these traditional experimental paradigms do not represent our daily life where we freely move around while simultaneously making decisions, recollecting memories or learning new tasks. Yet, experimental setups involving movements cause artifacts in EEG data, which can only be removed with sophisticated analyses.

Independent component analysis (ICA) is an analysis tool that disentangles a mixture of signals into individual reconstructed signals, which allows us to remove clear artifacts such as eye-blinks from the data. This mathematical method allows researchers to identify and filter out sources that generate noise relative to the brain activity of interest. (For an extensive review on ICA analysis see (43). Figure 5 illustrates a simplified schematic model of the ICA methodology where two sources A and B are generating a brain signal which is picked up by three electrodes. An additional noisy source is illustrated with C. Each electrode records a combination of the three signal sources (electrodes pick up a combined signal because the brain is highly conductive, also known as the volume conduction problem) illustrated with the time series at each electrode. The ICA analysis weights the contribution of each

1

source at the electrode level to reconstruct the initial source activity (here illustrated with the crossing arrows). Depending on the overall data quality, a greater number of electrodes is more likely to result in clean brain component data, as there are more electrodes that contribute information from a common component source compared to potential noise.

Importantly, ICA component rejection during removal of noise should be done with care since "noisy" components will also contain "brain" activity containing important information for further analyses (I use quotation marks, because although a component may mostly contain noise, there will often be some brain related activity in the background of that noisy component).
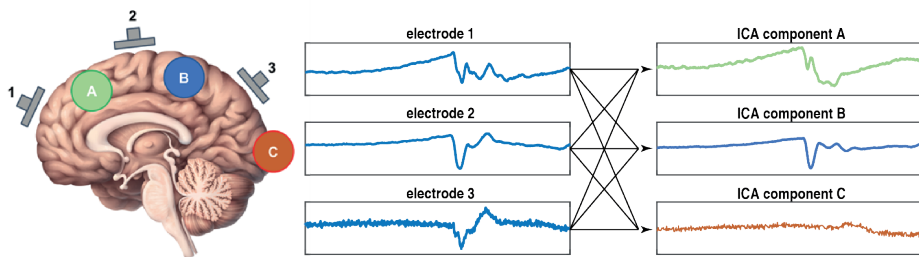
Figure 5. Independent component analysis. Schematic representation of signal de-mixing of time series brain data into time series component data. Electrodes are indicated with the numbers 1,2 & 3. Signal sources are indicated with A,B & C.

Aggregated neural activity is rhythmic and organized into bands, and therefore appropriate signal processing involves isolating these frequency band dynamics. Time-frequency analysis of EEG data allows us to interpret these spectral characteristics of the EEG time series data (Figure 6A) relative to a time-locked event (such as the perturbation onset; figure 6 C). The red colors indicate a relative increase of a certain frequency, while a blue color indicates a relative decrease in that frequency band. Several studies identified cortical dynamics over multiple frequency bands expressed as; theta (3-8Hz), alpha (10 -12Hz), beta (15-25Hz) and gamma (40-80Hz). Each of these frequency bands is known for its involvement in cortical processing such as cognitive control (theta; (44), sensory processes (alpha), and sensorimotor processes (beta; (45)). It is proposed that cortical brain regions interact over specific frequency bands through synchrony (i.e. distinct regions being simultaneously active in the same frequency; Fries 2005) and similarly the cortex may exert top-down control with specific muscles.

Functional connectivity of cortico-cortical (between brain regions) and cortico-muscle (between brain and muscles) activity is determined through a temporal interaction between spatially distant signals. Connectivity analyses allows us to determine to which extent the signal at a muscle (measured through electromyography; EMG) is dependent on cortical activity at a specific time and frequency. Several studies applied this analysis to experimental paradigms involving intentional leg movements, finding an interaction between cortical and muscle activity in the beta frequency band (46,47). Therefore, such analyses are interesting when investigating the cortical interaction with specific muscles during the balance response.

Cortical correlates of human postural balance control

Balance perturbations evoke a cortical electrophysiological marker known as the perturbation evoked potential (PEP; figure 6 A). The PEP is associated with destabilizing conditions and scales with perturbation intensity (15,48–52). This suggests that the PEP represents the integration of sensory information related to the perturbation induced changes on postural stability. The PEP was found to modulate under contextual factors such as predictability of perturbation onset or intensity (50,51,53–55), indicating that anticipation plays an important role in PEP dynamics (53). In addition, the PEP is often reported over the midfrontal scalp topography (figure 6 B) and EEG source localization analysis suggest that the signal originates from the supplementary motor area (SMA; (41,49,56), pre-SMA and Anterior Cingulate Cortex (ACC; (57)), which would support the interpretation of the PEP facilitating a monitoring or cognitive control process of balance responses (51,58). Besides PEP time series analysis, EEG data from balance paradigms has been analyzed in the time-frequency domain.

Time-frequency analysis of EEG times series data during balance paradigms suggests that midfrontal theta dynamics may facilitate postural control. Cortical theta dynamics during balance control scale with task difficulty and signal the loss of balance (59). In addition, unipedal stance showed greater theta dynamics increase compared to bipedal stance (60). Moreover, theta dynamics scale with stability, resulting in stronger theta dynamics when stability is at risk (61) and when balance is lost (62). Also, a study investigating the cortical involvement during anticipation of a perturbation reported that theta power increased for both feet-in-place and stepping responses following perturbation (41). Similar results were reported for feet-in-place responses following lateral balance perturbations (63).

This same study reported increased cortico-muscle-coherence in the theta frequency band between the SMA and the leg muscles, suggesting that the cortex actively interacts top-down with the muscles following a perturbation. Interestingly, in traditional cognitive neuroscience paradigms midfrontal theta dynamics are known to facilitate cognitive control and feedback related processes (64–67). Theta dynamics are known to increase following response conflicts (68,69), they scale with performance error (70) and are thought to signal for cognitive control (66). This indicates that midfrontal theta dynamics play an important role in action monitoring of behavior.

Altogether, these findings hint towards midfrontal theta dynamics during balance paradigms facilitating an action monitoring role. Yet, no study reported on any relation between theta dynamics and the monitoring of human postural control in response to external perturbations. Also, little is known about the characteristics of cortico-muscle interactions during the reactive balance stepping response and whether these cortical dynamics are specific to either leg throughout the response.
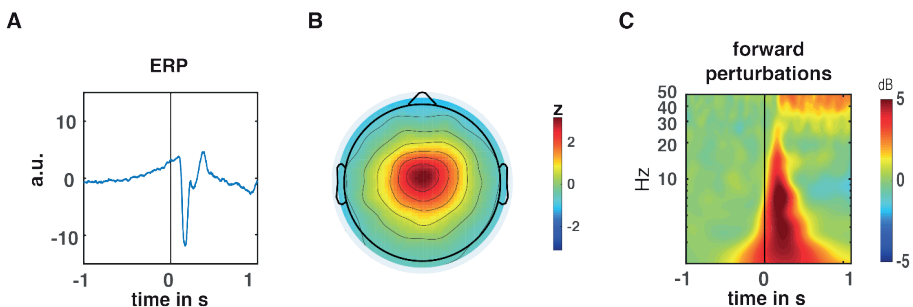
Figure 6. Mobile brain imaging EEG data. A, Average event related potential (ERP) time series data of midfrontal (FCz) electrode time locked to perturbation onset (time = 0s). **B**, Midfrontal scalp topography of EEG activity. Colors indicate the magnitude of the signal. **C**, Time-frequency decomposition of EEG time series time locked to perturbation onset (time = 0s). The Y-axis informs us on the frequency band, the X-axis indicates the time relative to time locked event. The colors indicate an increase (red) or decrease (blue) in power at a frequency at a given time point relative to baseline activity (-1500 to -500ms in this example).

The aims and outline of this thesis

In this thesis I investigated cortical involvement during the reactive postural balance response using EEG. The overall aim of this thesis was to gain more insight in the fundamentals of cortical involvement during the reactive balance response. In particular, I investigated theta dynamics underlying the balance monitoring process

of reactive balance feet-in-place and stepping responses. In addition, I explored the spectral dynamics of cortico-muscular interactions following perturbations. To achieve this, I addressed cortical electrophysiological markers that have been reproduced by many previous studies investigating human postural control in a wide variety of mobile balance-challenging conditions. I included healthy young participants (18-30 years old) that had no history of restrictions in their balance performance and had no experience with balance tasks on the Radboud Falls Simulator. To assess these goals, specific aims were addressed per chapter.

In **chapter 2** of this thesis, we assessed whether cortical responses elicited by whole body balance perturbations are similar to established cortical markers of action monitoring. We focused on multiple cortical frequency bands as a response of forward and backward balance perturbations at different perturbation intensities to identify cortical dynamics that scale with behavioral parameters which indicate balance monitoring. In addition, we investigated how theta dynamics relate to perturbation intensity and whether theta dynamics predict the ensuing behavioral response. To address these questions, EEG data of a total of 15 healthy young participants was analyzed. Participants were instructed to respond to whole-body balance perturbations in the forward and backward direction while maintaining feet-in-place if possible.

Chapter 3 continues on the cortical aspect of balance monitoring in the theta frequency range. I investigated whether midfrontal theta dynamics index the monitoring of postural control given different states of postural stability. In this chapter I manipulated postural stability prior to balance perturbations to investigate whether this would influence the relation of theta dynamics in response to different perturbation intensities. A relation between perturbation intensity and theta dynamics in combination with observing stronger theta dynamics in stepping responses does not imply monitoring of balance perse. Therefore, a balance monitoring role of theta dynamics during reactive balance responses can only be interpreted if theta dynamics scale with the cumulative induced postural threat. For this study, a total of 20 healthy young participants took part in an experiment where they had to assume different leaning angles prior to perturbations that were randomized in direction and intensity.

In **chapter 4** I determined whether midfrontal theta power in reactive stepping responses scale with postural stability at foot strike. In particular, I investigated the potential balance monitoring role of theta dynamics at reactive balance response foot strikes. As stepping responses facilitate extension of the BoS, I anticipated

1

that a new balance assessment is made at foot strike which is characterized by mid frontal theta dynamics. I addressed this question by analyzing data of 15 healthy young participants who were instructed to step in response to external balance perturbations while measuring high-density EEG.

In **chapter 5** I explored cortico-muscle coherence (CMC) during reactive balance responses in healthy young participants. In particular, I was interested in the initial onset of cortico-muscle coherence during the reactive balance response. In addition, I explored muscle specific CMC differences between step and stance leg time locked to perturbation onset and foot-off event. I anticipated to find differences over multiple CMC frequency bands as a function of their different role in the stepping response. I analyzed data of 18 healthy young participants measuring high density EEG and EMG activity of 5 leg muscles on both legs during forward and backward balance perturbations.

In **chapter 6** I summarize the results of this thesis and discuss their interpretation in a broader perspective.

A Dutch summary of this thesis is given in **chapter 7**.

References

1. Belgen B, Beninato M, Sullivan PE, Narielwalla K. The association of balance capacity and falls self-efficacy with history of falling in community-dwelling people with chronic stroke. Arch Phys Med Rehabil. 2006 Apr;87(4):554–61.

2. Harris JE, Eng JJ, Marigold DS, Tokuno CD, Louis CL. Relationship of balance and mobility to fall incidence in people with chronic stroke. Phys Ther. 2005 Feb;85(2):150–8.

3. Hyndman D, Ashburn A. Stops walking when talking as a predictor of falls in people with stroke living in the community. J Neurol Neurosurg Psychiatr. 2004 Jul;75(7):994–7.

4. Jørgensen L, Engstad T, Jacobsen BK. Higher incidence of falls in long-term stroke survivors than in population controls: depressive symptoms predict falls after stroke. Stroke. 2002 Feb;33(2):542–7.

5. Lamb SE, Ferrucci L, Volapto S, Fried LP, Guralnik JM. Risk Factors for Falling in Home-Dwelling Older Women With Stroke. Stroke. 2003 Feb;34(2):494–501.

6. Mackintosh SFH, Hill K, Dodd KJ, Goldie P, Culham E. Falls and injury prevention should be part of every stroke rehabilitation plan. Clin Rehabil. 2005 Jun;19(4):441–51.

7. Mackintosh SF, Hill KD, Dodd KJ, Goldie PA, Culham EG. Balance score and a history of falls in hospital predict recurrent falls in the 6 months following stroke rehabilitation. Arch Phys Med Rehabil. 2006 Dec;87(12):1583–9.

8. Suzuki T, Sonoda S, Misawa K, Saitoh E, Shimizu Y, Kotake T. Incidence and consequence of falls in inpatient rehabilitation of stroke patients. Exp Aging Res. 2005 Dec;31(4):457–69.

9. Teasell R, McRae M, Foley N, Bhardwaj A. The incidence and consequences of falls in stroke patients during inpatient rehabilitation: factors associated with high risk. Arch Phys Med Rehabil. 2002 Mar;83(3):329–33.

10. Brown LA, Shumway-Cook A, Woollacott MH. Attentional demands and postural recovery: the effects of aging. J Gerontol A Biol Sci Med Sci. 1999 Apr;54(4):M165-71.

11. Norrie RG, Maki BE, Staines WR, McIlroy WE. The time course of attention shifts following perturbation of upright stance. Exp Brain Res. 2002 Oct;146(3):315–21.

12. McIlroy WE, Norrie RG, Brooke JD, Bishop DC, Nelson AJ, Maki BE. Temporal properties of attention sharing consequent to disturbed balance. Neuroreport. 1999 Sep 29;10(14):2895–9.

13. Redfern MS, Müller MLTM, Jennings JR, Furman JM. Attentional dynamics in postural control during perturbations in young and older adults. J Gerontol A Biol Sci Med Sci. 2002 Aug;57(8):B298-303.

14. Brauer SG, Woollacott M, Shumway-Cook A. The influence of a concurrent cognitive task on the compensatory stepping response to a perturbation in balance-impaired and healthy elders. Gait Posture. 2002 Feb;15(1):83–93.

15. Maki BE, McIlroy WE. Cognitive demands and cortical control of human balance-recovery reactions. J Neural Transm. 2007 Jun 8;114(10):1279–96.

16. Jacobs JV, Horak FB. Cortical control of postural responses. J Neural Transm. 2007 Mar 29;114(10):1339–48.

1

17. Müller MLTM, Jennings JR, Redfern MS, Furman JM. Effect of preparation on dual-task performance in postural control. J Mot Behav. 2004 Jun;36(2):137–46.

18. Taube W, Schubert M, Gruber M, Beck S, Faist M, Gollhofer A. Direct corticospinal pathways contribute to neuromuscular control of perturbed stance. J Appl Physiol. 2006 Aug;101(2):420–9.

19. Keck ME, Pijnappels M, Schubert M, Colombo G, Curt A, Dietz V. Stumbling reactions in man: influence of corticospinal input. Electroencephalogr Clin Neurophysiol. 1998 Jun;109(3):215–23.

20. Takakusaki K. Functional neuroanatomy for posture and gait control. J Mov Disord. 2017 Jan 18;10(1):1–17.

21. Weerdesteyn V, de Niet M, van Duijnhoven HJR, Geurts ACH. Falls in individuals with stroke. J Rehabil Res Dev. 2008;45(8):1195–213.

22. van der Marck MA, Klok MPC, Okun MS, Giladi N, Munneke M, Bloem BR, et al. Consensus-based clinical practice recommendations for the examination and management of falls in patients with Parkinson's disease. Parkinsonism Relat Disord. 2014 Apr;20(4):360–9.

23. Campbell AJ, Borrie MJ, Spears GF, Jackson SL, Brown JS, Fitzgerald JL. Circumstances and consequences of falls experienced by a community population 70 years and over during a prospective study. Age Ageing. 1990 Mar;19(2):136–41.

24. O'Loughlin JL, Robitaille Y, Boivin JF, Suissa S. Incidence of and risk factors for falls and injurious falls among the community-dwelling elderly. Am J Epidemiol. 1993 Feb 1;137(3):342–54.

25. Rubenstein LZ. Falls in older people: epidemiology, risk factors and strategies for prevention. Age Ageing. 2006 Sep;35 Suppl 2:ii37–41.

26. Pickering RM, Grimbergen YAM, Rigney U, Ashburn A, Mazibrada G, Wood B, et al. A meta-analysis of six prospective studies of falling in Parkinson's disease. Mov Disord. 2007 Oct 15;22(13):1892–900.

27. Carroll NV, Slattum PW, Cox FM. The cost of falls among the community-dwelling elderly. J Manag Care Pharm. 2005 May;11(4):307–16.

28. Mansfield A, Inness EL, Mcilroy WE. Stroke. Handb Clin Neurol. 2018;159:205–28.

29. Marigold DS, Eng JJ. Altered timing of postural reflexes contributes to falling in persons with chronic stroke. Exp Brain Res. 2006 Jun;171(4):459–68.

30. de Kam D, Kamphuis JF, Weerdesteyn V, Geurts ACH. The effect of weight-bearing asymmetry on dynamic postural stability in people with chronic stroke. Gait Posture. 2017 Mar;53:5–10.

31. Galvan A, Devergnas A, Wichmann T. Alterations in neuronal activity in basal ganglia-thalamocortical circuits in the parkinsonian state. Front Neuroanat. 2015 Feb 5;9:5.

32. Hughes AJ, Daniel SE, Kilford L, Lees AJ. Accuracy of clinical diagnosis of idiopathic Parkinson's disease: a clinico-pathological study of 100 cases. J Neurol Neurosurg Psychiatr. 1992 Mar;55(3):181–4.

33. Sauerbier A, Qamar MA, Rajah T, Chaudhuri KR. New concepts in the pathogenesis and presentation of Parkinson's disease. Clin Med. 2016 Aug;16(4):365–70.

34. Goetz CG, Tilley BC, Shaftman SR, Stebbins GT, Fahn S, Martinez-Martin P, et al. Movement Disorder Society-sponsored revision of the Unified Parkinson's Disease Rating Scale (MDS-UPDRS): scale presentation and clinimetric testing results. Mov Disord. 2008 Nov 15;23(15):2129–70.

35. Matinolli M, Korpelainen JT, Korpelainen R, Sotaniemi KA, Virranniemi M, Myllylä VV. Postural sway and falls in Parkinson's disease: a regression approach. Mov Disord. 2007 Oct 15;22(13):1927–35.

36. Playfer JR. Falls and Parkinson's disease. Age Ageing. 2001 Jan;30(1):3–4.

37. Carpenter MG, Allum JHJ, Honegger F, Adkin AL, Bloem BR. Postural abnormalities to multidirectional stance perturbations in Parkinson's disease. J Neurol Neurosurg Psychiatr. 2004 Sep;75(9):1245–54.

38. Horak FB, Dimitrova D, Nutt JG. Direction-specific postural instability in subjects with Parkinson's disease. Exp Neurol. 2005 Jun;193(2):504–21.

39. Curtze C, Nutt JG, Carlson-Kuhta P, Mancini M, Horak FB. Levodopa Is a Double-Edged Sword for Balance and Gait in People With Parkinson's Disease. Mov Disord. 2015 Sep;30(10):1361–70.

40. Nonnekes J, Scotti A, Oude Nijhuis LB, Smulders K, Queralt A, Geurts ACH, et al. Are postural responses to backward and forward perturbations processed by different neural circuits? Neuroscience. 2013 Aug 15;245:109–20.

41. Solis-Escalante T, van der Cruijsen J, de Kam D, van Kordelaar J, Weerdesteyn V, Schouten AC. Cortical dynamics during preparation and execution of reactive balance responses with distinct postural demands. Neuroimage. 2019 Mar;188:557–71.

42. Tudor M, Tudor L, Tudor KI. [Hans Berger (1873-1941)--the history of electroencephalography]. Acta Med Croatica. 2005;59(4):307–13.

43. Onton J, Westerfield M, Townsend J, Makeig S. Imaging human EEG dynamics using independent component analysis. Neurosci Biobehav Rev. 2006 Aug 14;30(6):808–22.

44. Karakaş S. A review of theta oscillation and its functional correlates. Int J Psychophysiol. 2020 Nov;157:82–99.

45. Barone J, Rossiter HE. Understanding the role of sensorimotor beta oscillations. Front Syst Neurosci. 2021 May 31;15:655886.

46. Gwin JT, Ferris DP. Beta- and gamma-range human lower limb corticomuscular coherence. Front Hum Neurosci. 2012 Sep 11;6:258.

47. Gwin JT, Gramann K, Makeig S, Ferris DP. Electrocortical activity is coupled to gait cycle phase during treadmill walking. Neuroimage. 2011 Jan 15;54(2):1289–96.

48. Dietz V, Quintern J, Berger W, Schenck E. Cerebral potentials and leg muscle e.m.g. responses associated with stance perturbation. Exp Brain Res. 1985;57(2):348–54.

49. Goel R, Ozdemir RA, Nakagome S, Contreras-Vidal JL, Paloski WH, Parikh PJ. Effects of speed and direction of perturbation on electroencephalographic and balance responses. Exp Brain Res. 2018 Jul;236(7):2073–83.

50. Mochizuki G, Boe S, Marlin A, McIlRoy WE. Perturbation-evoked cortical activity reflects both the context and consequence of postural instability. Neuroscience. 2010 Oct 13;170(2):599–609.

51. Payne AM, Hajcak G, Ting LH. Dissociation of muscle and cortical response scaling to balance perturbation acceleration. J Neurophysiol. 2019 Mar 1;121(3):867–80.

52. Staines WR, McIlroy WE, Brooke JD. Cortical representation of whole-body movement is modulated by proprioceptive discharge in humans. Exp Brain Res. 2001 May;138(2):235–42.

1

53. Adkin AL, Quant S, Maki BE, McIlroy WE. Cortical responses associated with predictable and unpredictable compensatory balance reactions. Exp Brain Res. 2006 Jun;172(1):85–93.

54. Mochizuki G, Sibley KM, Cheung HJ, McIlroy WE. Cortical activity prior to predictable postural instability: is there a difference between self-initiated and externally-initiated perturbations? Brain Res. 2009 Jul 7;1279:29–36.

55. Mochizuki G, Sibley KM, Esposito JG, Camilleri JM, McIlroy WE. Cortical responses associated with the preparation and reaction to full-body perturbations to upright stability. Clin Neurophysiol. 2008 Jul;119(7):1626–37.

56. Mierau A, Hülsdünker T, Strüder HK. Changes in cortical activity associated with adaptive behavior during repeated balance perturbation of unpredictable timing. Front Behav Neurosci. 2015 Oct 14;9:272.

57. Bonini F, Burle B, Liégeois-Chauvel C, Régis J, Chauvel P, Vidal F. Action monitoring and medial frontal cortex: leading role of supplementary motor area. Science. 2014 Feb 21;343(6173):888–91.

58. Varghese JP, McIlroy RE, Barnett-Cowan M. Perturbation-evoked potentials: Significance and application in balance control research. Neurosci Biobehav Rev. 2017 Dec;83:267–80.

59. Hülsdünker T, Mierau A, Neeb C, Kleinöder H, Strüder HK. Cortical processes associated with continuous balance control as revealed by EEG spectral power. Neurosci Lett. 2015 Apr 10;592:1–5.

60. Hülsdünker T, Mierau A, Strüder HK. Higher Balance Task Demands are Associated with an Increase in Individual Alpha Peak Frequency. Front Hum Neurosci. 2015;9:695.

61. Slobounov S, Cao C, Jaiswal N, Newell KM. Neural basis of postural instability identified by VTC and EEG. Exp Brain Res. 2009 Oct;199(1):1–16.

62. Sipp AR, Gwin JT, Makeig S, Ferris DP. Loss of balance during balance beam walking elicits a multifocal theta band electrocortical response. J Neurophysiol. 2013 Nov;110(9):2050–60.

63. Peterson SM, Ferris DP. Group-level cortical and muscular connectivity during perturbations to walking and standing balance. Neuroimage. 2019 Sep;198:93–103.

64. Botvinick MM, Braver TS, Barch DM, Carter CS, Cohen JD. Conflict monitoring and cognitive control. Psychol Rev. 2001;108(3):624–52.

65. Ridderinkhof KR, Ullsperger M, Crone EA, Nieuwenhuis S. The role of the medial frontal cortex in cognitive control. Science. 2004 Oct 15;306(5695):443–7.

66. Cavanagh JF, Frank MJ. Frontal theta as a mechanism for cognitive control. Trends Cogn Sci (Regul Ed). 2014 Aug;18(8):414–21.

67. van Gaal S, de Lange FP, Cohen MX. The role of consciousness in cognitive control and decision making. Front Hum Neurosci. 2012 May 7;6:121.

68. Nigbur R, Cohen MX, Ridderinkhof KR, Stürmer B. Theta dynamics reveal domain-specific control over stimulus and response conflict. J Cogn Neurosci. 2012 May;24(5):1264–74.

69. Cohen MX. A neural microcircuit for cognitive conflict detection and signaling. Trends Neurosci. 2014 Sep;37(9):480–90.

70. Pereira M, Sobolewski A, Millán JDR. Action monitoring cortical activity coupled to submovements. eNeuro. 2017 Oct 24;4(5).
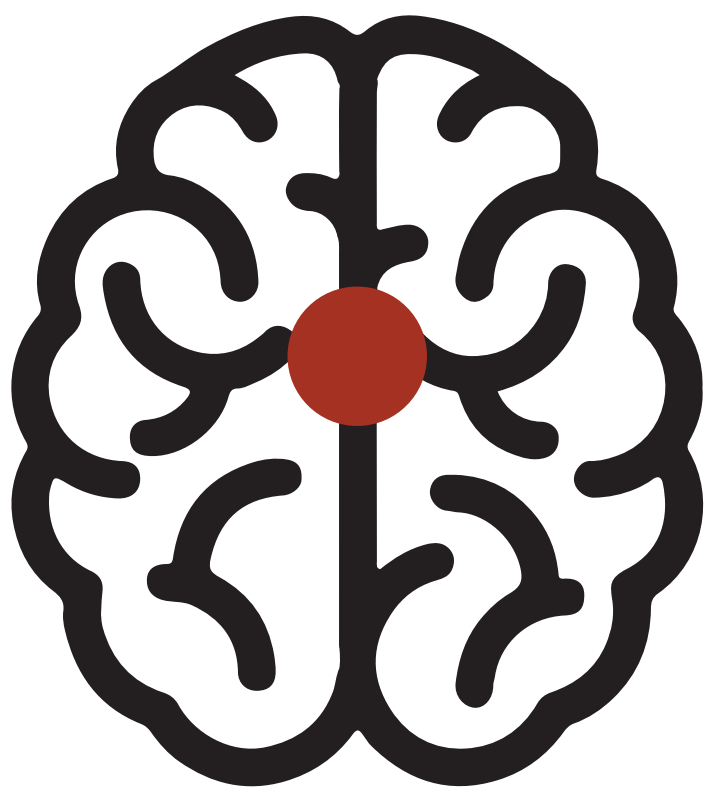
Chapter 2

Cortical responses to whole-body balance perturbations index perturbation magnitude and predict reactive stepping behavior

Abstract

The goal of this study was to determine whether the cortical responses elicited by whole-body balance perturbations were similar to established cortical markers of action monitoring. Postural changes imposed by balance perturbations elicit a robust negative potential (N1) and a brisk increase of theta activity in the electroencephalogram recorded over midfrontal scalp areas. Because action monitoring is a cognitive function proposed to detect errors and initiate corrective adjustments, we hypothesized that the possible cortical markers of action monitoring during balance control (N1 potential and theta rhythm) scale with perturbation intensity and the eventual execution of reactive stepping responses (as opposed to feet-in-place responses). We recorded high-density electroencephalogram from eleven young individuals, who participated in an experimental balance assessment. The participants were asked to recover balance following anteroposterior translations of the support surface at various intensities, while attempting to maintain both feet in place. We estimated source-resolved cortical activity using independent component analysis. Combining time-frequency decomposition and group-level general linear modeling of single-trial responses, we found a significant relation of the interaction between perturbation intensity and stepping responses with multiple cortical features from the midfrontal cortex, including the N1 potential, and theta, alpha, and beta rhythms. Our findings suggest that the cortical responses to balance perturbations index the magnitude of a deviation from a stable postural state to predict the need for reactive stepping responses. We propose that the cortical control of balance may involve cognitive control mechanisms (i.e., action monitoring) that facilitate postural adjustments to maintain postural stability.

2

Introduction

In everyday activities, we must continuously adjust our posture to maintain balance and avoid falling. The control of human balance and posture requires fast and robust coordination of neural ensembles distributed across multiple levels of the central nervous system (1–3). Although the traditional view is that balance and posture are controlled by the brainstem, basal ganglia, and cerebellum, the cerebral cortex may interact with these structures to maintain balance during goal-directed movement with varying environmental demands (4–6).

The cerebral cortex presumably contributes to maintaining postural stability by detecting deviations from a stable postural state and by modulating or initiating appropriate corrective actions, either by adapting the excitability of subcortical postural circuits or by directly contributing to postural responses (1). The likelihood of cortical contributions to reactive postural responses increases with the latency of the postural response (2). Yet, the cortical responses to external balance perturbations appear in the electroencephalogram (EEG) as early as 30 ms after perturbation onset. Robust cortical responses to balance perturbations appear with broad scalp distribution and rich spectral composition (7–9) and likely reflect cognitive and sensorimotor processes related to the integration of sensory information associated with sudden postural changes (10,11), and to the detection of a mismatch between expected and current postural stability (12,13).

The earliest cortical responses to balance perturbations appear over fronto-centro-parietal scalp areas as characteristic event-related potentials comprising a small positive peak (P1) and a large negative peak (N1), with respective latencies of 30–90 and 90–160 ms relative to perturbation onset (see Varghese et al., 2017 for a comprehensive review). These so-called perturbation-evoked potentials (PEP) P1 and N1 are modulated by the physical characteristics (i.e., displacement, velocity, acceleration, and duration) of the balance perturbations. The early P1 potential is thought to represent initial sensory afferences related to proprioception (10,11) because the P1 potential is suppressed by ischemic deafferentation (11), suppressed by peripheral nerve stimulation (14), and presumably suppressed due to presynaptic inhibition during gait (10,11,15). The N1 potential increases with the intensity of the perturbation and its associated destabilizing effect (11,14,16–19), which suggests that the N1 potential is at least partially involved in the processing of the multisensory input associated with a sudden change in posture and postural stability. However, the N1 potential is unlikely to represent cortical contributions to early-phase reactive postural responses as demonstrated by its latency (~150 ms)

and its weak correlation with fast reactive muscle responses (11,16,19,20). Instead, the N1 potential may represent cognitive and sensorimotor processes that modulate late-phase postural responses (e.g., stepping). Consistent with a possible cognitive function, the N1 potential is strongly affected by psychological factors such as perceived postural threat (18,21), the predictability of perturbation characteristics such as onset and intensity (12,18,22,23), attention to concurrent tasks (24,25), and habituation (19,20). For example, imposed changes to postural stability of the same magnitude elicit stronger N1 potentials under conditions of increased postural threat and reduced predictability (21), whereas attention to a concurrent task or repeated exposure to balance perturbations gradually decreases the N1 potential (20). These observations indicate that the N1 potential is internally regulated according to an expected deviation from a current stable posture.

The N1 potential could represent mechanisms of cognitive control (i.e., error detection and action monitoring) for self-regulation of performance via adaptive behavior. Interestingly, it has been proposed that the N1 potential represents a form of error detection (12,19,26) because it shares several characteristics with classical error-related cortical responses. The error-related negativity (ERN) and the error-related potentials (ErrP) are cortical responses to the realization of an erroneous action, and have similar latencies and scalp topographies to those of the N1 potential (27,28). Furthermore, the error-related responses (ERN/ErrP) scale with the magnitude and consequence of the perceived error and are modulated by prior knowledge about error occurrence (e.g., magnitude, consequence, and timing). This is comparable to how the N1 potential scales with analogous characteristics of a balance perturbation (i.e., perceived postural threat and onset predictability). Direct comparison of the N1 potential elicited by imposed postural changes (low-intensity balance perturbations) and the ERN/ErrP elicited by erroneous actions (incorrect left/right hand button press during a flanker task) showed that these responses arise from different cortical areas, i.e., the ERN/ErrP originates in the anterior cingulate cortex (ACC), whereas the N1 potential originates from the supplementary motor area (SMA; (26)). The localization of the N1 potential to the SMA has been repeatedly confirmed (8,17,20) and interpreted as evidence in favor of a role of the N1 potential in sensorimotor processes (e.g., movement preparation and initiation) over mechanisms of cognitive control (9). Nonetheless, it is important to mention that different aspects of cognitive control (e.g., decision conflict and response error) are associated with activity (including ERN/ErrP) from multiple structures in the posterior midfrontal cortex, including the SMA, pre-SMA, and the ACC (29–31). Therefore, it is possible that the N1 potential and the ERN/ErrP represent different aspects of a general action monitoring system (13).

2

Action monitoring refers to the capacity to evaluate the outcome of our actions in order to detect errors and initiate corrective adjustments (30,31). This implies that cortical markers of action monitoring are closely related to adaptive goal-directed behavior. Indeed, the amplitude of ERN/ErrP correlates with the magnitude of a perceived error and the required corrective response (32,33). Similarly, the power of the midfrontal theta rhythm (3–7 Hz) correlates with error detection, response conflict (or uncertainty), and the associated behavioral adaptations (34,35). Besides the ERN/ErrP and the theta rhythm being both correlated with error detection and adaptive behavior, it has been proposed that the ERN/ErrP may be generated through phase resetting of the ongoing theta rhythm (36–38), suggesting a close interrelation between the ERN/ErrP and the midfrontal theta rhythm. The ERN/ErrP and the midfrontal theta rhythm are considered cortical markers of action monitoring and may be part of a feedback control loop for top-down regulation of behavior. It remains to be established whether similar mechanisms take part in the control of balance and posture, where the neural activity at cortical levels of the postural control system could reflect action monitoring mechanisms for an internal assessment of postural stability that determines the need for late-phase balance recovery responses.

In this study we evaluated the association of the cortical responses elicited by balance perturbations with the intensity of the perturbation (as a form of perceived error), the ensuing reactive postural response (as necessary corrective actions), and the interaction between these factors. We were particularly interested in the interaction between perturbation intensity and reactive postural response (stepping vs. non-stepping) because it underlies a behavioral model of stepping probability and balance capacity, and this behavioral model may mirror the internal processes that regulate postural stability. We hypothesized that the cortical responses to balance perturbations would scale with perturbation intensity and its interaction with the type of postural response, suggesting that the cortical responses to balance perturbations follow the magnitude of the imposed change to postural sta-bility and its associated corrective response. In this way, we investigated whether the cortical responses elicited by whole-body balance perturbations are consistent with known cortical markers of action monitoring.

We analyzed temporal and spectral parameters of these cortical responses, with special focus on the time period around the N1 potential. We used a wide range of perturbation intensities to investigate the cortical responses elicited by balance perturbations covering the extent of the transition between non-stepping and stepping responses. This was important because previous studies have been largely limited by the use of small sets of low-intensity perturbations that exclusively

elicit non-stepping responses (11,15–19) or by the use of two distinct perturbation intensities (high - low) to elicit stepping and non-stepping responses (18,39). Furthermore, we analyzed a wide range of spectral components to better understand the modulations of cortical rhythms with respect to the perturbation intensity and reactive responses. We anticipated that the power of the theta rhythm would be modulated by perturbation intensity and reactive responses, due to the known role of the midfrontal theta rhythm as cortical marker of action monitoring, but also because transient conditions of reduced postural stability (caused by external perturbations or natural sway) elicit a brief power increase of the theta rhythm in fron-to-centro-parietal scalp areas (7,8,40) and because the power of the theta rhythm covaries with postural demand (41,42). Other spectral features were analyzed because perturbations to standing balance elicit a broadband power increase of frequencies between 3–17 Hz within 500 ms from the perturbation onset (7,8,43); yet, their association with perturbation intensity remains largely unexplored. Our analysis offered the possibility to identify specific cortical rhythms that may be associated with distinct cognitive and motor functions. An association of temporal or spectral parameters of the cortical responses with perturbation intensity and reactive postural responses would provide further evidence about the neural correlates of top-down regulation of reactive postural responses.

Materials and Methods

Participants
Eleven young able-body individuals participated in this study (age: 26 ± 3 years old, four female). None of the participants had self-reported history of neurological or neuromuscular disease or any other impairments that limited their involvement in the experiment. The experiments were undertaken with the understanding and written consent of each participant. The study protocol was approved by the Research Ethics Committee of the Radboud University Medical Center (Nijmegen, The Netherlands; Dossier 2018-4970). The experiments were conducted in accordance with the Declaration of Helsinki.

Experimental paradigm
The experiments were conducted with the Radboud Falls Simulator, a dynamic posturography system for investigating standing balance (44). During the experiments, the participants stood in the middle of a movable platform with arms crossed and feet placed apart at shoulder width. Figure 1 illustrates the experimental setup and the trial timing.
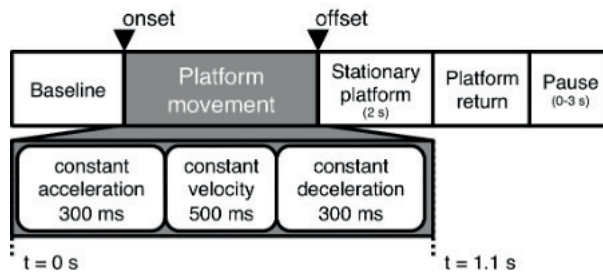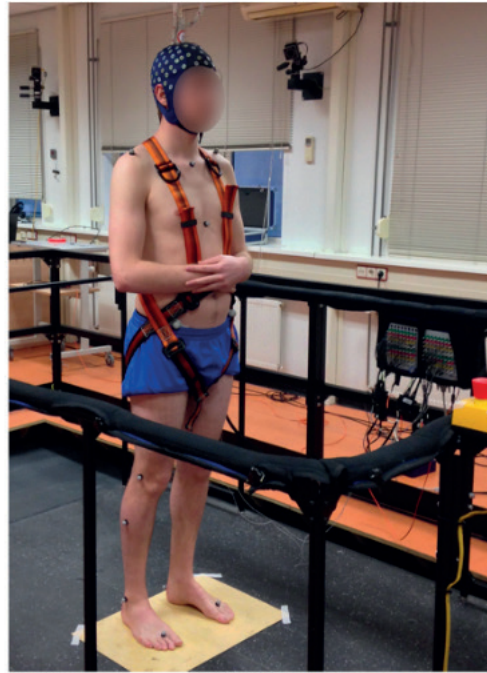
Figure 1. Experimental setup and trial timing. Top: The participants stood in the middle of a movable platform with arms crossed and feet placed apart at shoulder width. Bottom: The balance perturbations were ramp-and-hold platform translations consisting of three phases: constant acceleration, constant velocity, and constant deceleration. At the end of the displacement the platform remained stationary for 2 s

The participants were instructed to maintain standing balance by keeping both feet in place, in response to sudden balance perturbations. The balance perturbations were ramp-and-hold translations of the movable platform consisting of three phases: constant acceleration (300 ms), constant velocity (500 ms), and constant deceleration (300 ms). At the end of the displacement the platform remained stationary for 2 s before gently returning to its initial position. The intensity of the perturbations was controlled by varying the acceleration of the translations from 0.125 to 2.5 m/s2 (increments of 0.125 m/s2, leading to 20 accelerations). The direction of

the translation was either forward or backward, and thus there were a total of 40 different perturbations (20 accelerations × 2 directions). The higher perturbation intensities required the execution of reactive stepping to maintain standing balance. Forward translation of the platform elicited postural sway and an eventual step in the backward direction; similarly, backward translation of the platform elicited postural sway and an eventual step in the forward direction. Henceforth, we refer to the direction of the postural sway and eventual stepping response, unless specifically indicated as the direction of the platform translation. Participants were made aware of this and they were assured that stepping could not be avoided for a fair amount of perturbation intensities. Nonetheless, participants were encouraged to keep both feet in place throughout the experiment.

The perturbations were arranged into blocks of 10 forward and 10 backward translations with intensities uniformly distributed across the range of accelerations (same intensities in both directions per block). The order of the perturbations was randomized within each block and across participants. The inter-trial interval randomly varied between 3 and 5 s (with uniform distribution). Depending on the duration of preparation time and resting breaks, participants completed 120 or 160 experimental trials in one experimental session. Due to the arrangement of the perturbation blocks, each distinct perturbation was tested three to four times. Importantly, the participants could not predict timing onset, direction, or intensity of the perturbation.

To prevent fatigue, short pauses lasting 3–5 min were encouraged between blocks. Prior to the experiment, participants practiced with one block of perturbations to familiarize themselves with the task. The familiarization trials were not included in the analysis.

Data collection

We recorded high-density EEG using an electrode cap with 126 Ag-AgCl electrodes (WaveGuard, ANT Neuro, The Netherlands). The electrodes were distributed across the scalp according to the five percent electrode system (45). The ground electrode was placed on the left mastoid using an adhesive Ag-AgCl electrode. In addition, two-channel electrooculogram (EOG) was recorded using adhesive Ag-AgCl electrodes placed slightly above the nasion and at the outer canthus of the left eye. The ground electrode was used for both the EEG and the EOG channels. A biosignal amplifier (REFA System, TMSi, The Netherlands) recorded the EEG/EOG at 2048 Hz without any filters, except for a built-in antialiasing low-pass filter. The 128 signals (i.e., EEG and EOG) were referenced to the common average during acquisition. Ground reaction forces were recorded from two force plates (AMTI custom 6 axis composite force platform, Watertown, MA, USA; size: 60 × 180 cm each; sampling rate: 2,000

Hz) embedded in the movable platform. Each force plate recorded ground reaction forces from one foot. Synchronization triggers indicating the onset and offset of the platform movement were generated by the platform controller and simultaneously recorded with the EEG/EOG signals and the ground reaction forces.

Before beginning the experiment, EEG (and EOG) signals were recorded for a set of control conditions during quiet stance. These control conditions were short recordings (approx. one minute each) involving overt eye movement (blinking, lateral movement, eye rolling), head/neck movement (rotation, flexion/extension, lateral flexion), facial expressions (movements of mouth, lips, nose, and eyebrows), and jaw clenching; with an additional one minute of quiet stance with eyes open. These recordings were intended to assist the separation of sources of physiological noise by providing clear examples of their source activity that could be modeled as independent sources.

Detection of reactive stepping responses
The ground reaction forces were exported to C3D format and later imported into MATLAB (The Mathworks, Inc.) for analysis. Reactive stepping responses were detected from the vertical component of the ground reaction forces using threshold detection. The vertical component of the ground reaction forces measures the force applied to each side of the movable platform, corresponding with each leg. During quiet stance the sum of the left and right ground reaction forces equals the bodyweight of the participants (mass in kg) multiplied by the acceleration of gravity on Earth (~9.8 m/s^2). The vertical force components from each force plate were low-pass filtered at 20 Hz (5th order Butterworth IIR filters, zero-phase shift) and compared against a threshold of 10 N (~1 kg). Values below this threshold indicate that one of the feet has been lifted from one of the force plates. Reactive stepping responses were detected if they occurred within 1 s from perturbation onset; otherwise, the response was classified as non-stepping (feet-in-place). Participants were allowed to step with either leg.

EEG analysis

Preprocessing
The EEG was analyzed with MATLAB using custom scripts and incorporating functions from EEGLAB (46). The EEG was filtered between 1 and 200 Hz (consecutive high-pass and low-pass 5th order Butterworth IIR filters, zero-phase shift) and downsampled to 512 Hz. The EEG and EOG recordings from control conditions and experimental

blocks were concatenated. Highly contaminated channels were identified by visual inspection and removed from the recordings. On average, 126 channels remained for analysis ($SD \pm 1.7$). The remaining channels were re-referenced to the common average. The data were visually inspected for segments with cable movements or electrode disconnection, which were removed from the data.

Estimation of source-resolved activity

Independent component analysis (ICA) was used to estimate source-resolved brain activity from the high-density EEG (47,48) and to reduce the influence of other sources of physiological noise (e.g., electromyogram and electrocardiogram; (49–52). This approach is in line with previous studies on cortical dynamics during whole-body movement and balance control (7,8,43,53,54). Because the EEG was referenced to the common average, a principal component analysis was used before ICA simply to remove the principal component with the lowest eigenvalue (null-space; (55)).

Following the ICA, the source-resolved activity was segmented into epochs from −2 to 9 s relative to perturbation onset. Per participant, one independent component (IC) was identified as the likely source of the N1 potential by inspection of the event-related potential associated with each IC. All candidate ICs were further evaluated as likely brain sources based on the residual variance of an equivalent current dipole fitted to their scalp projections. The equivalent current dipoles were fitted using a four-shell spherical head model and standard electrode positions (DIPFIT toolbox within EEGLAB, (56). The equivalent current dipoles provide an estimation (limited in spatial resolution) of the likely location of the source-resolved N1, which assists the validation of a dipolar topography of the scalp projection and a physiologically plausible location (50,52). Thus the objective of the source localization analysis was to provide additional information on the distribution of individual IC scalp maps, to answer the questions whether the scalp map has a dipolar distribution (indicated by its residual variance) and whether the scalp map is likely to represent a cortical source (indicated by its spatial location).

The location of the equivalent current dipoles calculated by the DIPFIT toolbox are given in Talairach coordinates. The corresponding Broadmann areas were found using the online application mni2tal (available at https://bioimagesuiteweb.github.io/webapp/mni2tal.html) from the Yale BioImage Suite Package (57).

Time and time-frequency domain cortical parameters

The signal of the estimated source-resolved N1 potential was analyzed to quantify single-trial amplitude and latency. A copy of the source-resolved signal was low-pass

filtered at 30 Hz (5th order Butterworth IIR filter, zero-phase shift) and the single-trial amplitude and latency were identified as the largest negative peak within 300 ms from perturbation onset. The single-trial amplitude and latency were stored for analysis.

To quantify spectral parameters, the estimated source-resolved signal was analyzed in the time-frequency domain by convolving this signal with a set of complex Morlet wavelets, defined as complex sine waves tapered by a Gaussian (58). The frequencies of the wavelets ranged from 2 to 50 Hz in 30 steps (logarithmically spaced). The full-width at half-maximum (FWHM) ranged from 800 to 200 ms, decreasing with increasing wavelet peak frequency. This corresponded to a spectral FWHM range of 1.7–7.2 Hz.

Event-related parameters were extracted from the single-trial source-resolved signal in time domain and the time-frequency domain for 101 time points within ±500 ms (time resolution: 10 ms), relative to the trial-specific N1 latency. Thus, there were 101 time domain parameters and 101 × 30 time-frequency domain parameters. All parameters were transformed to logarithmic power ($10 \log_{10} (|\text{parameter}_x|^2)$), for consistency in analyses and interpretation of temporal and spectral features.

Trial rejection

After selection of the N1 component, the source-resolved activity was visually inspected once again for possible artifacts (e.g., movement artifacts or excessive contamination from muscular activity) within ±2 s from perturbation onset. Then, single-trials with N1 amplitudes or latencies beyond ±3 *SD* from the mean were rejected. Trial rejection was separately conducted for each participant. The remaining trials were time-locked to the N1 latency and visually inspected in the interval −1 to 1.5 s (relative to N1 latency). On average, there were 125 trials (*SD* ± 24) per participant.

Event-related potentials and spectral modulations

For the purpose of visualization, grand average event-related potentials associated with stepping and non-stepping responses were computed in the forward and backward direction. The source-resolved signals were normalized on a trial-by-trial basis (z-score across time points), time-locked to the N1 latency, and averaged across trials from the same condition.

Similarly, the grand average event-related spectral modulations were computed per condition. Single-trial spectrograms were computed following the time-frequency analysis described in the previous section (i.e., convolution with complex Morlet

wavelets). The spectrograms were transformed to logarithmic power and a trial-specific baseline was computed as the mean (log transformed) spectrum from the interval −1.5 to −0.5 s, relative to perturbation onset. The baseline was subtracted from its corresponding trial and the baseline-corrected spectrograms were time-locked to the N1 latency. Finally, time-frequency maps showing the mean event-related spectral modulations (i.e., power changes relative to baseline) were computed by averaging the spectrograms across trials from the same condition. The statistical significance of the spectral modulations was estimated for each time-frequency bin from its 95% confidence interval (bootstrap, $n = 200$).

Relation of cortical parameters with perturbation intensity and stepping behavior

The effects of perturbation intensity and stepping behavior on the cortical parameters were analyzed with the model for general linear regression:

$$C_x \sim \beta_0 + \beta_1 \cdot ACCEL + \beta_2 \cdot STEP + \beta_3 \cdot ACCEL \times STEP$$

where the regression coefficients β_1 and β_2 indicate the main effects of the perturbation intensity (i.e., acceleration: ACCEL) and the dummy-coded stepping behavior (STEP), respectively; and the regression coefficient β_3 indicates the effect of their interaction (ACCEL × STEP). The null-hypothesis that there is no significant relation with the cortical parameters Cx corresponds to regression coefficients equal to zero. The null-hypothesis can be rejected if the confidence interval of a given regression coefficient does not include zero.

Regression analyses were conducted at group-level using pooled trials from all participants, after participant-specific normalization (z-score across trials) of the cortical parameters. The analyses were performed separately for forward and backward stepping directions, with time and time-frequency parameters. An additional regression analysis was conducted to determine the effects of perturbation intensity and stepping behavior on the N1 latency (after participant-specific normalization).

The significance of the regression analysis was evaluated with an F test and the significance of the regression coefficients with a t test. Statistical significance was assessed for critical $\alpha = 0.01$. Given the multiple regression analyses computed in time and time-frequency domains, p-values were corrected for false discovery rate (FDR; (59).

Results

Reactive stepping responses (behavior analysis)

Table 1 presents the total number of trials per condition and the mean latencies of the reactive stepping responses (foot-off detection). Importantly, the forward and backward directions refer to the direction of postural sway and eventual stepping. The conditions were defined on basis of postural sway direction (forward vs. backward) and the ensuing reactive response (stepping vs. non-stepping), irrespective of the perturbation intensity. These latencies are relative to perturbation onset and averaged across stepping responses at varying perturbation intensities. Figure 2 shows the distribution of trials over perturbation intensities (i.e., accelerations) and the estimated stepping probability (computed via logistic regression).

Table 1. Number of trials and average stepping response latency (ms) per condition

	Backward			Forward		
	Stepping		Non-stepping	Stepping		Non-stepping
	Trials	Foot-off latency	Trials	Trials	Foot-off latency	Trials
S01	25	411.7	17	20	572.5	15
S02	31	598.5	23	31	632.5	22
S03	35	600.9	24	24	745.9	35
S04	41	318.2	18	31	387.8	27
S05	43	472.2	36	36	688.7	36
S06	51	448.5	22	35	607.7	38
S07	40	443.6	16	31	468.6	25
S08	45	306.3	9	27	386.7	31
S09	33	371.1	30	27	540.6	36
S10	41	499.2	37	45	450.4	31
S11	57	287.2	21	54	397.9	19
Pooled	442	422.4	253	361	521.8	315
SD (pooled)		170.1			172.8	
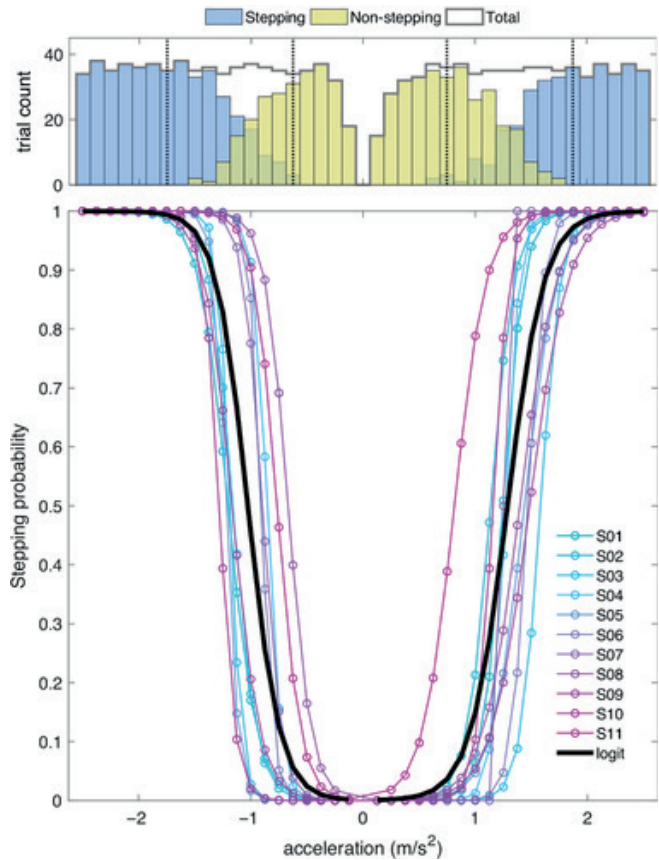
Figure 2. Trial distribution and stepping probabilities (group-level). Top: Total trial count per acceleration and distribution of stepping (blue) and non-stepping (yellow) trials. The distribution of the total number of trials was near-uniform in the backward stepping (negative accelerations) and forward stepping (positive accelerations) direction. Consistent with anatomical and functional constraints, the proportion of stepping trials was higher in the backward direction (see text). Bottom: The stepping probability as a function of perturbation intensity was computed for each direction using logistic regression. Individual probability curves are shown in cold colors (blue to magenta) and the group-level probability is shown with a thick black line

There were 695 trials challenging postural stability in the backward direction and 676 trials challenging postural stability in the forward direction. The mean number of trials per participant was not significantly different between the two directions (two-tailed paired t test; $t(10) = 1.71$, $p = .118$) and the distribution of trials over intensities was close to uniform (Kolmogorov–Smirnov tests for uniform distributions between 0.125 and 2.500 m/s²; backward: $D(695) = 0.051$, $p = .052$; forward: $D(676) = 0.054$, $p = .038$; see figure 2). In both directions, more than half of the trials elicited reactive stepping responses (backward: 63.3%, forward: 53.4%), but the proportion

of stepping trials was significantly larger for the backward direction (chi-squared test; $\chi^2 = 14.68$, $p = 1.27e^{-04}$). Consistent with these observations, the stepping probability models estimate that 50% stepping probability (at group level) corresponds to 1.02 m/s^2 for the backward stepping and 1.28 m/s^2 for the forward stepping direction; with the limits for 25% and 75% stepping probability at [0.87, 1.18] m/s^2 and [1.10, 1.46] m/s^2 respectively. The pooled data showed only non-stepping responses for perturbation intensities smaller or equal to 0.5 m/s^2 in both directions. Similarly, stepping responses were only observed for perturbation intensities greater than 1.5 m/s^2 for backward stepping and 1.75 m/s^2 for forward stepping (see histogram in figure 2). The mean stepping latency was significantly shorter for the backward stepping direction (two-tailed paired t test; $t(10) = -4.33$, $p = .001$).

Visualization of event-related cortical responses

In figure 3, the event-related potentials show the strong negative peak of the N1 potential ($t = 0$ s) and the characteristics of the cortical response to balance perturbations (9); namely, a slow potential shift preceding perturbation onset, followed by P1 (positive) and N1 (negative) potentials and late potentials of varying latency and amplitude approximately within 400 ms after perturbation onset. The event-related spectral modulations show a broadband power increase over the frequencies of the theta, alpha, beta, and gamma rhythms, occurring shortly after perturbation onset and coinciding with the N1 potential. In general, the initial broadband power increase is followed by power decrease over the frequencies of the alpha and low-gamma rhythms. This spectral modulation pattern is characteristic of cortical responses to balance perturbations (7–9). The visualization of event-related cortical responses is meant to provide an overview of the time and time-domain characteristics of the conditions defined on basis of postural sway direction (forward vs. backward) and the ensuing reactive response (stepping vs. non-stepping), irrespective of the perturbation intensity.
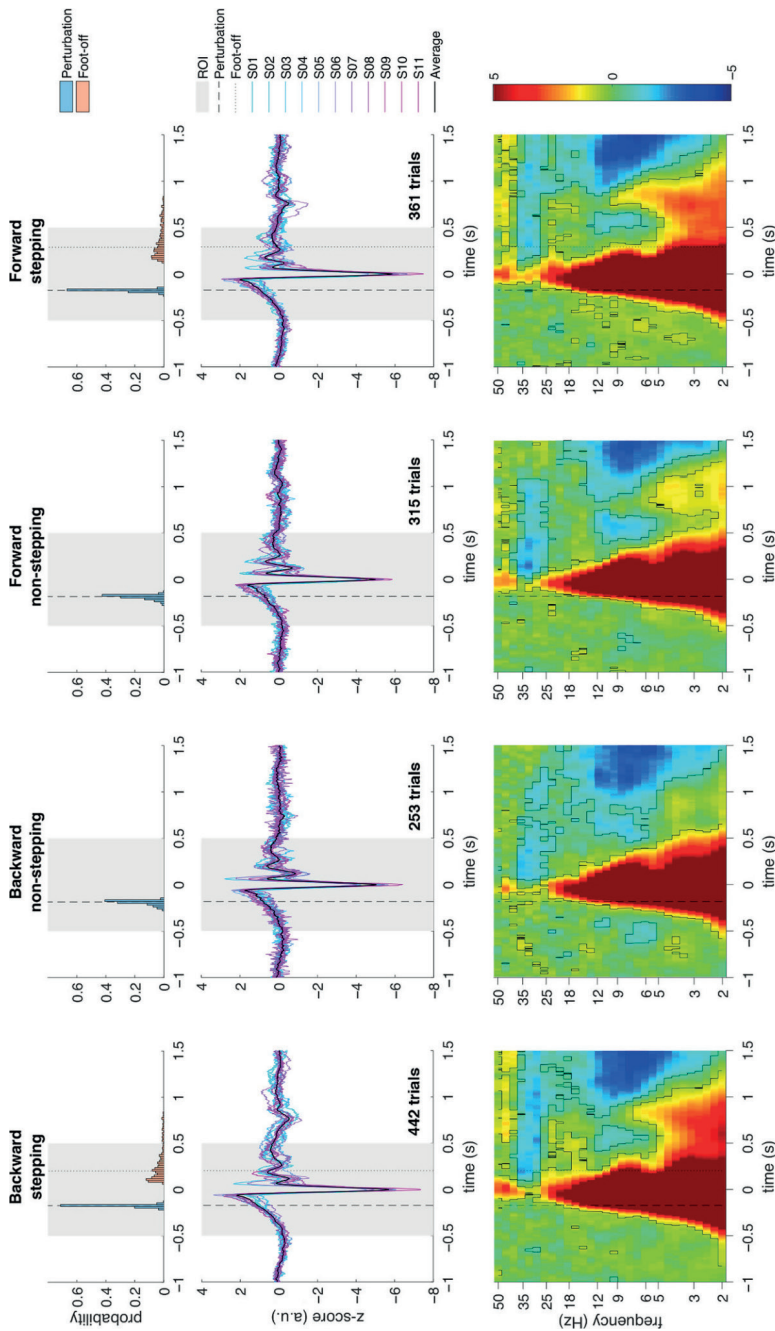
Figure 3. Event-related potentials and event-related spectral modulations. Characteristic cortical responses to balance perturbations in time domain (middle row) and time-frequency domain (bottom row), shown relative to the peak amplitude of the N1 potential (t = 0 s) and in comparison with the distribution (top row) of perturbation onset (blue) and foot-off onset (pink) latencies. The vertical dashed line indicates the median latency of the perturbation onset (backward: stepping −171.9 ms, non-stepping −183.6 ms; forward: stepping −173.8 ms, non-stepping −183.6 ms) and the vertical dotted line indicates the median foot-off latency (backward: 202.6 ms; forward: 289.9 ms). The region of interest (ROI, shown with a gray band) extended from −500 to 500 ms relative to the N1 potential, including the period between median perturbation onset and foot-off latencies. The time domain plots show a typical N1 potential for each individual (blue to magenta) and the group-level average (thick black line). The time-frequency domain maps show the grouplevel average power modulations, with typical broadband power increase (warm colors). The black contour shows power increase/decrease significantly different from baseline ($p < .05$)

Mean N1 latency

Table 2 presents the mean N1 latency (relative to perturbation onset) for each participant and for the pooled data. Noteworthy, the mean latency per condition was obtained by averaging across trials within the conditions defined on basis of postural sway direction (forward vs. backward) and the ensuing reactive response (stepping vs. non-stepping), irrespective of the perturbation intensity. Within each direction, the mean N1 latency was significantly shorter for stepping responses than for non-stepping responses (two-tailed paired t tests; backward: $t(10) = -13.3$, $p = 1.08e^{-07}$; forward: $t(10) = -7.05$, $p = 3.50e^{-05}$). The mean N1 potential latency (cortical response) preceded the mean stepping response latency (behavioral response) in either direction (two-tailed paired t test; backward: $t(10) = -8.05$, $p = 1.11e^{-05}$; forward: $t(10) = -9.60$, $p = 2.29e^{-06}$; average mean latency difference backward stepping: 257 ms, range: 117–433 ms; average mean latency difference forward stepping: 358 ms, range: 212–569 ms). Histograms of the stepping response latency, relative to the N1 potential, are shown in figure 3 (previous section), together with the average event-related potentials and event-related spectral modulations per condition.
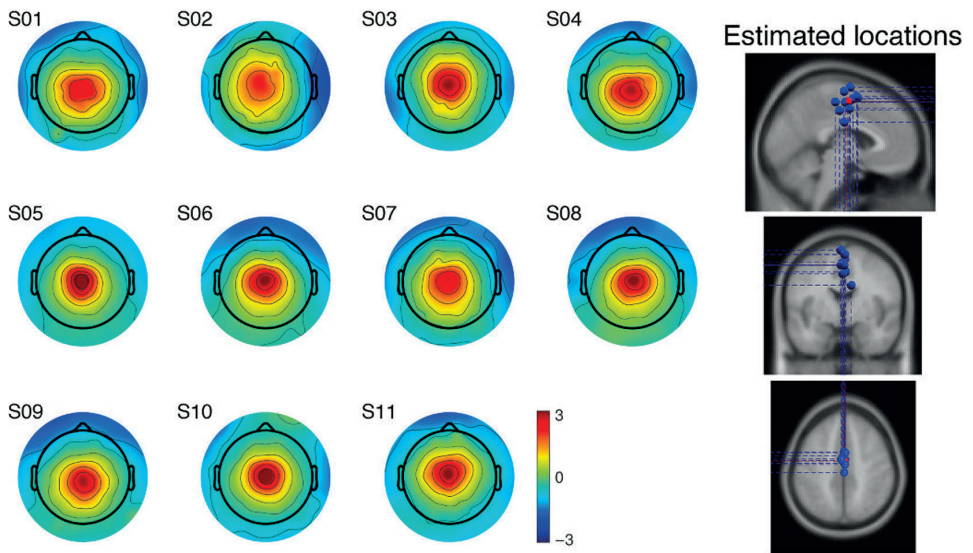
Figure 4. Individual IC scalp maps and estimated cortical source locations. The IC scalp maps of each participant are qualitatively similar and suggest a dipolar topography consistent with the residual variance in Table 3. The similarities are also shown in the estimated cortical location of the equivalent current dipoles (blue, individual participants; red, cluster centroid)

Table 2. Average N1 latency (ms) per condition

	Backward		Forward	
	Stepping	Non-stepping	Stepping	Non-stepping
S01	179.0	195.4	176.4	190.4
S02	189.9	206.2	193.2	203.8
S03	167.9	187.9	176.3	184.4
S04	174.1	183.5	175.7	182.0
S05	177.3	192.1	180.6	187.2
S06	168.4	177.9	170.0	175.1
S07	178.0	196.4	177.9	196.4
S08	176.4	190.3	173.3	188.7
S09	168.4	185.0	167.1	177.4
S10	175.8	188.7	173.2	193.4
S11	170.2	191.4	173.8	195.2
Pooled	174.5	190.2	176.0	187.1
SD (pooled)	11.7	23.5	11.8	23.1

Table 3. Estimated location of the N1 Cortical source

	Talairach coordinates			Residual variance (%)	Location and Brodmann area
	X	Y	Z		
S01	0	−16	40	2.23	Posterior cingulate L Left BA24
S02	9	−12	28	4.27	Posterior cingulate R —
S03	−2	−6	49	3.19	Paracentral L Left BA6
S04	1	−21	49	4.03	Paracentral R Right BA6
S05	−2	−3	64	1.25	Paracentral L —
S06	1	4	53	2.02	Superior frontal R Right BA6
S07	3	−5	42	2.44	Posterior cingulate R Right BA32
S08	3	3	54	3.05	Superior frontal R Right BA6
S09	1	−10	49	2.13	Paracentral R Right BA6
S10	2	−10	60	2.18	Paracentral R Right BA6
S11	0	−1	52	2.3	Superior frontal L Left BA6
Centroid	2	−7	49	—	Right BA6

Relation of cortical parameters with perturbation intensity and stepping behavior

Single-trial N1 characteristics

Figure 5 shows the pooled single-trial latency and power of the peak N1 amplitude together with the corresponding regression models. All determination and regression coefficients indicate a significant ($p < .01$) relation of perturbation intensity, stepping behavior, and the interaction between these factors with the characteristics of the N1 potential. In general, for perturbations that challenge postural stability in either direction, the latency and power of the peak N1 rapidly change with perturbation intensity in trials with non-stepping responses. The scaling with perturbation intensity is attenuated in trials with stepping responses, which is indicative of the interaction effect.
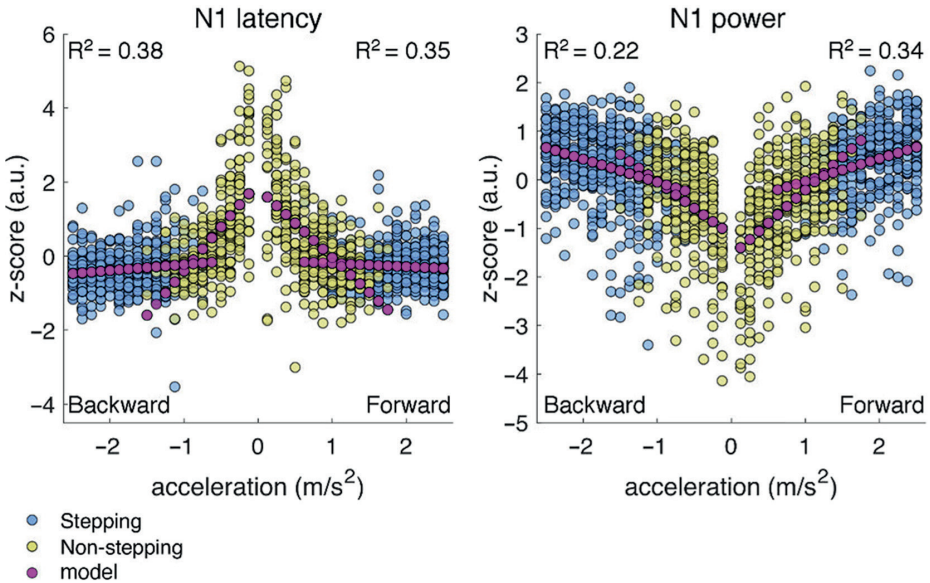
Figure 5. Relation of perturbation intensity and stepping responses with N1 characteristics. Distribution of the pooled single-trial latency (left) and power of the peak N1 amplitude (right). The data of each participant was normalized by computing the z-score across trials (including all perturbation intensities and directions). In a previous step, the peak N1 amplitude was transformed to logarithmic power for comparison with the analyses on spectral parameters. The x-axis indicates perturbation intensity (i.e., acceleration magnitude) multiplied by the sign of the sway direction (negative: backward sway; positive: forward sway). Blue circles indicate trials with a stepping response and yellow circles indicate trials with a non-stepping response. The corresponding regression models are shown with magenta circles. The determination (R2) and regression coefficients (β, not shown) are significant (p < .01). The relation with stepping behavior is indicated by the change in slope of the regression models seen between trials with stepping and nonstepping responses

The distribution of the pooled data and the corresponding regression models for the power of the peak N1 amplitude (figure 5) are representative of the temporal and spectral parameters (see figure S1). Overall, the temporal and spectral cortical parameters analyzed here scale with perturbation intensity and this scaling is attenuated from non-stepping to stepping responses. The cortical parameters related to stepping responses have larger magnitudes and are less affected by perturbation intensity than the cortical parameters related to non-stepping responses.

Time domain parameters

Figure 6 shows the adjusted determination coefficient, together with the corresponding regression coefficients, obtained from the regression analyses using time domain parameters. The coefficients of the regression model indicate: β_0 the intercept, β_1 the effect of acceleration, β_2 the effect of distinct reactive postural responses (dummy values: non-stepping = 0 and stepping = 1), and β_3 the effect of the interaction between acceleration and distinct reactive postural responses. The regression coefficients show a statistically significant effect of perturbation intensity from −140 to 30 ms (relative to the N1 potential), for perturbations that challenge postural stability in the backward ($p < .0012$) and forward ($p < .0026$) directions. A statistically significant effect of stepping behavior is shown from −130 to −50 ms for backward direction ($p < .0007$); and from −90 to −50 ms and from −10 to 20 ms for forward direction ($p < .0002$). The interaction between perturbation intensity and stepping behavior is also statistically significant in these intervals (backward: $p < .0010$; forward: $p < .0007$). These results show a relation of the N1 potential with perturbation intensity and stepping behavior, as well as their interaction.

Time-frequency domain parameters

Figure 7 shows time-frequency maps of the adjusted determination coefficient and the corresponding regression coefficients obtained from the regression analyses using spectral parameters. These maps show statistically significant effects of perturbation intensity, stepping behavior, and their interaction, in the time interval between perturbation onset and reactive responses and over a broad frequency band. The time interval corresponds with the expected interval of the N1 potential and the broad frequency band corresponds with power increase revealed from the event-related spectral modulations time-frequency maps (figure 4).
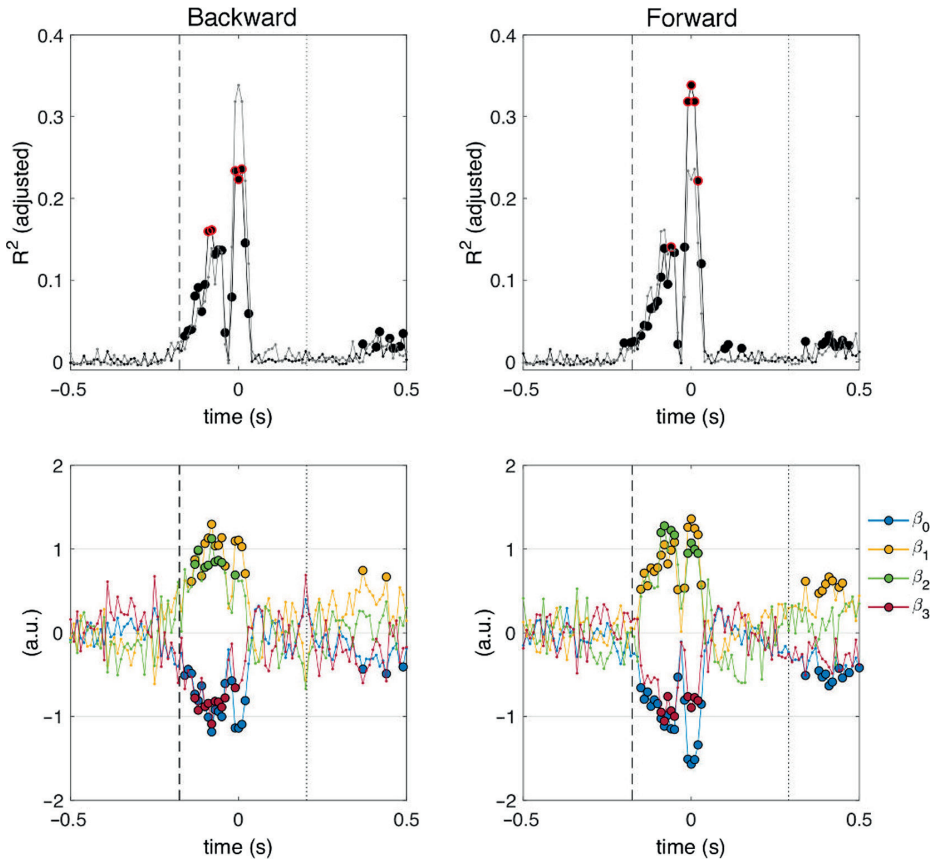
Figure 6. Relation of perturbation intensity and stepping responses with time domain parameters. Timedependent adjusted determination coefficient (top) and regression coefficients (bottom) shown relative to the peak amplitude of the N1 potential (t = 0 s). The regression coefficient β0 is the intercept of the model, β1 indicates the effect of acceleration, β2 indicates the effect of distinct reactive postural responses, and β3 indicates the effect of the interaction between acceleration and distinct reactive postural responses. The vertical dashed line indicates the median perturbation onset latency (backward and forward: −175.8 ms) and the vertical dotted line indicates the median foot-off latency (backward: 202.6 ms; forward: 289.9 ms) Filled circles indicate significant coefficient values (p < .01, FDR corrected). The top 5% determination coefficients (per direction, across all time points) are indicated with a red edge (top row only). For comparison, the time-dependent determination coefficient for the opposite direction is overlaid with a gray thin line.

The strongest relation with spectral parameters (indicated by the highest determination coefficient) occurred at ~4 Hz and −20 ms for the backward direction (R^2 = .3079, $F(691)$ = 104, p = 1.61e^{-55}) and ~4 Hz and −10 ms for the forward direction (R^2 = .3895, $F(672)$ = 145, p = 2.83e^{-72}); with statistically significant effects of perturbation intensity (backward: p = 9.54e^{-15}; forward: p = 2.91e^{-33}), stepping behavior (backward: p = 7.49e^{-07}; forward: p = 3.09e^{-08}), and the interaction between them (backward: p = 5.70e^{-06}; forward: p = 7.74e^{-11}).

The spectral distribution of the determination coefficients at the best-fit time points (shown in figure 8), shows distinct peaks in the determination coefficients at ~11 Hz (forward) and ~15 Hz (backward). Although a direct comparison between the two directions was not pursued, it is clear that the distribution of their determination coefficients is different, with higher determination coefficients for the forward direction and slightly different peak frequencies (indicated by the regression coefficients) between directions. The effect of perturbation intensity was statistically significant for both directions from 2 to 21 Hz (backward: p < .00026; forward: p < .0039), but the effect of stepping behavior was statistically significant between 2–5 Hz and 9–15 Hz for the backward direction (p < .0012) and between 3–15 Hz for the forward direction (p < .0011). Furthermore, peak coefficients occurred at 3 and 15 Hz (backward), and 5 and 9 Hz (forward). The interaction between perturbation intensity and stepping behavior followed a similar pattern (backward: p < .0015; forward: p < .0018). Figure 9 shows the time course of the regression analyses for 4, 11, and 15 Hz. Overall, the time course of the adjusted determination coefficients shows statistically significant effects of perturbation intensity, stepping behavior, and their interaction slightly preceding the time of the N1 potential (t = 0 s).
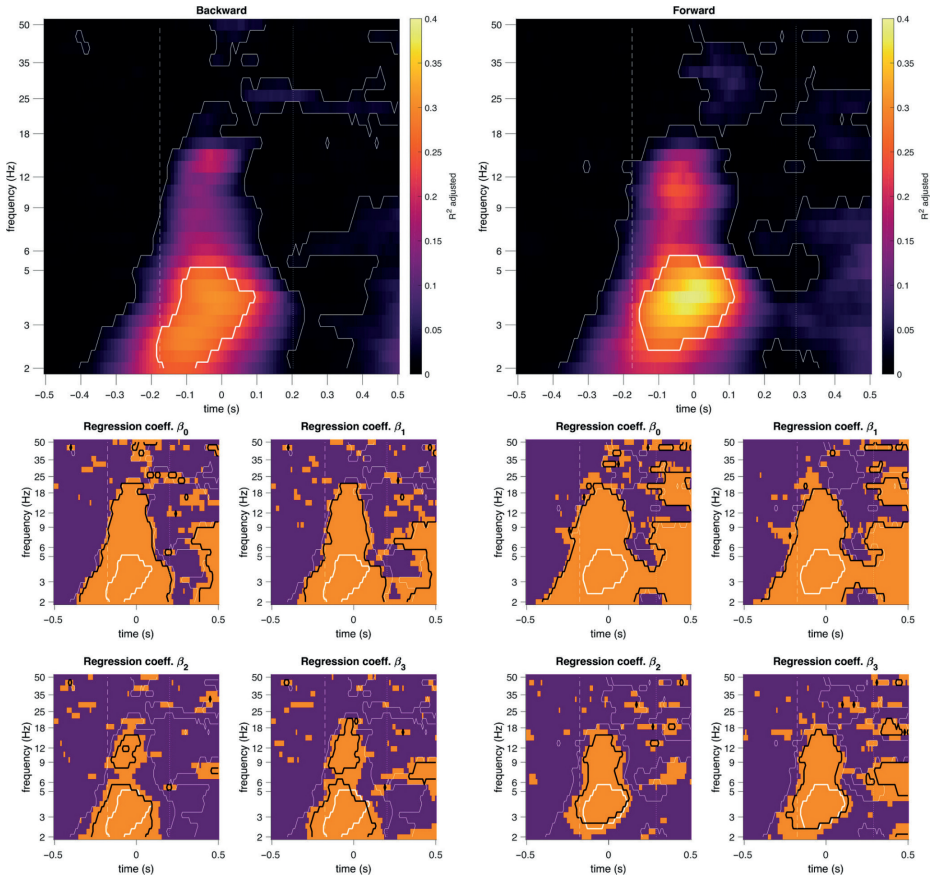
**Figure 7. Relation of perturbation intensity and stepping responses with time-frequency domain parameters.** Time-frequency maps of adjusted determination coefficients (top row) and regression coefficients (middle and bottom rows) shown relative to the peak amplitude of the N1 potential (t = 0 s). The regression coefficient β0 is the intercept of the model, β1 indicates the effect of acceleration, β2 indicates the effect of distinct reactive postural responses, and β3 indicates the effect of the interaction between acceleration and distinct reactive postural responses. The vertical dashed line indicates the median perturbation onset latency (backward and forward: −175.8 ms) and the vertical dotted line indicates the median foot-off latency (backward: 202.6 ms; forward: 289.9 ms). A thin white contour indicates statistically significant determination coefficients, whereas a thick white contour line highlights the top 5% determination coefficients. Time-frequency bins with non-zero regression coefficients (estimated from the 95% confidence intervals) are shown in orange. A thick black contour indicates statistically significant regression coefficients. All significance levels are p < .01, FDR corrected.
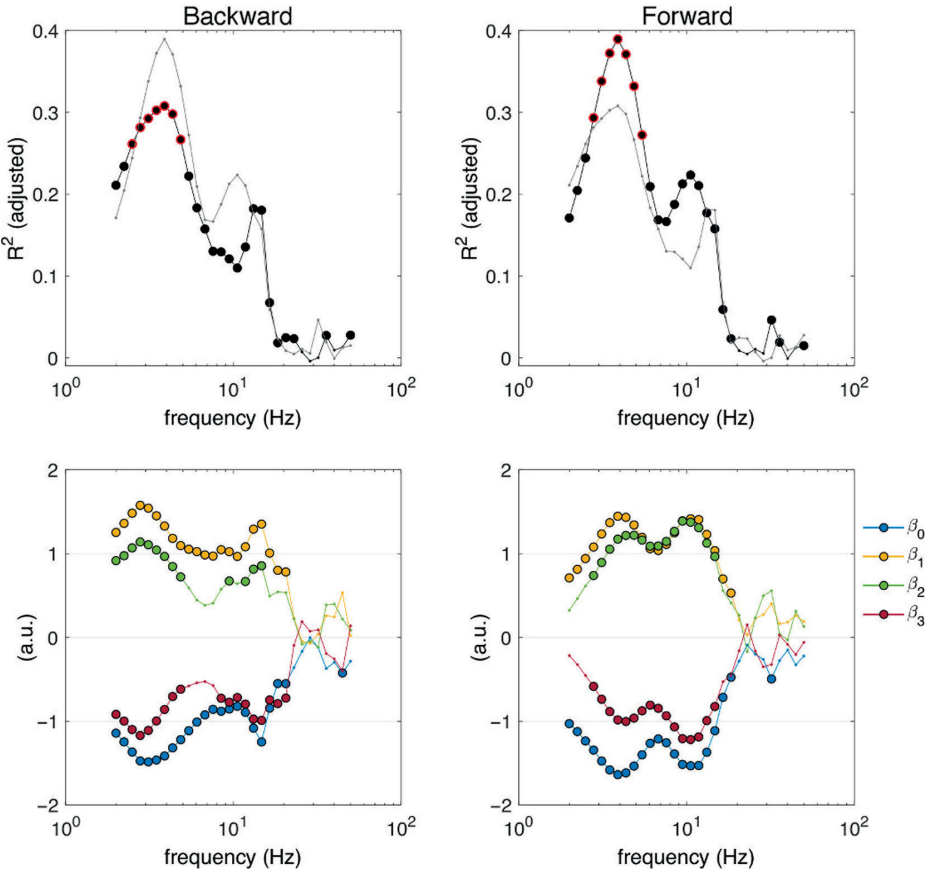
Figure 8. Spectral distribution of determination and regression coefficients. Frequency-dependent adjusted determination coefficient (top) and regression coefficients (bottom) for the time point with the highest determination coefficient (backward: −20 ms; forward: −10 ms). For comparison, the determination coefficient for the opposite direction is overlaid with a gray thin line. Filled circles indicate significant coefficient values (p < .01, FDR corrected). The top 5% determination coefficients across all time frequency bins per direction are indicated with a red edge (top row only). The regression coefficient β0 is the intercept of the model, β1 indicates the effect of acceleration, β2 indicates the effect of distinct reactive postural responses, and β3 indicates the effect of the interaction between acceleration and distinct reactive postural responses
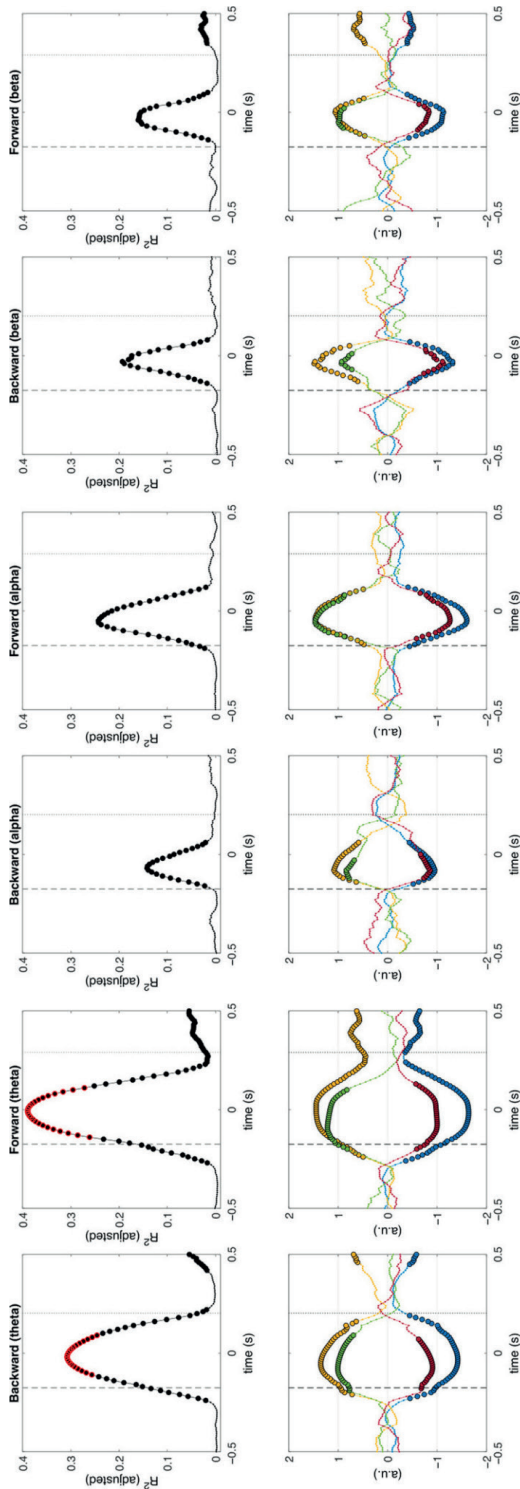
Figure 9. Temporal evolution of determination and regression coefficients for theta, alpha, and beta frequencies. Time-dependent adjusted determination coefficient (top row) and regression coefficients (bottom row) shown relative to the peak amplitude of the N1 potential (t = 0 s). The regression coefficient β0 is the intercept of the model, β1 indicates the effect of acceleration, β2 indicates the effect of distinct reactive postural responses, and β3 indicates the effect of the interaction between acceleration and distinct reactive postural responses. The vertical dashed line indicates the median perturbation onset latency (backward and forward: −175.8 ms) and the vertical dotted line indicates the median foot-off latency (backward: 202.6 ms; forward: 289.9 ms). Filled circles indicate significant coefficient values (p < .01, FDR corrected). The top 5% determination coefficients across all time-frequency bins per direction are indicated by a red edge (top row only).

2

Discussion

The key finding in our study is that the association between early cortical responses and the perturbation intensity differs according to the ensuing behavioral response to restore balance. This could not have been revealed in previous studies because differences in cortical responses between stepping and non-stepping behavior were confounded by the effects of perturbation intensity (i.e., different behavioral responses were elicited by different perturbation intensities). Our analyses show that the characteristics of the N1 potential (peak power and latency) and the power of the theta, alpha, and beta rhythms index the magnitude of an imposed deviation from postural stability and the execution of late-phase reactive postural responses, in both forward and backward perturbation directions. The peak power and latency of the N1 potential rapidly scales with increasing perturbation intensities that elicit feet-in-place responses (consistent with previous studies), but the scaling is attenuated when the perturbation intensities are high enough to elicit stepping responses. Additionally, our analyses show that the power of theta, alpha, and beta rhythms is similarly modulated, but that the theta rhythm has a stronger association with the interaction between perturbation intensity and the ensuing postural response than the alpha and beta rhythms. Our results indicate that scaling of cortical responses with perturbation intensity appears to be consistent with a behavioral model of stepping probability. Hence our study presents evidence that ties together the cortical responses to balance perturbations and balance recovery behavior.

Cortical balance control: Monitoring postural stability to predict balance recovery behavior

Our finding on the significant association of cortical responses with the interaction between perturbation intensity and the ensuing postural response (figures 5-8), provides new evidence of the possible cortical contributions to the decision-making process for selection of appropriate postural responses. The cerebral cortex may contribute to maintaining postural stability by monitoring deviations from a stable postural state and modulating or initiating appropriate balance corrective responses. Whole-body perturbations to standing balance elicit bouts of multisensory information (visual, vestibular, proprioceptive) that are proportional to the direction, magnitude, and rate of change in postural stability. This multisensory information is quickly integrated at subcortical levels of the central nervous system to produce very fast, yet highly coordinated, automatic postural responses (60–63). At the cortical level, multisensory information may be further processed to determine the need for late-phase responses and/or an update to the current motor plan (1–3). The need for late-phase balance recovery responses (e.g., stepping)

2

could be determined by comparing an ongoing change in postural stability against an internal reference of expected or acceptable deviation from a stable posture (60,63–65). This internal reference may be dynamically adapted (60) according to experience (e.g., predictability or habituation) and physical (e.g. biomechanical configuration, posture), environmental, and task constraints (e.g. postural threat or postural demand). Indeed, the perturbation-induced N1 potential has previously been suggested to represent the deviation from stable posture, as a form of error detection (12,13), as it scales with perturbation intensity and its corresponding destabilizing effect. Furthermore, the factors that could adapt the internal reference for acceptable deviations from postural stability are known to have an impact on the amplitude of the N1 potential (see Section 1). Our results provide further evidence that support the role of the N1 potential (and associated cortical rhythms) in monitoring postural stability as a deviation from a stable postural state.

Because the N1 potential and the accompanying modulations of theta, alpha, and beta rhythms, precede the actual stepping responses by hundreds of milliseconds, we suggest that these reflect cortical processes involved in monitoring postural stability to predict the need for stepping responses. Our regression models for behavioral (figure 2) and cortical responses (figure 5) show that as perturbation intensity and stepping probability increase, the peak power of the N1 potential increases and its latency shortens. The experimental data shows rapid changes in peak power and latency associated with low-intensity perturbations and near-zero stepping probability, which are followed by modest changes in peak power and latency associated with higher-intensity perturbations and higher stepping probability. We propose that the marked changes in peak power and latency associated with increasing perturbation intensity represent the neural computations that signal the growing need for stepping responses, which is more evident at low-intensity perturbations before the need for stepping responses becomes certain at high-intensity perturbations.

The mapping between cortical responses and stepping probabilities could be modulated by the experimental paradigm. The perceived growing need for stepping responses may be modulated by the uncertainty regarding perturbation onset, intensity, and direction, and the relatively high probability of high-intensity perturbations that require stepping responses. When uncertainty about postural demand or postural threat exists, the central nervous system is conservatively driven toward a default state in anticipation of high postural demand/threat (18). Thus, the experimental conditions and task instructions could set the relation between stepping probability and cortical responses. To further validate the role

of the cerebral cortex in the prediction of stepping responses it will be necessary to manipulate the internal reference for postural stability, perhaps by altering the distribution of perturbation intensities (e.g., including catch trials) or directly manipulating postural stability. Manipulating postural stability could be achieved, for instance, by controlled displacement of the center of mass relative to the base of support, prior to the onset of a balance perturbation.

Although our results show an association between cortical responses and the ensuing balance recovery behavior, further analyses are necessary to uncover any causal effect of cortical and postural responses (see Peterson and Ferris (2019) (66)). Future studies must pursue time-dependent analyses of (effective) cortico-muscular connectivity to better understand the top-down regulation of balance recovery responses.

Estimated cortical source and interpretation of the N1 potential

We estimated the cortical source of the N1 potential in the posterior midline frontal cortex (Table 3; Figure 4), near the SMA. Although the spatial resolution of our source localization analysis is limited by the use of standard electrode positions and head model, the estimated cortical source is consistent with previous studies on cortical involvement in balance control (20,26). The localization of the N1 potential to the SMA has been considered as an indication that the N1 potential may be related to sensorimotor processes (e.g., movement preparation and initiation) instead of mechanisms of cognitive control (8,9,20,26). However, different aspects of cognitive control are associated with error-related potentials ERN/ErrP and modulations of the theta rhythm from the SMA and other structures in the posterior midfrontal cortex. The SMA has been long implicated in action monitoring and adaptive behavior (29– 31,67). Error-related potentials and modulations of theta rhythm in or near the SMA signal the need for corrective actions (33,68). In our study, the presumed cortical source of the N1 potential provides further evidence for its involvement in cognitive control, for example, in action monitoring.

Different rhythms and distinct aspects of the control of balance and posture

Our results show that, in addition to the modulations in the midfrontal theta rhythm discussed above, the power of the alpha and beta rhythms was also related to perturbation intensity and balance recovery behavior (figures 7 and 8). Because different rhythms have been associated with distinct cognitive and sensorimotor functions (69), it is plausible that the theta, alpha, and beta rhythms represent distinct aspects of the cortical control of balance. The midfrontal theta rhythm is a known marker of cognitive control and action monitoring (34,35), whereas the

alpha and beta rhythms are classical sensorimotor rhythms with cortical sources over bilateral sensorimotor cortices (70). Since it has been shown that the SMA acts as a hub for information flow related to sensorimotor and cognitive processes elicited by external perturbations (66), it is possible that the alpha and beta rhythms observed in our analyses are related to communication between the SMA and the sensorimotor cortices. With respect to balance control, power modulations of alpha and beta rhythms have been reported near the bilateral M1/S1 and the midfrontal SMA during the preparation and execution of balance recovery responses with feet-in-place and stepping responses (7,8). Future studies should consider frequency-specific analyses to disentangle the functional role of individual cortical rhythms.

Relevance of perturbation direction
Although we did not formally evaluate the effect of perturbation direction on the cortical responses, it is worth mentioning that we found higher determination coefficients for perturbations that elicit postural sway in the forward direction (figures 6 and 8), and distinct spectral distributions of the determination and regression coefficients between perturbation directions (figure 8). Moreover, our behavioral analyses (figure 2; Table 1) showed differences in the proportions of stepping trials and mean stepping latencies of the two perturbation directions. These results suggest the existence of functional differences in the cortical responses to distinct perturbations that may be of interest for future studies.

Previous studies have found that the amplitude of the N1 potential is not modulated by the direction of the perturbation (11,17,19). However, reactive postural responses are direction-specific (71–73), and therefore, cortical processes involved in top-down control of balance and posture could carry direction-specific information. Future studies may focus on finding direction-specific modulations of the multiple cortical rhythms that accompany the N1 potential.

Limitations
In our experiment, we controlled the distribution of the balance perturbations to maintain the unpredictability of perturbation intensity and perturbation direction. The near-uniform distribution of the perturbation intensities led to different proportions of feet-in-place and stepping responses in the two stepping directions, with a slight bias toward stepping responses in the backward (63%) and forward (53%) stepping directions. It could be argued that the effect of stepping behavior is overestimated in the regression models for cortical responses. However, the visualization of the data (figure 5) suggests that the effect of stepping behavior is primarily driven by the responses to low-intensity perturbations and feet-in-

place responses. Moreover, the significantly different proportions of stepping trials comparing the backward and forward stepping directions led to qualitatively similar results, suggesting that an effect of sampling bias is negligible.

Conclusions

Our study expands the understanding of cortical contributions to balance control by demonstrating that the N1 potential, theta (~4 Hz), alpha (~11 Hz), and beta (~15 Hz) rhythms, arising from the midfrontal cortex, index the magnitude of a sudden deviation from postural stability during quiet stance and appear to be involved in the prediction of eventual stepping responses. The relation of the cortical responses to whole-body balance perturbations with the intensity of the perturbation (as a form of perceived error), and the ensuing reactive postural response (as necessary corrective actions), provide further evidence that cognitive control mechanisms (e.g., action monitoring) may regulate reactive postural adjustments for maintaining postural stability.

Acknowledgements

Conflict of interests

None

Author contributions

TSE, VW, MXC conceived and designed research; TSE performed experiments; TSE, MXC contributed analysis tools; TSE analyzed data; TSE, VW, MXC, MS interpreted results of experiments; TSE drafted manuscript; TSE, MS, VW, MXC edited and revised manuscript. All authors approved the final version of manuscript.

References

1. Bolton DAE. The role of the cerebral cortex in postural responses to externally induced perturbations. Neurosci Biobehav Rev. 2015 Oct;57:142–55.

2. Jacobs JV, Horak FB. Cortical control of postural responses. J Neural Transm. 2007 Mar 29;114(10):1339–48.

3. Maki BE, McIlroy WE. Cognitive demands and cortical control of human balance-recovery reactions. J Neural Transm. 2007 Jun 8;114(10):1279–96.

4. Jacobs JV. Why we need to better understand the cortical neurophysiology of impaired postural responses with age, disease, or injury. Front Integr Neurosci. 2014 Aug 29;8:69.

5. Nutt JG, Horak FB, Bloem BR. Milestones in gait, balance, and falling. Mov Disord. 2011 May;26(6):1166–74.

6. Takakusaki K. Functional neuroanatomy for posture and gait control. J Mov Disord. 2017 Jan 18;10(1):1–17.

7. Peterson SM, Ferris DP. Differentiation in Theta and Beta Electrocortical Activity between Visual and Physical Perturbations to Walking and Standing Balance. eNeuro. 2018 Aug 13;5(4).

8. Solis-Escalante T, van der Cruijsen J, de Kam D, van Kordelaar J, Weerdesteyn V, Schouten AC. Cortical dynamics during preparation and execution of reactive balance responses with distinct postural demands. Neuroimage. 2019 Mar;188:557–71.

9. Varghese JP, McIlroy RE, Barnett-Cowan M. Perturbation-evoked potentials: Significance and application in balance control research. Neurosci Biobehav Rev. 2017 Dec;83:267–80.

10. Dietz V, Quintern J, Berger W, Schenck E. Cerebral potentials and leg muscle e.m.g. responses associated with stance perturbation. Exp Brain Res. 1985;57(2):348–54.

11. Dietz V, Quintern J, Berger W. Afferent control of human stance and gait: evidence for blocking of group I afferents during gait. Exp Brain Res. 1985;61(1):153–63.

12. Adkin AL, Quant S, Maki BE, McIlroy WE. Cortical responses associated with predictable and unpredictable compensatory balance reactions. Exp Brain Res. 2006 Jun;172(1):85–93.

13. Payne AM, Ting LH, Hajcak G. Do sensorimotor perturbations to standing balance elicit an error-related negativity? Psychophysiology. 2019 Jul;56(7):e13359.

14. Staines WR, McIlroy WE, Brooke JD. Cortical representation of whole-body movement is modulated by proprioceptive discharge in humans. Exp Brain Res. 2001 May;138(2):235–42.

15. Dietz V, Quintern J, Berger W. Cerebral evoked potentials associated with the compensatory reactions following stance and gait perturbation. Neurosci Lett. 1984 Sep 7;50(1–3):181–6.

16. Dietz V, Horstmann GA, Berger W. Perturbations of human posture: influence of impulse modality on EMG responses and cerebral evoked potentials. J Mot Behav. 1989 Dec;21(4):357–72.

17. Goel R, Ozdemir RA, Nakagome S, Contreras-Vidal JL, Paloski WH, Parikh PJ. Effects of speed and direction of perturbation on electroencephalographic and balance responses. Exp Brain Res. 2018 Jul;236(7):2073–83.

18.   Mochizuki G, Boe S, Marlin A, McIlRoy WE. Perturbation-evoked cortical activity reflects both the context and consequence of postural instability. Neuroscience. 2010 Oct 13;170(2):599–609.

19.   Payne AM, Hajcak G, Ting LH. Dissociation of muscle and cortical response scaling to balance perturbation acceleration. J Neurophysiol. 2019 Mar 1;121(3):867–80.

20.   Mierau A, Hülsdünker T, Strüder HK. Changes in cortical activity associated with adaptive behavior during repeated balance perturbation of unpredictable timing. Front Behav Neurosci. 2015 Oct 14;9:272.

21.   Adkin AL, Campbell AD, Chua R, Carpenter MG. The influence of postural threat on the cortical response to unpredictable and predictable postural perturbations. Neurosci Lett. 2008 Apr 18;435(2):120–5.

22.   Mochizuki G, Sibley KM, Esposito JG, Camilleri JM, McIlroy WE. Cortical responses associated with the preparation and reaction to full-body perturbations to upright stability. Clin Neurophysiol. 2008 Jul;119(7):1626–37.

23.   Mochizuki G, Sibley KM, Cheung HJ, McIlroy WE. Cortical activity prior to predictable postural instability: is there a difference between self-initiated and externally-initiated perturbations? Brain Res. 2009 Jul 7;1279:29–36.

24.   Little CE, Woollacott M. EEG measures reveal dual-task interference in postural performance in young adults. Exp Brain Res. 2015 Jan;233(1):27–37.

25.   Quant S, Adkin AL, Staines WR, Maki BE, McIlroy WE. The effect of a concurrent cognitive task on cortical potentials evoked by unpredictable balance perturbations. BMC Neurosci. 2004 May 17;5:18.

26.   Marlin A, Mochizuki G, Staines WR, McIlroy WE. Localizing evoked cortical activity associated with balance reactions: does the anterior cingulate play a role? J Neurophysiol. 2014 Jun 15;111(12):2634–43.

27.   Chavarriaga R, Sobolewski A, Millán JDR. Errare machinale est: the use of error-related potentials in brain-machine interfaces. Front Neurosci. 2014 Jul 22;8:208.

28.   Crowley MJ. Error-related negativity. Encyclopedia of autism spectrum disorders. 2013;1159–60.

29.   Bonini F, Burle B, Liégeois-Chauvel C, Régis J, Chauvel P, Vidal F. Action monitoring and medial frontal cortex: leading role of supplementary motor area. Science. 2014 Feb 21;343(6173):888–91.

30.   Luu P, Flaisch T, Tucker DM. Medial frontal cortex in action monitoring. J Neurosci. 2000 Jan 1;20(1):464–9.

31.   Ridderinkhof KR, Ullsperger M, Crone EA, Nieuwenhuis S. The role of the medial frontal cortex in cognitive control. Science. 2004 Oct 15;306(5695):443–7.

32.   Debener S, Ullsperger M, Siegel M, Fiehler K, von Cramon DY, Engel AK. Trial-by-trial coupling of concurrent electroencephalogram and functional magnetic resonance imaging identifies the dynamics of performance monitoring. J Neurosci. 2005 Dec 14;25(50):11730–7.

33.   Pereira M, Sobolewski A, Millán JDR. Action monitoring cortical activity coupled to submovements. eNeuro. 2017 Oct 24;4(5).

34.   Cavanagh JF, Frank MJ. Frontal theta as a mechanism for cognitive control. Trends Cogn Sci (Regul Ed). 2014 Aug;18(8):414–21.

35. Cohen MX, Donner TH. Midfrontal conflict-related theta-band power reflects neural oscillations that predict behavior. J Neurophysiol. 2013 Dec;110(12):2752–63.

36. Luu P, Tucker DM, Makeig S. Frontal midline theta and the error-related negativity: neurophysiological mechanisms of action regulation. Clin Neurophysiol. 2004 Aug;115(8):1821–35.

37. Trujillo LT, Allen JJB. Theta EEG dynamics of the error-related negativity. Clin Neurophysiol. 2007 Mar;118(3):645–68.

38. Yeung N, Bogacz R, Holroyd CB, Nieuwenhuis S, Cohen JD. Theta phase resetting and the error-related negativity. Psychophysiology. 2007 Jan;44(1):39–49.

39. Omana Moreno H. The Influence of Dual-tasking on Cortical Responses Associated with Instability. 2017 Oct 12;

40. Slobounov S, Cao C, Jaiswal N, Newell KM. Neural basis of postural instability identified by VTC and EEG. Exp Brain Res. 2009 Oct;199(1):1–16.

41. Hülsdünker T, Mierau A, Neeb C, Kleinöder H, Strüder HK. Cortical processes associated with continuous balance control as revealed by EEG spectral power. Neurosci Lett. 2015 Apr 10;592:1–5.

42. Mierau A, Pester B, Hülsdünker T, Schiecke K, Strüder HK, Witte H. Cortical correlates of human balance control. Brain Topogr. 2017 Jul;30(4):434-46.

43. Varghese JP, Marlin A, Beyer KB, Staines WR, Mochizuki G, McIlroy WE. Frequency characteristics of cortical activity associated with perturbations to upright stability. Neurosci Lett. 2014 Aug 22;578:33–8.

44. Nonnekes J, de Kam D, Geurts ACH, Weerdesteyn V, Bloem BR. Unraveling the mechanisms underlying postural instability in Parkinson's disease using dynamic posturography. Expert Rev Neurother. 2013 Dec;13(12):1303–8.

45. Oostenveld R, Praamstra P. The five percent electrode system for high-resolution EEG and ERP measurements. Clin Neurophysiol. 2001 Apr;112(4):713–9.

46. Delorme A, Makeig S. EEGLAB: an open source toolbox for analysis of single-trial EEG dynamics including independent component analysis. J Neurosci Methods. 2004 Mar 15;134(1):9–21.

47. Gramann K, Ferris DP, Gwin J, Makeig S. Imaging natural cognition in action. Int J Psychophysiol. 2014 Jan;91(1):22–9.

48. Makeig S, Gramann K, Jung T-P, Sejnowski TJ, Poizner H. Linking brain, mind and behavior. Int J Psychophysiol. 2009 Aug;73(2):95–100.

49. Gwin JT, Gramann K, Makeig S, Ferris DP. Removal of movement artifact from high-density EEG recorded during walking and running. J Neurophysiol. 2010 Jun;103(6):3526–34.

50. Kline JE, Huang HJ, Snyder KL, Ferris DP. Isolating gait-related movement artifacts in electroencephalography during human walking. J Neural Eng. 2015 Aug;12(4):046022.

51. Oliveira AS, Schlink BR, Hairston WD, König P, Ferris DP. Induction and separation of motion artifacts in EEG data using a mobile phantom head device. J Neural Eng. 2016 Jun;13(3):036014.

52. Snyder KL, Kline JE, Huang HJ, Ferris DP. Independent Component Analysis of Gait-Related Movement Artifact Recorded using EEG Electrodes during Treadmill Walking. Front Hum Neurosci. 2015 Dec 1;9:639.

53. Gwin JT, Gramann K, Makeig S, Ferris DP. Electrocortical activity is coupled to gait cycle phase during treadmill walking. Neuroimage. 2011 Jan 15;54(2):1289–96.

54. Sipp AR, Gwin JT, Makeig S, Ferris DP. Loss of balance during balance beam walking elicits a multifocal theta band electrocortical response. J Neurophysiol. 2013 Nov;110(9):2050–60.

55. Artoni F, Delorme A, Makeig S. Applying dimension reduction to EEG data by Principal Component Analysis reduces the quality of its subsequent Independent Component decomposition. Neuroimage. 2018 Jul 15;175:176–87.

56. Oostenveld R, Oostendorp TF. Validating the boundary element method for forward and inverse EEG computations in the presence of a hole in the skull. Hum Brain Mapp. 2002 Nov;17(3):179–92.

57. Lacadie CM, Fulbright RK, Rajeevan N, Constable RT, Papademetris X. More accurate Talairach coordinates for neuroimaging using non-linear registration. Neuroimage. 2008 Aug 15;42(2):717–25.

58. Cohen MX. A better way to define and describe Morlet wavelets for time-frequency analysis. Neuroimage. 2019 Oct 1;199:81–6.

59. Benjamini Y, Yekutieli D. The control of the false discovery rate in multiple testing under dependency. Ann Statist. 2001 Aug;29(4):1165–88.

60. Lockhart DB, Ting LH. Optimal sensorimotor transformations for balance. Nat Neurosci. 2007 Oct;10(10):1329–36.

61. Welch TDJ, Ting LH. A feedback model reproduces muscle activity during human postural responses to support-surface translations. J Neurophysiol. 2008 Feb;99(2):1032–8.

62. Welch TDJ, Ting LH. A feedback model explains the differential scaling of human postural responses to perturbation acceleration and velocity. J Neurophysiol. 2009 Jun;101(6):3294–309.

63. Welch TDJ, Ting LH. Mechanisms of motor adaptation in reactive balance control. PLoS ONE. 2014 May 8;9(5):e96440.

64. Scott SH. The computational and neural basis of voluntary motor control and planning. Trends Cogn Sci (Regul Ed). 2012 Nov;16(11):541–9.

65. Safavynia SA, Ting LH. Long-latency muscle activity reflects continuous, delayed sensorimotor feedback of task-level and not joint-level error. J Neurophysiol. 2013 Sep;110(6):1278–90.

66. Peterson SM, Ferris DP. Group-level cortical and muscular connectivity during perturbations to walking and standing balance. Neuroimage. 2019 Sep;198:93–103.

67. Cohen MX. A neural microcircuit for cognitive conflict detection and signaling. Trends Neurosci. 2014 Sep;37(9):480–90.

68. Töllner T, Wang Y, Makeig S, Müller HJ, Jung T-P, Gramann K. Two Independent Frontal Midline Theta Oscillations during Conflict Detection and Adaptation in a Simon-Type Manual Reaching Task. J Neurosci. 2017 Mar 1;37(9):2504–15.

69. Buzsáki G. Rhythms of the Brain. Oxford University Press; 2006.

70. Pfurtscheller G, Lopes da Silva FH. Event-related EEG/MEG synchronization and desynchronization: basic principles. Clin Neurophysiol. 1999 Nov;110(11):1842–57.

71. Chvatal SA, Torres-Oviedo G, Safavynia SA, Ting LH. Common muscle synergies for control of center of mass and force in nonstepping and stepping postural behaviors. J Neurophysiol. 2011 Aug;106(2):999–1015.

72. Torres-Oviedo G, Ting LH. Muscle synergies characterizing human postural responses. J Neurophysiol. 2007 Oct;98(4):2144–56.

73. de Kam D, Geurts AC, Weerdesteyn V, Torres-Oviedo G. Direction-Specific Instability Poststroke Is Associated With Deficient Motor Modules for Balance Control. Neurorehabil Neural Repair. 2018 Jun 29;32(6–7):655–66.

2
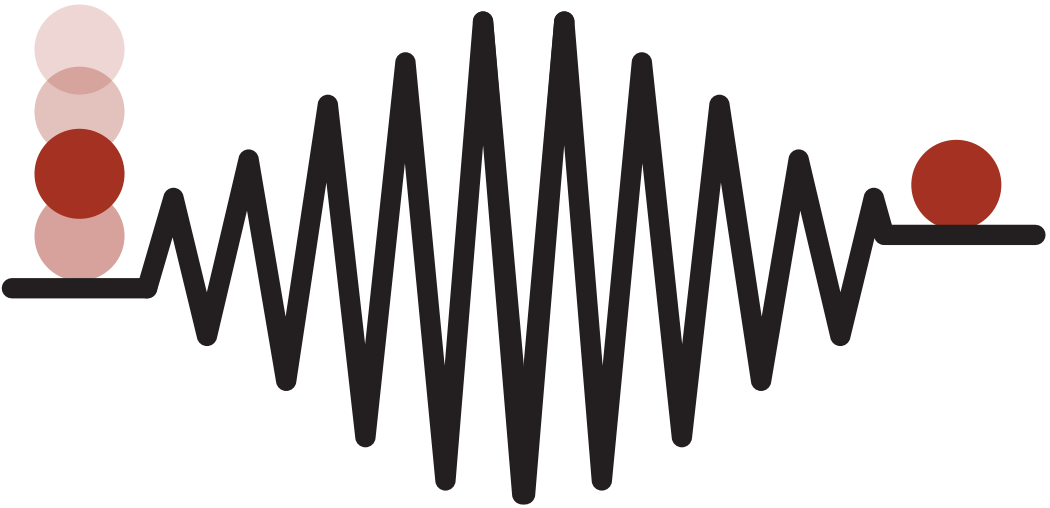
Midfrontal theta dynamics index the monitoring of postural stability

Abstract

Stepping is a common strategy to recover postural stability and maintain upright balance. Postural perturbations have been linked to neuroelectrical markers such as the N1 potential and theta frequency dynamics. Here, we investigated the role of cortical midfrontal theta dynamics of balance monitoring, driven by balance perturbations at different initial standing postures. We recorded electroencephalography, electromyography, and motion tracking of human participants while they stood on a platform that delivered a range of forward and backward whole-body balance perturbations. The participants' postural threat was manipulated prior to the balance perturbation by instructing them to lean forward or backward while keeping their feet-in-place in response to the perturbation. We hypothesized that midfrontal theta dynamics index the engagement of a behavioral monitoring system and, therefore, that perturbation-induced theta power would be modulated by the initial leaning posture and perturbation intensity. Targeted spatial filtering in combination with mixed-effects modeling confirmed our hypothesis and revealed distinct modulations of theta power according to postural threat. Our results provide novel evidence that midfrontal theta dynamics subserve action monitoring of human postural balance. Understanding of cortical mechanisms of balance control is crucial for studying balance impairments related to aging and neurological conditions (e.g. stroke).

Introduction

Maintaining balance is crucial for humans, and indeed, falling due to reduced balance ability is a serious health risk for the elderly and individuals with movement disorders such as Parkinson's disease. Postural stability is challenged with every intentional movement and by unpredicted changes in our surroundings. The central nervous system has a remarkable ability to monitor balance and sudden postural changes and rapidly engage corrective postural responses (1–3).

The traditional view was that balance is mainly regulated by subcortical brain regions (4,5). However, it has become increasingly clear that the cerebral cortex also contributes to postural control (1,6–8). The cortex may contribute by monitoring deviations from a desired stable posture, related to an internal model of postural stability (9), and by initiating corrections, for example through regulation of subcortical excitability of the automatic postural response or through direct corrective responses at later-phase response latency (3).

Balance studies with electroencephalography (EEG) recordings identified 2 key electrophysiological signatures of cortical involvement in balance control. The N1 potential is a robust negative event-related potential occurring at ~150 ms following a balance perturbation and is presumably related to sensory integration and cognitive processes (10–12). Time–frequency analysis shows a strong increase over multiple frequency bands, of which the theta frequency band (3–8 Hz) dominates, suggesting a strong relationship between the N1 potential and the underlying theta dynamics (13–16). The event-related nature and scaling of N1/theta with perturbation intensity suggest involvement in sensory processing (1–3). However, these indices are not simply sensory markers: the N1 is modulated by anticipated perturbations (17), and both N1 and theta modulate according to ensuing recovery behavior, with theta power better describing the variance within the data compared to the N1 amplitude (18). The latter is of particular interest, as it hints at midfrontal theta dynamics playing a role in balance monitoring and predicting the need for a corrective step. Yet, the intimate relationship between both strong perturbation accelerations and stepping behavior obscures the interpretation of theta involvement in balance monitoring, because stronger perturbations are more likely to elicit step responses which does not directly imply the monitoring of balance.

While monitoring balance and predicting the need for corrective responses, the CNS may use an internal representation of the postural changes and body dynamics. The predictive coding theorem is proposed to be involved in the monitoring of upright

3

stance (19), by comparing external sensory postural information with expected sensory information stored in an internal model of stability (9,20). A mismatch between these 2 results in a prediction error of the sensory information stored in the internal model. It has been suggested that the transient increase of theta power is representative of the prediction error and, therefore, indicates the deviation of current and expected posture.

Here, we manipulated the relationship between acceleration and stepping behavior by altering the initial standing posture, which changes the distance between the center of mass (CoM) and the boundaries of the base of support prior to perturbations. Therefore, perturbations with identical intensities would differently impact postural stability depending on the direction of perturbation and the initial posture. If midfrontal theta indeed subserves an action monitoring role of postural balance, different initial leaning postures should modulate midfrontal theta dynamics. In the event of a balance perturbation, the internal processes of action monitoring must identify the impact of the perturbation in accordance with the internal model of postural stability and initiate an appropriate corrective response. When manipulating the initial postural state, the internal model of stability may be updated to correctly represent the current postural state and evaluate the threat imposed by a given perturbation. The evaluation of the perturbation's impact on stability may then be reflected in the midfrontal theta dynamics.

Our goal was to investigate the participation of midfrontal theta dynamics in a behavioral monitoring system for reactive balance responses. Based on previous findings implicating midfrontal theta in action monitoring, we hypothesized that midfrontal theta reflects the phasic activation of a cortical system that monitors balance and signals threats to postural stability (i.e. we expect that theta dynamics are stronger when the leaning direction and perturbation direction are congruent). To test this hypothesis, we recorded EEG and motion tracking data while participants were instructed to try to maintain their balance with feet-in-place responses following sudden movements of the support surface. Furthermore, we instructed participants to lean forward or backward to manipulate their initial stability state and, thereby, manipulate the impact of a given perturbation on postural stability.

Materials and Methods

Participants

Twenty young healthy adults (10 female; age mean 23.9 years, SD 3.6 years) participated in this study. All participants received ample information about the experiment. In addition, all participants were naïve participants and did not have previous experience on the platform. Afterwards, the participants voluntarily signed an informed consent form and were financially compensated after completion of the study. None of the participants had previous history of neuromuscular disease or any other impairment that could affect their performance in the experiment. The experimental procedure was approved by the Research Ethics Committee of the Radboud University Medical Center (Nijmegen, The Netherlands; Dossier 2018-4970). The experiments were conducted in line with the Declaration of Helsinki.

Experimental paradigm

Participants were familiarized with the experimental procedure through a series of 28 forward and backward perturbations with increasing acceleration, as delivered by the Radboud Falls Simulator (18,21,22). Participants stood barefoot on the movable platform with their feet at shoulder width and the arms crossed in front of the body. They were instructed to do their best to keep the feet-in-place in response to a balance perturbation. Platform perturbation profiles consisted of 300 ms platform acceleration, 500 ms constant velocity, and 300 ms deceleration (Fig. 1B). Platform accelerations were randomized and ranged from 0.25 to 1.9 m/s2 with a higher resolution at lower accelerations in both forward and backward perturbation directions (0.25, 0.4, 0.7, 1.0, 1.3, 1.6, 1.9 m/s2). This distribution was chosen, because we expected theta modulations to be more pronounced during the feet-in-place responses at lower platform accelerations, as illustrated in our previous study (18). In addition, this distribution allowed us to also record a fair number of feet-in-place responses in the conditions with congruent leaning and perturbation directions (i.e. those with a greater necessity for stepping responses). Forward translation of the platform elicited postural sway and an eventual step in the backward direction; similarly, backward translation of the platform elicited postural sway and an eventual step in the forward direction. Henceforth, we refer to the movement of the body with respect to the feet, meaning that in the forward perturbation direction, the body moved in the forward direction and backward perturbations moved the body in the backward direction. Prior to a sequence, participants were instructed to maintain a leaning posture throughout the whole sequence. In total, participants underwent 5 sequences of each 3 leaning conditions. Leaning conditions were altered from neutral stance to forward leaning and then backward leaning followed again by

neutral stance to prevent fatigue due to the leaning posture. The experiment consisted of 15 sequences containing 29 balance perturbations each (435 total). The first perturbation of a sequence always consisted of a low-intensity dummy trial and was not included in the analyses, resulting in 420 trials for analysis per participant.

To control the initial posture, participants received feedback with respect to their leaning angle, which was computed as the angle between reflective markers located at the left and right ankle and the seventh cervical vertebra. Neutral stance was assigned to a 90° angle, whereas forward leaning was set to 85° and backward leaning to 95° of lean. Participants were instructed to maintain a straight posture, preventing any flexion at the knee or hip while maintaining the leaning position. Prior to each perturbation, participants received real-time visual feedback of their leaning angle, which was presented on a projection screen in front of the participants for a fixed 2 s (figure 1A). The feedback was replaced with a fixation cross 1–3 s prior to the perturbation onset and remained on the screen throughout the trial. Real-time data stream allowed the experimenter to control participants' posture and performance, such as maintaining leaning angle, excessive knee flexion, and changes in leg weight bearing (which may indicate the use of specific strategies to counteract balance perturbations).

To prevent fatigue, participants took a small break of 5 min after 3 consecutive sequences and were seated on a chair. After 9 sequences, participants were given a 20-min lunch break. The active experiment time was 2.5 h and the preparation time was 2.5 h, the complete lab visit lasted a maximum of 6 h (including resting breaks).

Data Acquisition

We recorded high-density EEG using a cap with 126 Ag-AgCl electrodes (WaveGuard, ANT Neuro, The Netherlands). The electrodes were fixed in the cap and distributed across the scalp according to the 5% electrode system (23). The EEG was referenced to the common average during acquisition. The ground electrode was placed on the left mastoid. A biosignal amplifier (REFA System, TMSi, The Netherlands) recorded the EEG at 2,048 Hz without any filters, except for a hardware low-pass filter at 552 Hz. To monitor physiological activity that could present artifacts in the EEG, we also recorded electrical activity of the left eye in the vertical and horizontal directions (electrooculogram, EOG) using adhesive Ag-AgCl electrodes. The EOG was recorded from electrodes placed slightly under the left eye (vertical eye movement) and at the outer canthus of the left eye (horizontal eye movement).
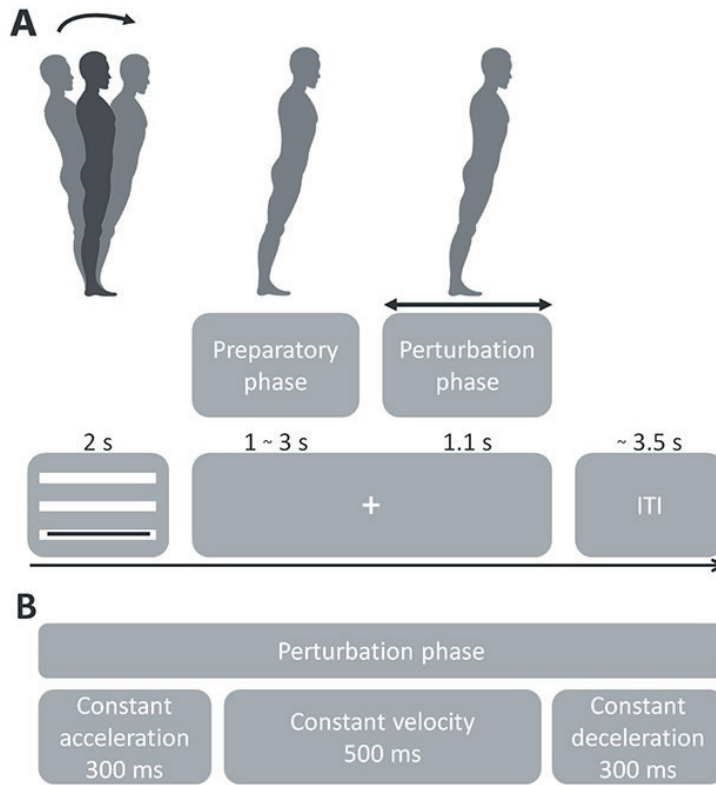
Figure 1. Experimental procedure. A) Participants were instructed to maintain 1 out of 3 postures during a sequence of perturbations. Perturbations were randomized in onset time, direction, and acceleration. The initial posture prior to perturbation was fixed per sequence. A trial consisted of a visual cue indicating the continuous leaning angle for 2 s, followed by a fixation cross. Platform onset was randomized from 1 to 3 s and the perturbation lasted for 1.1 s. After a perturbation, the platform slowly returned to the initial position in ~3.5 s. At platform return, the visual feedback of initial leaning angle was presented. Visual feedback for leaning posture was presented through 3 white bars representing forward leaning (bottom bar), neutral stance (middle bar), and backward leaning (top bar). A black bar presented in front of the white bars represented the participant's real-time leaning angle. Participants were instructed to keep the black bar on the white bar corresponding to the instructed leaning direction. The fixation cross was presented at the same height as the leaning bar for that sequence to guide the participant. Initial leaning posture had to be maintained throughout the fixation cross period, ensuring that postural stability was controlled at platform perturbation. B) Platform perturbation profiles.

Body movements were recorded using an 8-camera 3D motion analysis system (Vicon Motion Systems, United Kingdom) at a sample rate of 100 Hz. For this purpose, a total of 23 reflective markers (PlugInGait Full-body AI model excluding the head and arm markers; Vicon Nexus software 2.7.1) were attached to anatomical landmarks on the participants' body.

Ground reaction forces were recorded from 2 force plates (AMTI Custom 6 axis composite force platform, USA; size: 60 × 180 cm each; sampling rate: 2,000 Hz) embedded in the moveable platform. Trials were recorded from −2 to +5 s relative to the platform perturbation. Synchronization triggers were generated by the platform controller and recorded for post hoc alignment of motion data via Vicon, and EEG signals via the EEG acquisition computer.

Kinematic and behavioral data processing

Force plate data were used to identify the moment of foot-off (step onset) during a trial. The threshold for foot-off identification was set at a participant-specific level of 80% unloading of the weight borne on one leg. Steps occurring before 1.1 s post perturbation onset (i.e. termination of platform movement) were included in the analysis as stepping trials. A total of 194 trials (2.4% of total) with steps occurring outside this temporal window were excluded from further analysis.

Kinematic data were preprocessed using Vicon Nexus software (Vicon Motion Systems, UK, version 2.7.1). Markers were labeled and reconstructed in a batch preprocessing pipeline. Occluded markers on the hip or trunk segment were gap filled with a rigid body fill algorithm when at least 3 other markers of the body segment were visible. Other missing markers were gap filled using the Vicon Woltring filter, but only if they did not overlap platform perturbation onset (±0.5 s) and lasted a maximum of 50 frames. Marker data were imported to MATLAB and 10 Hz low-pass filtered (fifth order Butterworth IIR filters, zero-phase shift). Relative marker movement was computed by subtracting the platform marker movement from each individual body marker and imported to the EEG dataset.

Data analysis: stepping probability

The stepping probability quantifies the distribution of feet-in-place and stepping responses across platform acceleration. The responses were coded as feet-in-place (0) and stepping (1) responses and the probability of a stepping response is expressed in the ratio of step responses and the total number trials recorded at that specific acceleration and leaning condition. A stepping probability of zero indicated that stepping responses did not occur, whereas a probability of 1 indicated that steps occurred in all trials.

Data analysis: margin of stability

The margin of stability (MoS) (24,25) is a kinematic measure that reflects dynamic stability, by taking into account both the position and the velocity of the horizontal CoM projection relative to the boundary of the support base (BoS). We obtained

3

the CoM from the Vicon processed data and the BoS was determined by averaging the anterior posterior position of the toes in the forward perturbation direction and the heels in the backward perturbation direction. A low MoS indicates a less stable postural state as the CoM may be approaching the BoS. A MoS value of zero means there is no more room for the CoM to move before extending beyond the BoS and a negative value of MoS indicates that the CoM has traveled beyond the BoS. We calculated the MoS at 300 ms post perturbation onset, where the platform acceleration transitioned in a constant velocity. We used a fixed single-trial value for the BoS averaged over −2 to −1 s prior to perturbation, since we were only interested in dynamics prior to foot off. The MoS allowed us to verify whether the leaning conditions in combination with platform accelerations indeed posed different postural threats. The MoS was calculated according to (24).

EEG processing

EEG and EOG data were preprocessed in MATLAB using functions of the EEGLAB toolbox (26). Data were bandpass filtered (2–200 Hz, consecutive high-pass and low-pass fifth-order Butterworth IIR filters, zero-phase shift) using the filtfilt.m matlab function and averaged referenced. Continuous data were cut into epochs of 5 s (−2 to +3 s relative to perturbation onset) and concatenated per participant for further processing. Channels were flagged for rejection based on a kurtosis >3 and a variance >3 and rejected based on visual inspection (mean 5.5, SD 6.3 rejected channels). Additionally, epochs were rejected through visual inspection for noise. An independent component analysis (Infomax ICA) with a minimum of 90 and maximum of 126 principal components (depending on the rank of the EEG data) was run and independent components were rejected based on being excessively noisy and of non-brain origin (mean 91 rejected components, SD 16 rejected components). Artifact-reduced EEG was obtained by back projection of the retained independent components.

Generalized eigendecomposition

We applied a generalized eigendecomposition (GED), a multivariate source-separation method, on the clean EEG data in order to derive a spatial filter that is optimized for theta (3–8 Hz) activity (27). Computation of the GED on fewer components resulting from ICA cleaning does not reduce the rank of the GED as GED is defined for any rank matrix (28). Two covariance matrices are constructed corresponding to theta-filtered data (matrix S) and broadband data (matrix R) (Equation 1). The GED on these 2 matrices returns a set of eigenvectors (in matrix W) and corresponding eigenvalues (in matrix Λ), and the eigenvector associated with the largest eigenvalue is a set of channel weights that maximizes the relative energy in the theta band.

$$SW = RWΛ \tag{1}$$

This generalized eigenvalue equation solves the Rayleigh quotient and is often used in machine learning and brain-computer-interface research (29–31).

The eigenvector with the 1) greatest eigenvalue, 2) ERP average and 3) midline/midfrontal scalp topography was selected per participant for further analysis of the EEG data. The component time series was computed as $w^T X$, where X is the channel time series data, and the spatial map was computed as $w^T S$ (30).

Time-frequency analysis

The neural time series data after GED analysis were further characterized through time–frequency decomposition. This was implemented by narrow-band filtering the time series at a range of frequencies through trial-by-trial convolution with complex Morlet wavelets. Equations (2) and (3) show the construction of the complex Morlet wavelets.

$$\Psi_f = e^{i2\pi f t} e^{-\frac{t^2}{2s^2}} \tag{2}$$

$$s = \frac{n}{2\pi f} \tag{3}$$

Where t represents time, f is frequency, s is width of the Gaussian modulating the complex sine wave and n stands for the number of wavelet cycles. The number of cycles per wavelet controls the temporal and spectral precision tradeoff. We used 40 frequencies logarithmically spaced between 2 and 60 Hz. Wavelet widths were logarithmically spaced from 4 to 12 cycles.

For the visualization of average time–frequency data, we baseline corrected the data with a baseline window of 1 to −0.2 s prior to perturbation onset.

Single-trial EEG theta power calculations

Preprocessed single-trial EEG time series data were filtered in the 3–8 Hz range, (consecutive high-pass and low-pass fifth-order Butterworth IIR filters, zero-phase shift) and theta power was computed as the magnitude of the Hilbert transform. Applying the Hilbert transform to the data was done over the whole trial timeseries of 4 s, making sure that the timeseries was large enough to compare theta power over a whole wave cycle. Temporal single trial averaging over 0.1–0.3 s post perturbation was done after using the Hilbert transform in the theta band filtered data. This means that when averaging over a smaller time window, this accurately represents the theta power at that time, even though the theta oscillations may be related to

a longer lasting event. Trials with step responses occurring in the 0.1–0.3 s epoch were rejected to reduce potential step-related EEG interference. We did not subtract single-trial baseline power due to single-trial instability. Instead, single-trial theta power was normalized by computing the *z*-score over all trials per participant before statistical analysis. To verify that only theta dynamics scale with balance monitoring behavior, we similarly treated and analyzed the data in the alpha (9–12 Hz) and beta (15–25 Hz) frequency range.

Statistical analysis

Data quality check (EEG)
To determine whether EEG data quality was comparable for all leaning conditions, we computed single-trial variance and determined any effects of leaning conditions using a one-way ANOVA.

Leaning condition-specific average theta baseline power
Time–frequency average theta baseline dynamics were tested for an effect of leaning with a one-way ANOVA to indicate whether leaning conditions had an effect on theta dynamics prior to perturbation.

Theta dynamics (EEG)
EEG data were analyzed separately for forward and backward directions with 2 generalized linear mixed-effects models (GLME) with factors Acceleration, Stepping behavior, and Leaning condition. For the categorical factor Stepping behavior, the feet-in-place responses were dummy coded as zero, whereas the categorical factor Leaning condition was dummy coded per perturbation direction according to the most stable condition, i.e. the condition associated with a greater proportion of feet-in-place responses. Therefore, backward leaning feet-in-place responses were considered the most stable condition in the forward perturbation direction model and forward leaning feet-in-place responses in the backward perturbation direction model.

The GLME models are described by:

$$Y_{ij} = \beta_0 + \mu_{0j} + (\beta_1 + \mu_{1j})A_{ij} + (\beta_2 + \mu_{2j})S_{ij} + (\beta_3 + \mu_{3j})L_{ij} + \beta_4 A_{ij}L_{ij} + \beta_5 A_{ij}S_{ij} + \beta_6 S_{ij}L_{ij} + \beta_7 A_{ij}L_{ij}S_{ij} + \varepsilon_{ij} \qquad (4)$$

Here, β_0 is the fixed intercept, μ_{0j} the random intercept, ξ_{ij} is the error term, β_1 is the fixed effect slope for acceleration A_{ij}, and μ_{1j} is the random slope for acceleration A_{ij}, with μ_{1j} assumed to be normally distributed with mean 0 and variance $\sigma_{\mu 1}^2$. β_2 is the

fixed effect slope for stepping S_{ij}, and μ_{2j} is the random slope for stepping S_{ij}, with μ_{2j} assumed to be normally distributed with mean 0 and variance $\sigma_{\mu 2}^2$. β_3 is the fixed

effect slope for leaning L_{ij}, and μ_{3j} is the random slope for leaning L_{ij}, with μ_{3j} assumed to be normally distributed with mean 0 and variance $\sigma_{\mu 3}^2$. β_4 is the fixed interaction

effect slope for acceleration A_{ij}, and leaning L_{ij}, β_5 is the fixed interaction effect slope for acceleration A_{ij}, and stepping S_{ij}, β_6 is the fixed interaction effect slope for stepping S_{ij}, and leaning L_{ij}. β_7 is the fixed three-way interaction effect slope for acceleration A_{ij}, leaning L_{ij} and stepping S_{ij}. The null-hypothesis can be rejected if the confidence interval of a given regression coefficient does not include zero. The regression analyses were conducted at group-level using single trials from all participants, after participant-specific normalization (z-score across trials) of the cortical theta power.

Behavioral parameters

To test whether stepping probability was changed between leaning angles, the stepping probability was analyzed with a nested logistic regression of individual stepping probability values with platform "Acceleration" and "Leaning condition" as the independent variables. The MoS was analyzed with a GLME with factors "Acceleration" and "Leaning condition." See Equation 5 (as a simplified equation without the factor of Stepping from Equation 4).

$$Y_{ij} = \beta_0 + \mu_{0j} + (\beta_1 + \mu_{1j})A_{ij} + (\beta_2 + \mu_{2j})L_{ij} + \beta_3 A_{ij}L_{ij} + \varepsilon_{ij} \tag{5}$$

These statistical analyses were conducted to corroborate the effect of the experimental manipulation (changes to initial postural stability due to leaning posture) on the distribution of reactive stepping behavior across the experimental conditions.

Results

Behavioral data

A total of 7424 trials over 20 participants were analyzed from a total of 7972 recorded trials. 5 trials were rejected based on stepping prior to perturbation onset. A total of 270 trials were rejected based on steps occurring after the constant velocity phase of the motion platform. We rejected 195 trials based on artefacts in kinematic data and an additional 78 trials for artifacts in EEG data (see methods section for trial rejection criteria). The forward perturbation direction analyses contained 3715 trials, of which

2062 were feet-in-place and 1653 were step responses. The backward perturbation direction model contained a total of 3709 trials with 1830 feet-in-place and 1879 step responses. Overall, the proportion of stepping responses for forward and backward responses were significantly different (χ^2= 28.29, df = 3, p = 1.05e^{-7}; forward 43% and backward 51%). With more steps being taken in the backward direction. See figure 2 for the detailed distribution over the different accelerations and leaning conditions. Step onsets were earlier in the backward perturbation direction (median = 376ms, SD = 0.20ms) compared to the forward perturbation direction (median = 440ms, SD = 0.18ms) (Mann-Whitney U test, Z = 14.91, p = 2.71e^{-50}).
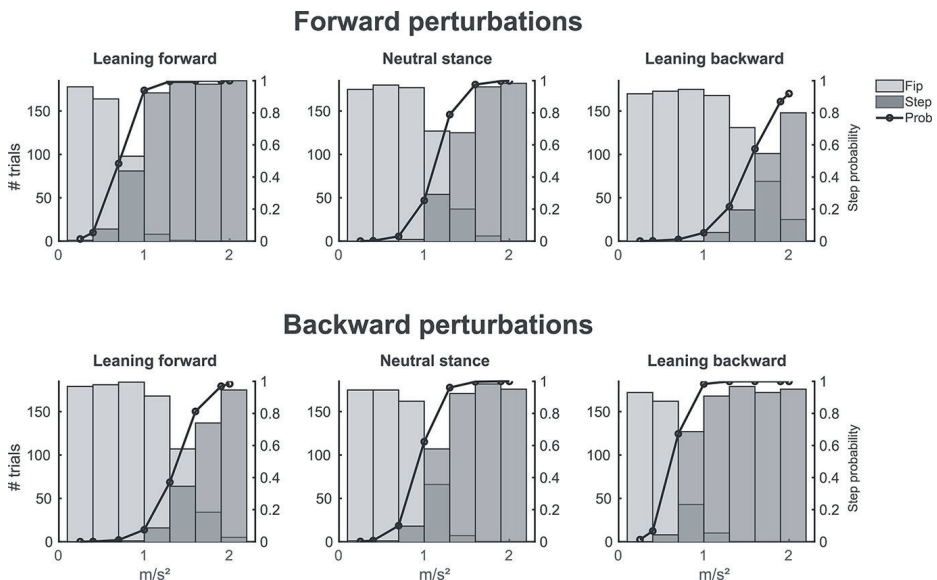
Figure 2. Group-level stepping probability. The top row histograms illustrate the forward-directed perturbation trial distribution for feet-in-place (Fip, light gray) and stepping (Step, dark gray) responses over the conditions forward leaning (left), neutral stance (middle), and backward leaning (right). The bottom row shows the trial distribution for backward-directed perturbation trials. The black curves represent the stepping probability per condition. Increased platform acceleration led to an increased stepping probability. Additionally, stepping probability increased when the leaning direction was congruent to the perturbation direction.

Stepping probability

Figure 2 shows the stepping probabilities for both perturbation directions and the different leaning conditions. The results indicate that stepping probability was affected by both leaning manipulation and platform acceleration, meaning that increased platform accelerations led to an increased stepping probability and when leaning condition and perturbation direction were congruent, stepping probabilities were closer to one. Stepping probability distributions of forward and backward

perturbation directions at neutral stance are similar to previous studies, indicating that the random selected group of participants did not under- or overperform the experiment (32,33).

The logistic regression model of the stepping probability in the forward perturbation direction showed an interaction of acceleration and congruent leaning condition ($t = -4.01$, dof $= 3711$, $P = 6.04e^{-5}$). This indicates that stepping probability increases with greater platform accelerations and that forward leaning additionally shifts the greater stepping probability to lower platform perturbation accelerations. Differences in stepping probability due to the imposed leaning conditions are mainly observed over the middle range of accelerations with 50% stepping probability varying from ~0.7 m/s^2 in the forward leaning condition to ~1.6 m/s^2 in the backward leaning condition. The backward perturbation direction logistic regression model showed an interaction effect for "Leaning condition" and "Acceleration" ($t = -6.21$, dof $= 3705$, $P = 5.27e^{-10}$) with a main effect for both "Leaning condition" ($t = 0.30$, dof $= 3705$, $P = 4.88e^{-6}$) and "Acceleration" ($t = -8.99$, dof $= 3705$, $P = 2.55e^{-19}$). Once again, the differences in stepping probability due to the imposed leaning conditions are mainly observed over the middle range of accelerations with 50% stepping probability varying from ~1.3 m/s^2 in the forward leaning condition to ~0.7 m/s^2 in the backward leaning condition.

Margin of stability

In Figure 3A, single-trial MoS timeseries are presented for all leaning conditions with a feet-in-place and step response in the forward perturbation direction at 1 m/s^2 (* = The forward leaning feet-in-place response trial intensity was 0.7 m/s^2, solid red line). Our results indicate that overall step trials reach lower and, in some cases, negative values of MoS compared to feet-in-place trials. Step latencies did not occur during the initial 300 ms post perturbation; therefore, we analyzed MoS dynamics at 300 ms to determine leaning-induced differences on MoS.

Figure 3B shows the margin of stability for both perturbation directions and the different leaning conditions. The results indicate that the MoS is influenced by the acceleration and leaning conditions, in both the forward and backward perturbation directions. In addition, within acceleration bin of a leaning condition MoS was overall greater in the forward compared to backward perturbation direction. In accordance with the stepping probability, when leaning condition and perturbation direction were congruent, the MoS was smaller (and stepping probability was closer to one). This is also indicated by the interaction effects of leaning condition and acceleration of the regression models. The forward perturbation direction model ($R^2 = 0.88$,

F(3439) =2529, p = 8.94e^{-204}) showed an interaction effect for the *Forward leaning condition x Acceleration* (β_3 = -3.89, CI: [-19.73 : 11.94], p = 0.016), and a main effect for the *Neutral leaning condition* (β_2 = -36.83, CI: [-44.08 : 29.57], p = 4.97e^{-23}). The backward perturbation direction model (R^2 = 0.90, F(3434) = 2782, p = 1.80e^{-284}) showed an interaction effect for both *Neutral leaning condition x Acceleration* (β_3 = -17.7, CI: [-31.52 : 3.89], p = 0.01) and *Backward leaning condition x Acceleration* (β_3 = -36.35, CI: [-55.04 : -17.67], p = 1.3e^{-4}).
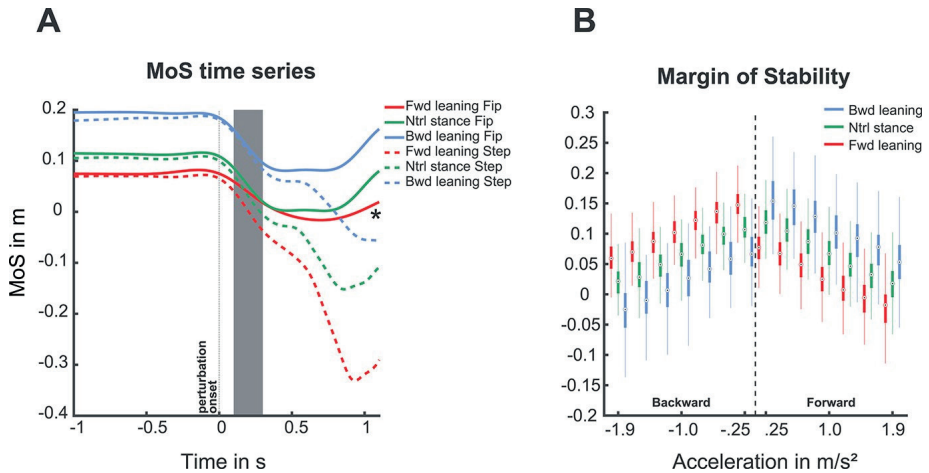
Figure 3. MoS. A) Single-trial MoS timeseries data of forward perturbations at 1 m/s2 (arbitrarily chosen from the experiment of one participant). Note that the MoS trajectory for the forward leaning feet-in-place trial (red solid line, indicated with an asterisk) was collected at an intensity of 0.7 m/s2, because no participant responded feet-in-place to 1 m/s2. Gray shaded area indicates time window of interest for theta analysis (100–300 ms). MoS values for further analysis were obtained from 300 ms post perturbation. **B)** MoS at 300 ms post perturbation for each leaning condition per acceleration. MoS illustrated over leaning conditions; forward leaning (red), neutral stance (green), and backward leaning (blue). The boxplots presented to the left of the dotted line represent MoS for backward perturbation directions, and the boxplots to the right of the dotted line represent the forward perturbation directions. The figure clearly illustrates that the leaning manipulation shifted the MoS for each individual acceleration (observed as the 3 boxplot colors per acceleration bin). Additionally, the MoS is reduced with increasing acceleration, which indicates a greater risk of losing postural stability.

Electroencephalography

Overall, EEG data quality was unaffected by leaning conditions as we found no effect on condition-specific trial variance ($F(2) = 1.05$, $P = 0.35$). Only 2 participants showed extensive noise, resulting in a greater amount of rejected components after ICA (mean 91 rejected components, SD 16 rejected components). Overall, ICA infomax was an appropriate method for over 95% of the participants and therefore considered suitable for the analysis pipeline. All leaning steps were conducted prior

to data analysis to prevent any bias toward the results.
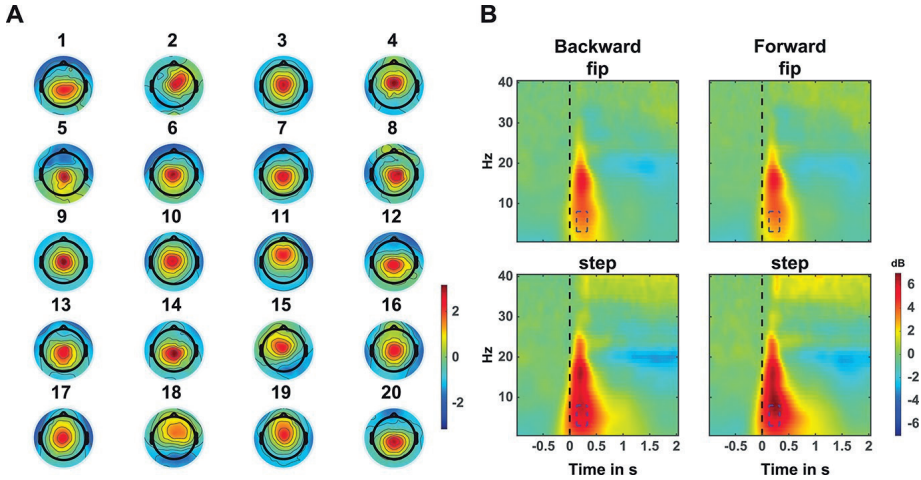
Figure 4. EEG data. A) Participant-specific scalp topographies of the eigenvector with the largest eigenvalue and a midfrontal topography. The scalp topography data were normalized per participant. **B)** Average time–frequency plots of 20 participants scaled power in dB. Plots are averaged over all leaning conditions. Top row panels show feet-in-place responses (fip), while bottom row panels show step responses. The left column illustrates backward perturbations, whereas the right column presents forward perturbations. The perturbation onset occurs at t = 0 s. Blue dashed boxes indicate the theta frequency and temporal window of interest.

GLME model fit of cortical dynamics

In addition to theta dynamics, similar analyses were conducted on the alpha and beta range on the forward perturbation model (see Supplementary Material).

Forward perturbation direction theta dynamics model

The forward perturbation direction GLME model was overall a highly significant fit to the data ($R^2 = 0.147$, $F(3703) = 29.70$, $P = 1.27e^{-60}$) (figure 5). There was a main effect of platform acceleration indicating greater theta power associated with higher platform accelerations ($\beta_1 = 0.622$, CI: [0.49 0.76], $P = 9.11e^{-19}$). An effect of "Forward leaning condition" ($\beta_3 = -0.37$, CI: [−0.63–0.11], $P = 4.76e^{-3}$) indicated that theta power was lower for backward leaning (most stable condition) than for forward leaning (least stable condition) at the same platform accelerations. There was an interaction effect of "Acceleration × Forward leaning" ($\beta_4 = 1.26$ CI: [0.78 1.75], $P = 2.91e^{-7}$), indicating greater increase of theta power with platform accelerations when leaning forward versus leaning backward. Furthermore, there was an "Acceleration × Forward leaning × Stepping" interaction ($\beta_7 = -1.13$, CI: [−1.79–0.46], $P = 8.86e^{-4}$), indicating that the different slopes in theta power observed due to the interaction effect of "Forward
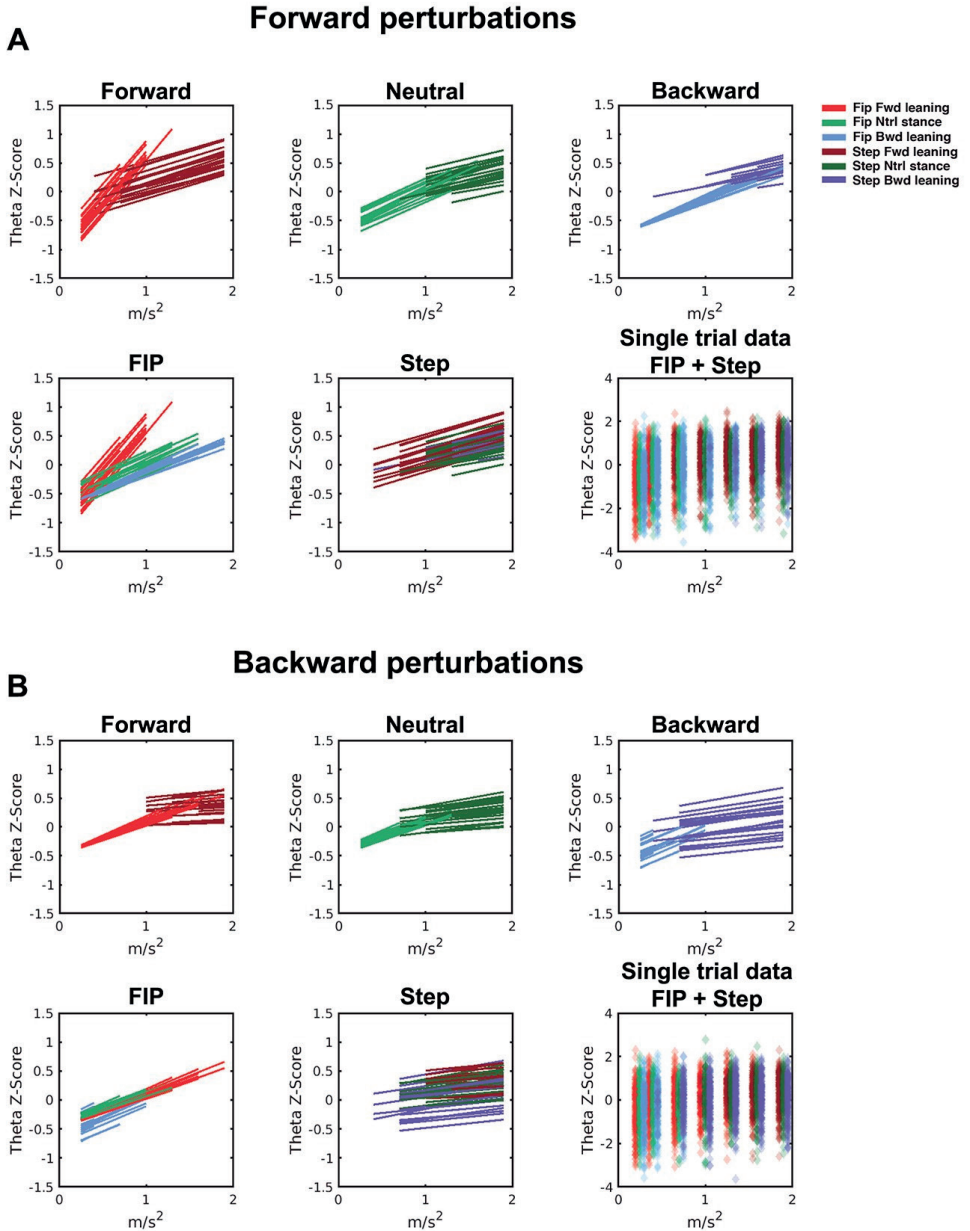
Figure 5. Theta power model fit. A) Forward perturbation model fit of single-trial theta dynamics. The top row shows theta dynamics of each leaning condition with fip (lighter color) or step response (darker color). In the bottom row, all leaning condition fip responses are presented left and step responses in the middle. The bottom right panel shows single-trial normalized theta power for each participant per leaning condition. A small offset on the x-axis was added to represent the 3 leaning conditions in the same platform acceleration bin. B) Backward perturbation model fit of single-trial theta dynamics. Data presented as forward leaning (red), neutral stance (green), and backward leaning (blue).

leaning condition × Acceleration" were only observed for the feet-in-place responses and not for the stepping responses.

Backward perturbation direction theta dynamics model

The backward perturbation direction GLME model ($R^2 = 0.084$, $F(3697) = 11,58$, $P = 1.46e^{-21}$) showed a main effect of "Acceleration" ($\beta_1 = 0.56$, CI: [0.40 0.72], $P = 3.52e^{-12}$) and an interaction effect for "Acceleration × Stepping" ($\beta_5 = -0.40$, CI: [−0.79–0.02], $P = 0.04$). This interaction indicates that the slope of theta power is different for the stepping responses compared to feet-in-place responses (i.e. steeper when maintaining feet-in-place; Fig. 5). Interestingly, in the backward perturbation direction, we did not find a main or interaction effect for the leaning conditions.

Discussion

Our goal was to demonstrate the participation of midfrontal theta dynamics in the behavioral monitoring of standing balance. We used whole-body balance perturbations of varying accelerations to probe the postural control system while manipulating the initial state of postural stability with a leaning task. This experimental paradigm allowed us to investigate the theta dynamics during altered states of postural stability. We found that different leaning conditions changed the relation between platform acceleration and midfrontal theta power. In particular, we found that the initial postural state, as imposed by the leaning instructions, led to different theta power modulations at identical platform accelerations. This is supporting evidence for the role of the midfrontal theta dynamics in balance monitoring and highlights that the role of midfrontal theta is nuanced and dependent on contextual postural factors.

Evidence of a monitoring role of midfrontal theta dynamics

We, and others, have speculated that midfrontal theta during balance monitoring reflects the activation of a cortical system that compares incoming postural information to an internal model of postural stability, and predicts the need for a corrective step. Consistent with the suggested monitoring role of midfrontal theta dynamics, the midfrontal theta power increases prior to loss of balance in a balance beam walking paradigm (13), near the instant of minimum MoS (34), and during continuous challenges to postural stability (16). In response to balance perturbations, theta power dynamics scale with perturbation intensity (15,35,36) and with different reactive responses (i.e. feet-in-place versus stepping, (18)), suggesting that theta dynamics scale with task difficulty. Our current results demonstrate that the

relation between theta power with acceleration and the ensuing postural response can be altered by the leaning condition (i.e. initial postural state). In the forward perturbation direction, the relation between theta power with acceleration and the postural response significantly changed when leaning forward (in contrast to leaning backward, see bottom left panel in figure 5). In particular, when being perturbed in the forward direction, theta power increases more rapidly over acceleration when leaning forward and maintaining feet-in-place compared to leaning backward. Importantly, we do not observe changes in theta dynamics during baseline periods of the different leaning conditions, indicating that theta dynamics are not altered during the leaning phase prior to perturbation resulting in the observed differences. In addition, analysis of alpha and beta frequency bands (Supplementary Material) did not show similar interaction effects, suggesting that only theta dynamics scale with behavioral balance monitoring parameters.

We propose that the leaning posture alters the internal representation of postural stability in such a way that balance perturbations of a given intensity and direction are perceived as different postural threats and may elicit distinct postural responses. The theta dynamics observed in the range of accelerations that elicit feet-in-place responses reflect the rapid increase in postural threat associated with perturbations toward the leaning direction. Following the perturbation onset, incoming sensory information (representing the perturbation characteristics) may be quickly integrated within the central nervous system and compared against the estimated sensory information (given by the internal model of postural stability; see (9,20,37); any deviation from the internal estimate would require adaptive postural responses, and the cortical involvement in this computation manifests as midfrontal theta (18). An important finding of the present study is that these theta dynamics depend on the initial postural situation in addition to the magnitude of the induced perturbation when feet-in-place responses are still feasible. An effect of initial leaning posture on midfrontal theta dynamics is not observed at higher perturbation intensities, where stepping responses are consistently elicited, and therefore, the midfrontal theta may have reached a threshold value indicating that a feet-in-place strategy is insufficient to maintain balance.

Interestingly, the balance-related cortical theta dynamics show strong similarities to cortical theta dynamics during other action monitoring paradigms. Many paradigms investigating action monitoring during dynamic tracking tasks show modulations of the midfrontal theta rhythm with similar latencies and scalp distributions to the results presented in our study (38). An increase of midfrontal theta power coincides with behavioral errors, and the magnitude of these errors (as well as the ensuing

corrective behavior) corresponds with the magnitude of theta power (39). In our study, the theta dynamics preceded the stepping responses and seemed to represent active monitoring of balance, which is most relevant when perturbation acceleration and initial leaning condition lead to feet-in-place responses.

Balance monitoring and perturbation direction

Our analyses of midfrontal theta dynamics revealed an effect of the initial leaning condition in the forward perturbation direction, but not in the backward perturbation direction. Albeit our goal was not to compare between the 2 postural perturbation directions, our results suggest that the initial postural state given by the leaning conditions prior to perturbation onset is less relevant for the backward perturbation direction. This may be explained by different anatomical and biomechanical constraints in the backward direction. The musculoskeletal system is primarily built to propel the human body in the forward direction. This can be observed in the greater distance of the ankle joint to the toes versus its distance to the heels, which creates a larger lever arm and allows generating greater ankle plantar flexion than dorsiflexion torques, and the greater range of motion of the hip joint in flexion than extension. These differences offer clear advantages for balance recovery in the forward direction. Ankle strategies help to maintain balance when CoM displacement is small; however, when the CoM displacement is larger, hip strategies help counteracting the CoM acceleration to prevent humans from falling forward. As these strategies are not applicable to the same extent for the backward perturbation direction, postural perturbations of equal magnitude lead to a higher likelihood of stepping responses in the backward than in the forward perturbation direction.

To prevent falls in the backward direction, it seems most effective to initiate stepping responses not only at lower platform intensities, but also sooner after perturbation. Indeed, we found that stepping latencies were faster in the backward direction (376 ms) compared to the forward direction (440 ms). Interestingly, in our previous study (18), we found no difference in forward and backward perturbations N1 latency, which suggests that monitoring postural stability occurs with a similar interval for forward and backward perturbation directions, but later response onset in the forward perturbation direction leads to more time available to determine the necessity of a stepping response (c.f. (40). Therefore, we speculate that in the backward direction, the shorter time until step onset may limit the role of midfrontal theta modulations in selecting the behavioral response, which appears in line with the overall lower explained variance of the backward perturbation direction GLME model (8.4% vs. 14.7% for the forward perturbation direction model).

3

Whether balance is monitored differently for perturbation directions has remained elusive. Despite previous studies reporting that the perturbation direction does not modulate the perturbation-evoked responses (10–12), recent studies suggest a cortical representation of direction-specific postural stability (33). Our results indicate that for the backward perturbation direction, the initial leaning posture does not change the relation between perturbation acceleration and theta power (see figure 5). We expected to observe a strong modulation of the midfrontal theta power during feet-in-place responses related to the initial leaning posture and indicating balance monitoring. Such modulation of the midfrontal theta power with initial leaning posture was indeed observed in the forward perturbation direction (see top right panel figure 5), yet the larger proportion of stepping responses in the backward perturbation direction (see Section 3.1) may have obscured a similar effect of leaning posture. On the other hand, the slopes of the backward perturbation direction in feet-in-place data in the top-left panel of Figure 5 seem to follow a parallel trend and do not seem to show a threshold of theta power indicating the necessity of a step.

Clinical implications

Postural balance control is an ongoing cognitive-motor process that all humans engage in every day of their lives. Impairments in postural control can be devastating to quality of life. In fact, instability (leading to high fall risk) is a major problem in people with neurological disorders, as well as in the rapidly growing older population. Despite the severity of this problem and the pivotal role of the brain in controlling the musculoskeletal system, we still have a remarkably poor understanding of the cortical mechanisms involved in postural control. Our present suggestion of theta activity representing action monitoring of postural balance according to an internal model of stability informs future studies where, for instance, we may want to seek further evidence for this hypothesis in patients with known deficits in internal modeling (e.g. cerebellar pathology). In addition, it may be of interest to investigate whether aberrant internal modeling may underlie (or contribute to) postural instability and falls in various neurological conditions (e.g. stroke or Parkinson's disease). For such studies, it is recommended to limit the experimental duration and perform a small subset of perturbations, while still allowing for a sufficient number of repetitions at each experimental condition. As we showed most cortical modulations related to balance monitoring at the lower end of the spectrum of perturbation intensities, perturbations may largely constitute those eliciting feet-in-place responses. In addition, it may be helpful to use 2 contrasting leaning conditions, instead of the 3 conditions as used in the present experiment. Importantly, for such clinical experiments, a sophisticated experimental setup such as

the Radboud Falls Simulator is not a prerequisite since there are affordable treadmill-based alternatives for delivering standardized anterior–posterior perturbations. The current study provides valuable insights on the specific experimental conditions that may be used to target cortical balance monitoring processes.

Future studies

We recommend that future studies investigate a wider range of low acceleration balance perturbations in the backward perturbation direction with different leaning postures, to investigate the effect on the modulation of midfrontal theta power in the backward perturbation direction. The current study illustrates that the cortical role in balance monitoring does not solely represent the characteristics of the perturbation itself but also accounts for contextual information (i.e. postural threat). This provides supporting evidence for future studies to investigate to what extent different sensory modalities contribute information to the internal model of stability.

Limitations

Changes in sensory information due to perturbation intensity and through the leaning conditions are hard to disentangle. Experimental manipulations of sensory inflow (e.g. vibration to Achilles tendon) would not allow for perfect dissociation with perturbation magnitude, due to reweighting mechanisms of the highly redundant sensory inputs that would remain unaffected by such manipulations (e.g. exteroceptive information from the foot soles). Therefore, one can only speculate how sensory information is altered by the induced leaning conditions and whether this might have interacted with observed balance monitoring theta dynamics. Noteworthy, our experimental manipulations maintained the intensity of external balance perturbations while allowing for natural (ecologically valid) sensory reweighting of the postural control system. An important finding of the present study is that these theta dynamics depend on the initial postural situation in addition to the magnitude of the induced perturbation when feet-in-place responses are still feasible.

In addition, the time window allows us to interpret theta dynamics in response to the imposed postural threats following the 100–300 ms post perturbations. Yet, postural balance control is a dynamic process with cortical dynamics changing over time. Although, the selected time window in this study may help explain the role of theta dynamics during the monitoring of postural balance, it should be mentioned that dynamics outside of this window may also contribute to the monitoring of postural balance.

While, at first glance, the GLME model fit seems to suggest that feet-in-place responses elicit greater theta dynamics compared to step responses for the highest accelerations resulting in feet-in-place responses, there are several factors that preclude making this inference. Primarily, we would like to point out there was an unequal amount of observations in either feet-in-place and step response per acceleration bin (i.e. gradually decreasing numbers of feet-in-place trials with increasing perturbation intensities, and vice versa for stepping trials). As the GLME model fit yields more uncertainty for the estimates at the extreme ends of the spectrum with low numbers of trials, it may have overestimated these feet-in-place response theta dynamics.

Another point of attention may be the differences in the stepping ratios for forward and backward perturbation directions, as we found significantly more step responses in the backward perturbation direction. Although the amount of responses seems more balanced in the backward direction compared to the forward direction, we expected that the leaning effect on cortical dynamics of balance monitoring to be more pronounced during feet-in-place trials. As stepping thresholds are lower in the backward direction, the current experimental setup may not have been adequate to elicit these monitoring dynamics in the backward direction. Therefore, backward perturbations at low intensities and small increments may illustrate similar balance monitoring dynamics.

Data and code availability statement
The data and code will be made available through a public repository.

References

1. Jacobs JV, Horak FB. Cortical control of postural responses. J Neural Transm. 2007 Mar 29;114(10):1339–48.

2. Maki BE, McIlroy WE. Cognitive demands and cortical control of human balance-recovery reactions. J Neural Transm. 2007 Jun 8;114(10):1279–96.

3. Bolton DAE. The role of the cerebral cortex in postural responses to externally induced perturbations. Neurosci Biobehav Rev. 2015 Oct;57:142–55.

4. Sherrington CS. Flexion-reflex of the limb, crossed extension-reflex, and reflex stepping and standing. J Physiol (Lond). 1910 Apr 26;40(1–2):28–121.

5. Diener HC, Dichgans J, Bootz F, Bacher M. Early stabilization of human posture after a sudden disturbance: influence of rate and amplitude of displacement. Exp Brain Res. 1984;56(1):126–34.

6. Jacobs JV. Why we need to better understand the cortical neurophysiology of impaired postural responses with age, disease, or injury. Front Integr Neurosci. 2014 Aug 29;8:69.

7. Nutt JG, Horak FB, Bloem BR. Milestones in gait, balance, and falling. Mov Disord. 2011 May;26(6):1166–74.

8. Takakusaki K. Functional neuroanatomy for posture and gait control. J Mov Disord. 2017 Jan 18;10(1):1–17.

9. Forbes PA, Chen A, Blouin J-S. Sensorimotor control of standing balance. Handb Clin Neurol. 2018;159:61–83.

10. Dietz V, Quintern J, Berger W, Schenck E. Cerebral potentials and leg muscle e.m.g. responses associated with stance perturbation. Exp Brain Res. 1985;57(2):348–54.

11. Goel R, Ozdemir RA, Nakagome S, Contreras-Vidal JL, Paloski WH, Parikh PJ. Effects of speed and direction of perturbation on electroencephalographic and balance responses. Exp Brain Res. 2018 Jul;236(7):2073–83.

12. Payne AM, Hajcak G, Ting LH. Dissociation of muscle and cortical response scaling to balance perturbation acceleration. J Neurophysiol. 2019 Mar 1;121(3):867–80.

13. Sipp AR, Gwin JT, Makeig S, Ferris DP. Loss of balance during balance beam walking elicits a multifocal theta band electrocortical response. J Neurophysiol. 2013 Nov;110(9):2050–60.

14. Marlin A, Mochizuki G, Staines WR, McIlroy WE. Localizing evoked cortical activity associated with balance reactions: does the anterior cingulate play a role? J Neurophysiol. 2014 Jun 15;111(12):2634–43.

15. Varghese JP, Marlin A, Beyer KB, Staines WR, Mochizuki G, McIlroy WE. Frequency characteristics of cortical activity associated with perturbations to upright stability. Neurosci Lett. 2014 Aug 22;578:33–8.

16. Hülsdünker T, Mierau A, Neeb C, Kleinöder H, Strüder HK. Cortical processes associated with continuous balance control as revealed by EEG spectral power. Neurosci Lett. 2015 Apr 10;592:1-5.

17. Adkin AL, Quant S, Maki BE, McIlroy WE. Cortical responses associated with predictable and unpredictable compensatory balance reactions. Exp Brain Res. 2006 Jun;172(1):85–93.

3

18. Solis-Escalante T, Stokkermans M, Cohen MX, Weerdesteyn V. Cortical responses to whole-body balance perturbations index perturbation magnitude and predict reactive stepping behavior. Eur J Neurosci. 2020 Dec;54(12):8120–38.

19. Yao Li, Levine WS. An optimal control model for human postural regulation. 2009 American Control Conference. IEEE; 2009. p. 4705–10.

20. Rasman BG, Forbes PA, Tisserand R, Blouin J-S. Sensorimotor Manipulations of the Balance Control Loop-Beyond Imposed External Perturbations. Front Neurol. 2018 Oct 26;9:899.

21. Nonnekes J, de Kam D, Geurts ACH, Weerdesteyn V, Bloem BR. Unraveling the mechanisms underlying postural instability in Parkinson's disease using dynamic posturography. Expert Rev Neurother. 2013 Dec;13(12):1303–8.

22. Solis-Escalante T, van der Cruijsen J, de Kam D, van Kordelaar J, Weerdesteyn V, Schouten AC. Cortical dynamics during preparation and execution of reactive balance responses with distinct postural demands. Neuroimage. 2019 Mar;188:557–71.

23. Oostenveld R, Praamstra P. The five percent electrode system for high-resolution EEG and ERP measurements. Clin Neurophysiol. 2001 Apr;112(4):713–9.

24. Hof AL, Gazendam MGJ, Sinke WE. The condition for dynamic stability. J Biomech. 2005 Jan;38(1):1–8.

25. McAndrew Young PM, Wilken JM, Dingwell JB. Dynamic margins of stability during human walking in destabilizing environments. J Biomech. 2012 Apr 5;45(6):1053–9.

26. Delorme A, Makeig S. EEGLAB: an open source toolbox for analysis of single-trial EEG dynamics including independent component analysis. J Neurosci Methods. 2004 Mar 15;134(1):9–21.

27. Cohen MX. Multivariate cross-frequency coupling via generalized eigendecomposition. eLife. 2017 Jan 24;6.

28. Cohen MX. A tutorial on generalized eigendecomposition for source separation in multichannel electrophysiology. arXiv:210412356v1 [q-bioQM] [Internet]. 2021 Apr 26 [cited 2021 May 27]; Available from: https://arxiv.org/pdf/2104.12356.pdf

29. Blankertz, B., Tomioka, R., Lemm, S., Kawanabe, M. & Muller, K. Optimizing spatial filters for robust EEG single-trial analysis. *IEEE Signal Process. Mag.* 25(1), 41–56 (2008)

30. Haufe S, Meinecke F, Görgen K, Dähne S, Haynes J-D, Blankertz B, et al. On the interpretation of weight vectors of linear models in multivariate neuroimaging. Neuroimage. 2014 Feb 15;87:96-110.

31. Blankertz B, Tomioka R, Lemm S, Kawanabe M, Muller K. Optimizing Spatial filters for Robust EEG Single-Trial Analysis. IEEE Signal Process Mag. 2008;25(1):41–56.

32. de Kam D, Kamphuis JF, Weerdesteyn V, Geurts ACH. The effect of weight-bearing asymmetry on dynamic postural stability in healthy young individuals. Gait Posture. 2016 Mar;45:56–61.

33. Solis-Escalante T, De Kam D, Weerdesteyn V. Classification of Rhythmic Cortical Activity Elicited by Whole-Body Balance Perturbations Suggests the Cortical Representation of Direction-Specific Changes in Postural Stability. IEEE Trans Neural Syst Rehabil Eng. 2020 Nov 6;28(11):2566–74.

34. Slobounov S, Cao C, Jaiswal N, Newell KM. Neural basis of postural instability identified by VTC and EEG. Exp Brain Res. 2009 Oct;199(1):1–16.

35. Varghese JP, Staines WR, McIlroy WE. Activity in Functional Cortical Networks Temporally Associated with Postural Instability. Neuroscience. 2019 Mar 1;401:43–58.

36. Payne AM, Ting LH. Worse balance is associated with larger perturbation-evoked cortical responses in healthy young adults. Gait Posture. 2020 Jul;80:324–30.

37. Scott SH. Optimal feedback control and the neural basis of volitional motor control. Nat Rev Neurosci. 2004 Jul;5(7):532–46.

38. Cohen MX, Donner TH. Midfrontal conflict-related theta-band power reflects neural oscillations that predict behavior. J Neurophysiol. 2013 Dec;110(12):2752–63.

39. Pereira M, Sobolewski A, Millán JDR. Action monitoring cortical activity coupled to submovements. eNeuro. 2017 Oct 24;4(5).

40. Manista GC, Ahmed AA. Stability limits modulate whole-body motor learning. J Neurophysiol. 2012 Apr;107(7):1952–61.

Supplementary material

Manuscript: Midfrontal theta dynamics index monitoring postural stability
Statistical analysis of the cortical alpha (9 – 12 Hz) and beta (15 – 25 Hz) frequency range was conducted similarly to the theta power GLME analysis for the forward perturbation direction. These results indicate that only theta dynamics facilitate the monitoring of human balance control.

Alpha dynamics

In the additional analysis of the alpha (9 – 12 Hz) frequency band range ($R^2 = 0.07$, $F(3703) = 16,24$, $p=1.28e^{-31}$, figure S1), we do observe main and interaction effects of *Acceleration x Stepping* ($\beta_5 = -0.48$, CI: [-0.88 -0.08], p = 0.02), indicating that over all leaning conditions the slope of alpha under feet-in-place responses is steeper than for step responses (observed in the top row of figure 2). In addition, we observe an interaction effect of *Acceleration x Leaning forward* ($\beta_4 =0.58$, CI: [0.10 1.1], p = 0.02), indicating that when leaning forward, alpha power increases faster over accelerations compared to leaning backward. However, there is no three-way interaction observed in slope between feet-in-place and step responses when leaning forward. The lack of an effect between feet-in-place and stepping response when leaning forward suggests that alpha only signals for an increase in postural threat explained by acceleration and leaning but not with the ensuing behavioral response as theta dynamics do.

Beta dynamics

In the beta (15 – 25Hz) frequency range ($R^2 = 0.03$, $F(3703)=9.9$, $p=6.6e^{-18}$, figure S2) we observe an effect of *Acceleration* ($\beta_1 = 0.21$, CI: [0.075 0.35], p = 0.002). In addition, we observe an interaction effect of *Stepping x Leaning* for both forward ($\beta_6 = -0.96$, CI: [-1.79 -0.13], p = 0.02) and at neutral stance ($\beta_6 = -95$, CI: [-1.85 -0.05], p = 0.04). This indicates that the slope of beta dynamics is different when leaning backward and stepping compared to the other leaning postures (observed in the bottom middle graph of figure s2). In addition, a three-way interaction is observed ($\beta_7 =0.66$, CI: [0.077 1.24], p = 0.03) which indicates that the slope of beta dynamics is different when leaning backward and stepping compared to feet in place. This is observed as the negative slope for backward leaning and stepping, compared to feet in place in the top right graph of figure s2.
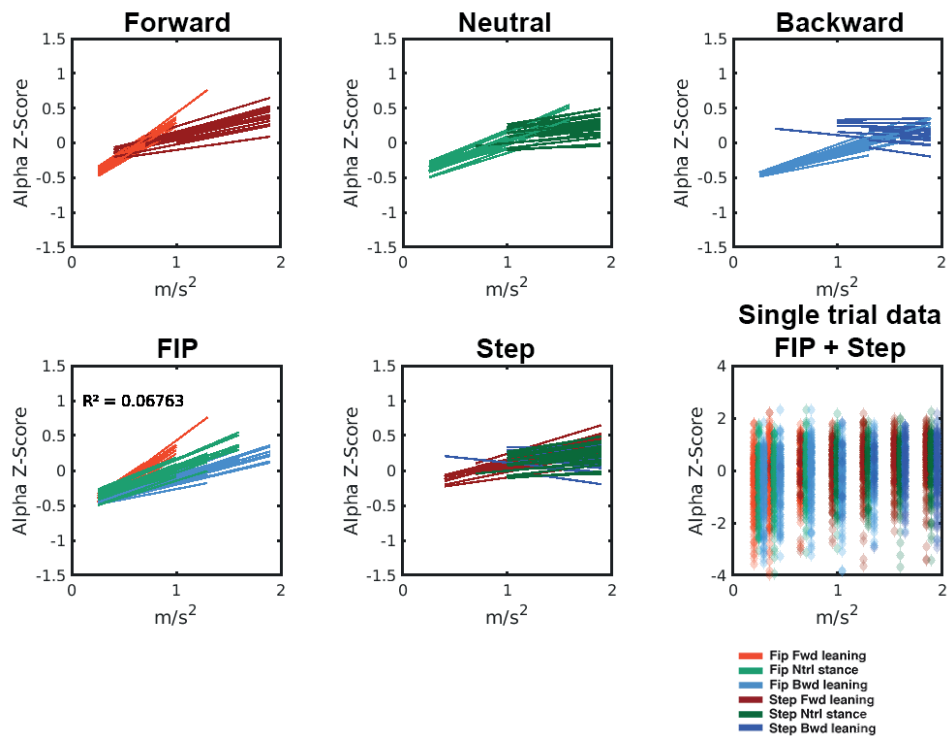
Figure S1: Alpha dynamics GLME model fit. The top row illustrates the different leaning conditions forward leaning (left), neutral stance (middle), backward leaning (right) with both feet-in-place (fip) (lighter color) and step response (darker color). The bottom row contains the fip response (bottom left) and the step response (middle) of the three leaning conditions. In the bottom right panel, the single trial data is presented with an offset on the x-axis to illustrate all three leaning conditions per acceleration bin.
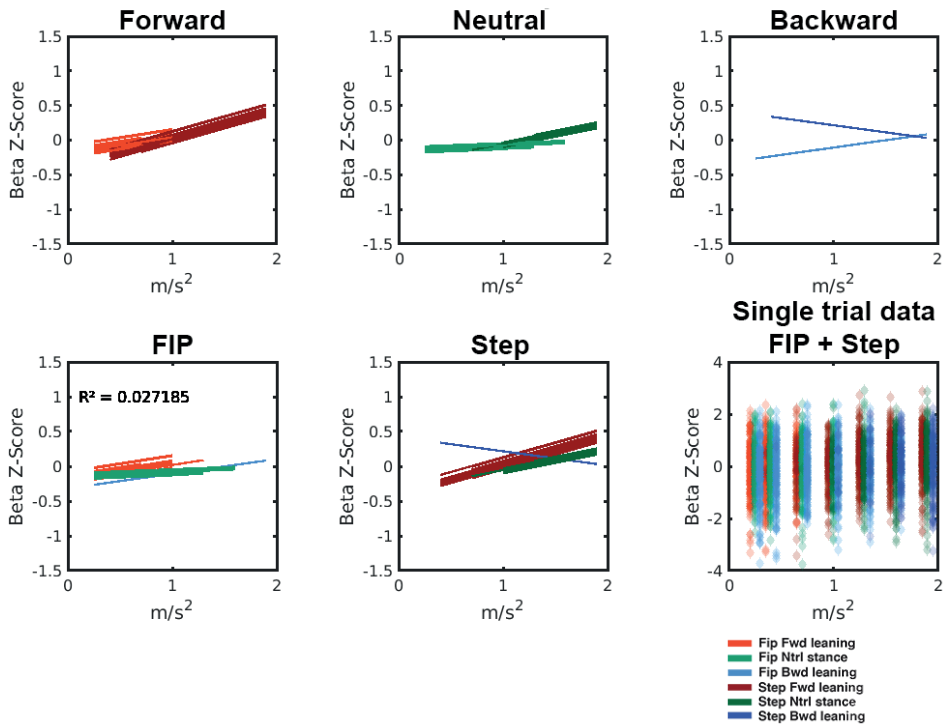
Figure S2: Beta dynamics GLME model fit. The top row illustrates the different leaning conditions forward leaning (left), neutral stance (middle), backward leaning (right) with both feet-in-place (fip) (lighter color) and step response (darker color). The bottom row contains the fip response (bottom left) and the step response (middle) of the three leaning conditions. In the bottom right panel, the single trial data is presented with an offset on the x-axis to illustrate all three leaning conditions per acceleration bin.

Although we observe a three-way interaction in the beta range, these observed interactions concern differences in beta dynamics for stepping between forward and backward leaning. Importantly, we do not consider this as monitoring of balance as we expect markers for monitoring to scale within the feet-in-place responses (when any response outcome is still possible), rather than the step responses as observed in the beta dynamics. Within the feet-in-place response there is a stability range to monitor postural balance before balance is lost, whereas in stepping trials the possibility for a feet-in-place response is exceeded and always results in the loss of stability and a step response.

Chapter 4

Cortical midfrontal theta dynamics following foot strike may index response adaptation during reactive stepping

Abstract

Reactive balance recovery often requires stepping responses to regain postural stability following a sudden change in posture. The monitoring of postural stability has been linked to neuroelectrical markers such as the N1 potential and midfrontal theta frequency dynamics. Here, we investigated the role of cortical midfrontal theta dynamics during balance monitoring following foot landing of a reactive stepping response to recover from whole-body balance perturbations. We hypothesized that midfrontal theta dynamics reflect the engagement of a behavioral monitoring system, and therefore that theta would increase time-locked to the moment of foot strike after a stepping response, coinciding with a re-assessment of postural balance to determine if an additional step is necessary. We recorded high-density EEG and kinematic data of 15 healthy young participants while they stood on a platform that delivered multi-directional balance perturbations. Participants were instructed to recover balance with a single step utilizing either their left or right leg (in separate blocks). We used targeted spatial filtering (generalized eigen decomposition) in combination with time–frequency analysis of the EEG data to investigate whether theta dynamics increase following foot strike event. In line with our hypothesis, the results indicate that the foot strike event elicits a midfrontal theta power increase, though only for backward stepping. Counter to our expectations, however, this theta power increase was positively correlated with the margin of stability at foot strike, suggesting a different role of foot strike related theta from monitoring stability. Post-hoc analysis suggests that midfrontal theta dynamics following foot landing may instead facilitate adaptation of stability margins at subsequent stepping responses. We speculate that increase of theta power following foot strikes was not related to stability monitoring but instead may indicate cortical dynamics related to performance monitoring of the balance response.

Introduction

On a daily basis, we experience challenges to our postural stability, either from errors when engaging in voluntary movements (e.g. misjudging the height of a step down) or from external perturbations (e.g. being pushed). Such instances often require a corrective step to maintain balance. This generally involves few difficulties for young healthy individuals but can be challenging or even dangerous in individuals with impaired balance or in elderly (1,2).

Although balance control was traditionally considered a subcortical function, it has become evident that the cerebral cortex is also involved. In particular, two cortical signals (measured through Electroencephalogram; EEG) have been consistently observed shortly after an unexpected balance perturbation: the N1 event-related potential, and power modulations of theta-band (3–8 Hz) activity (3,4). The roles of N1 and theta power increase have been linked to sensory integration and facilitating cognitive processes underlying postural control (e.g. balance monitoring), supporting evidence for these roles comes from studies that measured continuous balance performance and found that a less stable posture correlated with stronger theta power (5,6). Additionally, theta power scales with both balance perturbation intensity and with stepping or feet-in-place (i.e. to overcome a balance perturbation without making a step) response outcomes, suggesting that theta signals the loss of stability and predicts the necessity of a step (7). Furthermore, we recently showed that manipulating the leaning posture prior to random perturbation intensities resulted in theta power modulations that scaled with postural threat (i.e. greater postural threat caused theta dynamics to rise faster over smaller perturbation intensities (8). Altogether these results show that theta dynamics are intimately involved in balance monitoring.

In light of this supporting evidence for a role in balance monitoring shortly after an unexpected perturbation, we reasoned that a theta power increase may also be elicited at the moment when the stepping foot strikes the ground, based on the idea that the new postural stability after the recovery step is not guaranteed and may require a re-assessment of the new postural state.

In this study, we investigated foot strike related theta power dynamics in reactive stepping trials following unexpected balance perturbations in forward and backward directions. We hypothesized that the foot strike event is followed by a midfrontal theta power increase relative to baseline theta power and distinguishable from the initial perturbation-induced theta power increase. In addition, we expected that

4

these theta power dynamics represent a balance monitoring process of the new postural state after foot strike. We therefore expected that stronger theta dynamics scale with lower margins of stability at foot contact, as a commonly used measure of dynamic stability that captures the relationship between center of mass and the edge of the base of support at foot strike. We also studied whether theta power dynamics may differ between forward and backward reactive stepping responses, because there are behavioral differences between perturbation directions. Previous studies showed that there are evident biomechanical differences in the forward and backward reactive stepping response (9,10) and visual control of the step also differs between these directions. In addition, backward reactive steps occur faster than forward reactive steps (7,11) and at lower stepping thresholds (i.e. lower perturbation intensities (12,13)). Given the relatively greater challenge involved in backward as compared to forward steps, we expected theta dynamics to be stronger in the backward direction.

Materials and methods

Participants
Fifteen young healthy adults (6 female; mean age 24 years, sd 2 years) participated in this study. None of the participants had a previous history of neurological or musculoskeletal conditions or other impairments that could affect balance. They provided written informed consent before participating in the experiment according to the experimental procedures approved by the Research Ethics Committee of the Radboud University Medical Center (Nijmegen, The Netherlands; Dossier NL67690.091.18). The experiments were conducted in line with the Declaration of Helsinki.

Experimental paradigm
The Radboud Falls Simulator was used to deliver balance perturbations and to assess reactive stepping responses (14). This movable platform is equipped with embedded dual force plates, (60 by 180 cm each, AMTI Custom 6 axis composite force platform, USA) and a 3D motion capture system (Vicon Motion Systems, Oxford, UK). Translations of the movable platform elicit a reactive stepping response in the opposite direction of the platform translation (i.e. backward platform translations result in forward stepping). Henceforth, we will refer to stepping direction when mentioning perturbation direction. Participants were instructed to stand upright with their feet 5 cm apart (marked on the platform) and to recover their balance with a single step. Prior to each block of perturbations, participants were instructed to

use either their right or their left leg for stepping. Perturbations were given in five different directions for each leg (backward, diagonal backward, sideways, diagonal forward and forward). The perturbation profile consisted of an acceleration of 1.5 m/s2 for 300 ms followed by a constant velocity phase of 500 ms and a deceleration phase of 300 ms (see figure 1). During the experiment, participants wore a safety harness that was attached to a sliding rail on the ceiling.
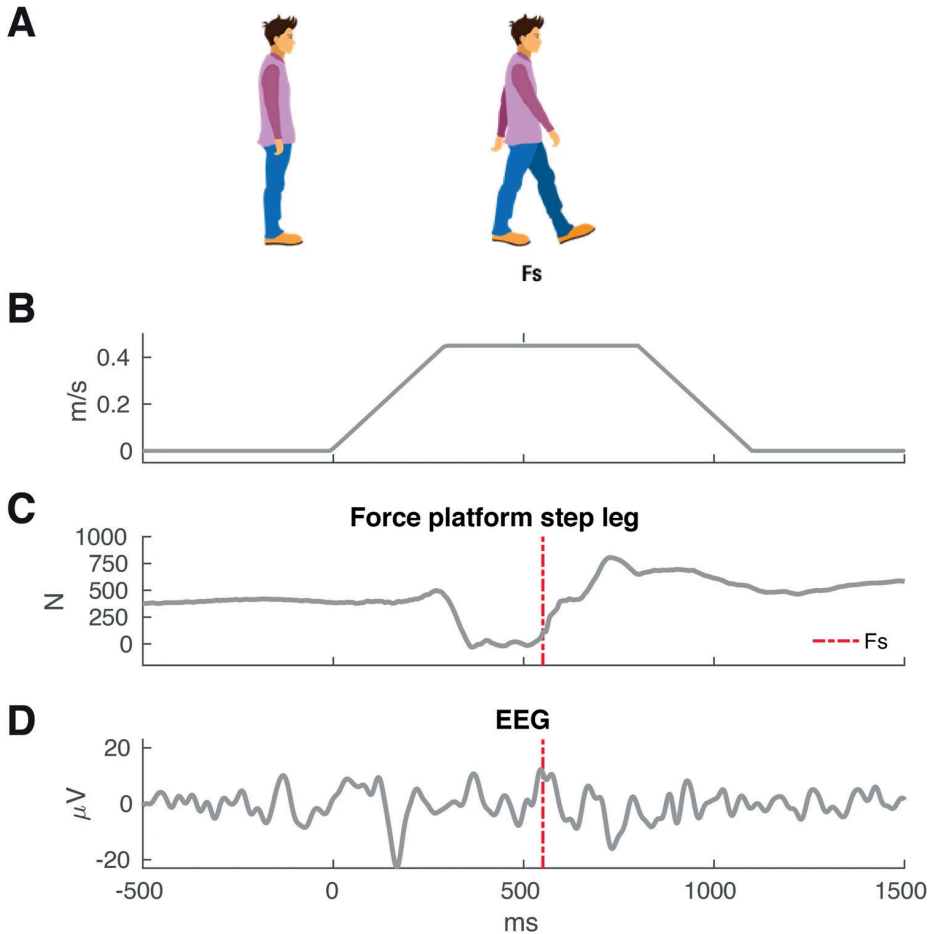
Figure 1. Experimental data alignment. (A) The participant's response to a forward perturbation (i.e. backward platform translation). Foot strikes (Fs) were identified from the force plate and marker data. (B) The perturbation profile used in the experiment expressed in velocity over time. The total perturbation duration was 1.1 s. (C) Vertical forces measured underneath the stepping leg, with the vertical dashed line indicating the instant of foot strike of the stepping leg (Fs). (D) Trial-specific Fs time stamps were used to time-lock EEG data for data analysis. For illustration purposes, EEG data shown in this figure is 10 Hz low-pass filtered single-trial EEG data time-locked to perturbation onset.

Participants performed four trial blocks with each leg. Each block consisted of 25 perturbations, with five repetitions in each perturbation direction in a random order. In this study we restricted our analyses to the forward and backward platform perturbations, merging the responses for the left and right-leg stepping trials (i.e. 40 trials in forward and 40 trials in backward directions).

Data collection

We recorded high-density EEG using a cap with 126 Ag–AgCl electrodes (WaveGuard, ANT Neuro, The Netherlands). The electrodes were fixed in the cap and distributed across the scalp according to the five percent electrode system (15). The EEG was referenced to the common average during acquisition. The ground electrode was placed on the left mastoid. A biosignal amplifier (REFA System, TMSi, The Netherlands) recorded the EEG at 2048 Hz without any filters, except for a hardware low-pass filter at 552 Hz. To monitor physiological activity that could present artifacts in the EEG, we also recorded electrical activity of the left eye in the vertical and horizontal direction (electrooculogram, EOG) using adhesive Ag–AgCl electrodes. The EOG was recorded from electrodes placed slightly under the left eye (vertical eye movement) and at the outer canthus of the left eye (horizontal eye movement).

Body movements were recorded using an 8-camera 3D motion analysis system (Vicon motion systems, United Kingdom) at a sample rate of 100 Hz. For this purpose, a total of 23 reflective markers (PlugInGait Full-body AI model excluding the head and arm markers; Vicon Nexus software 2.7.1) were attached to anatomical landmarks on the participants' body.

Processing and analysis

Force plate data were used to identify the moment of foot strike during a trial (see figure 1). The threshold for foot strike identification was set at a participant-specific level of 10% bodyweight loading on one leg. Foot strikes were visually verified by a subsequent lack of foot marker (ankle, heel or toe) movement following an identified foot strike. We discarded trials with foot strikes occurring beyond the constant velocity phase of the perturbation (i.e. 0.8 s post perturbation onset) for further analysis to avoid potential effects of platform deceleration on the balance recovery response (16).

Markers were labeled and reconstructed in a batch preprocessing pipeline. Occluded markers on the hip or trunk segment were gap-filled with a rigid body fill algorithm when at least three other markers of the body segment were visible. Other missing markers were gap filled using the Vicon Woltring filter, but only if they did not

overlap foot strike event (± 0.5 s) and lasted a maximum of 50 frames. Marker data were imported to MATLAB and 10 Hz low-pass filtered (5th order Butterworth IIR filters, zero-phase shift). The foot strike events were merged into the EEG datasets.

Margin of stability

Our behavioral outcome of interest was the margin of stability (MoS) at the instant of foot strike, as an instantaneous measure of postural stability. The MoS is an established measure of dynamic stability that takes into account both the position and the velocity of the center of mass (CoM) relative to the boundary of the base of support (BoS). The MoS (in meters) is calculated according to Eq. (1).

$$MoS = XcoM - BoS \tag{1}$$

$$XcoM = x + \frac{\dot{x}}{\omega_0} \tag{2}$$

with the extrapolated center of mass (XcoM, Eq. 2; 17) derived from the CoM position x and its velocity $\dot{x}$ in the anterior–posterior direction, normalized by ω_0 (the ratio between Earth's gravitational constant $g = 9.81$ m/s2 and leg length l in meters, Eq. 3).

$$\omega_0 = \sqrt{\frac{g}{l}} \tag{3}$$

A MoS well above zero indicates a stable posture. Yet, once some (theoretical) critical value of 'good stability' has been reached, any further increment in MoS is considered to not have additional relevance for maintaining dynamic stability. A low MoS indicates a less stable postural state as the CoM is approaching the boundary of the BoS. A MoS value of zero or lower means there is no more margin for the XcoM to the BoS and a fall is imminent if no corrective response is executed.

In forward trials, we used the toe marker of the stepping leg as the BoS. For backward foot strikes we used the heel marker of the stepping leg as the BoS.

EEG pre-processing

EEG and EOG data were preprocessed in MATLAB using functions of the EEGLAB toolbox (18). Data were bandpass filtered (2–200 Hz, consecutive high-pass and low-pass 5th order Butterworth IIR filters, zero-phase shift). Channels were checked for flat lines, outliers (amplitude and kurtosis > 5 SD) and low correlation with other channels (threshold 0.7). After removing noisy channels, the average reference was computed, and the power at 50 Hz is estimated and channels or trials above 4 SD are

rejected. Continuous data were downsampled to 512 Hz and epoched per trial with 3 s prior to and 6 s post perturbation onset. Noisy epochs were automatically rejected (amplitude threshold > 6 SD) before independent components analysis (Infomax ICA) was computed. Independent components were rejected based on being excessively noisy and of non-brain origin (mean = 10 accepted components, SD = 2.75 accepted components). Artifact-reduced EEG was obtained by back-projection of the retained independent components.

Generalized eigendecomposition

We applied generalized eigendecomposition (GED), a multivariate source-separation method, on the clean EEG data in order to derive a spatial filter that is optimized for theta (3–8 Hz) activity (19). We performed GED to create a spatio-temporal filter optimized for theta activity, which is superior to ICA for hypothesis-driven dimension-reduction (19). Computation of the GED on fewer components resulting from ICA cleaning does not affect the GED as GED is defined for any rank matrix (19). Two covariance matrices were constructed corresponding to theta-band filtered data (matrix S) and broadband data (matrix R) (Eq. 4). The generalized eigendecomposition on these two matrices returns a set of eigenvectors (W) and corresponding eigenvalues *(Λ)*, where the eigenvector associated with the largest eigenvalue is a set of channel weights (spatial filter) that maximizes the relative energy in the theta band.

$$SW = RW\Lambda \tag{4}$$

This generalized eigenvalue equation solves the generalized Rayleigh quotient and is often used in machine learning and brain-computer-interface research (19-21).

One spatial filter with a midfrontal topography and the largest eigenvalue, was selected per participant for further analysis of the EEG data. The GED component time series was computed as $w^T X$, where X is the channel time series data. The corresponding spatial map was computed as $w^T S$ (21).

Time-frequency analysis

The GED component time-series were further characterized through time–frequency decomposition. This was implemented by narrow-band filtering the time series at a range of frequencies through trial-by-trial convolution with complex Morlet wavelets. Equations (5) and (6) show the construction of the complex Morlet wavelets.

$$\Psi_f = e^{i2\pi f t} e^{-t^2/2s^2} \tag{5}$$

$$s = \frac{n}{2\pi f} \tag{6}$$

where t represents time, f is frequency, s is width of the Gaussian modulating the complex sine wave and n stands for the number of wavelet cycles. The number of cycles per wavelet controls the temporal and spectral precision tradeoff. We used 40 frequencies logarithmically spaced between 2 and 60 Hz. Wavelet widths were logarithmically spaced from 4 to 12 cycles. We selected a condition-specific baseline window of -1.4 to -0.7 s relative to perturbation onset. Individual time–frequency data were averaged in the frequencies of the theta rhythm (3–8 Hz) per direction.

Statistical analysis

To evaluate theta power increases after foot strike compared to baseline, sample-wise t tests of theta power were computed for each time point over 0–550 ms relative to foot strike to determine a difference relative to baseline theta power. This temporal window was selected based on the average time from foot strike to the end of platform motion (547 ms, that we rounded up to 550 ms for simplicity). The average baseline theta was averaged over a predefined window of -1400 to -700 ms relative to perturbation onset. To correct for multiple tests, p-values were corrected for false discovery rate (FDR; 22) with statistical significance assessed for critical $\alpha < 0.05$.

To evaluate directional differences in foot strike event latencies, we compared these latencies between backward and forward steps using t tests. In addition, to identify directional differences in theta dynamics time-locked to foot strike, we conducted sample-wise t tests over 0–550 ms. Given the multiple tests, p-values were corrected for FDR with statistical significance assessed for critical $\alpha < 0.05$.

To determine the relation between theta and dynamic stability at foot strike, we computed Spearman correlation coefficients between the margin of stability at foot strike (averaged across trials for each participant and direction) and theta power at each time point between 0 and 550 ms relative to foot strike.

Ethics approval and consent to participate

Participants provided written informed consent before participating in the experiment according to the experimental procedures approved by the Research Ethics Committee of the Radboud University Medical Center (Nijmegen, The Netherlands; Dossier NL67690.091.18). The experiments were conducted in line with the Declaration of Helsinki.

Results

Foot strike latency

From a total of 1203 collected trials (in the forward and backward direction) (mean = 80, SD = 1.7 trials per participant), 0.25% were rejected based on the stepping latency laying outside of the temporal window of constant velocity of the platform. An additional 1% of the trials were rejected due to missing marker data in the critical foot strike time window (see "Methods" section for rejection criteria).

Figure 2 shows the histograms of single trial foot strike latency distribution in the forward and backward direction. Across the forward and backward direction, we found an average foot strike latency of 611 ms (SD 58 ms) relative to perturbation onset. Foot strike latencies significantly differed between directions (t(14) = 3.09, p < 0.01) with faster foot strikes in the backward direction (mean = 596 ms, SD = 44 ms) compared to the forward direction (mean = 627 ms, SD = 46 ms).
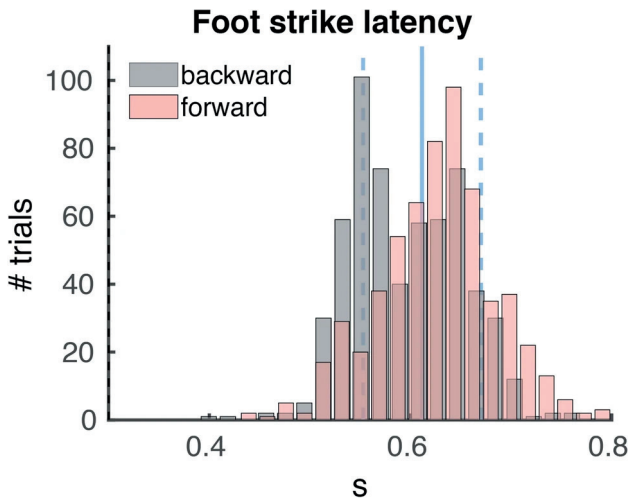
Figure 2. Foot strike latencies. Single trial foot strike latencies in the forward (red) and backward (grey) direction. The solid vertical blue line represents the overall mean foot strike latency (611 ms) and the dashed blue lines represent the standard deviation (58 ms). Presented foot strikes all occurred during the constant velocity phase of the platform perturbation (0.3–0.8 s).

EEG

The GED analysis yielded midfrontal topographies for all participants (figure 3A). Time–frequency analysis of midfrontal GED component data time-locked to perturbation onset showed the characteristic patterns of midfrontal theta frequency power increase

4
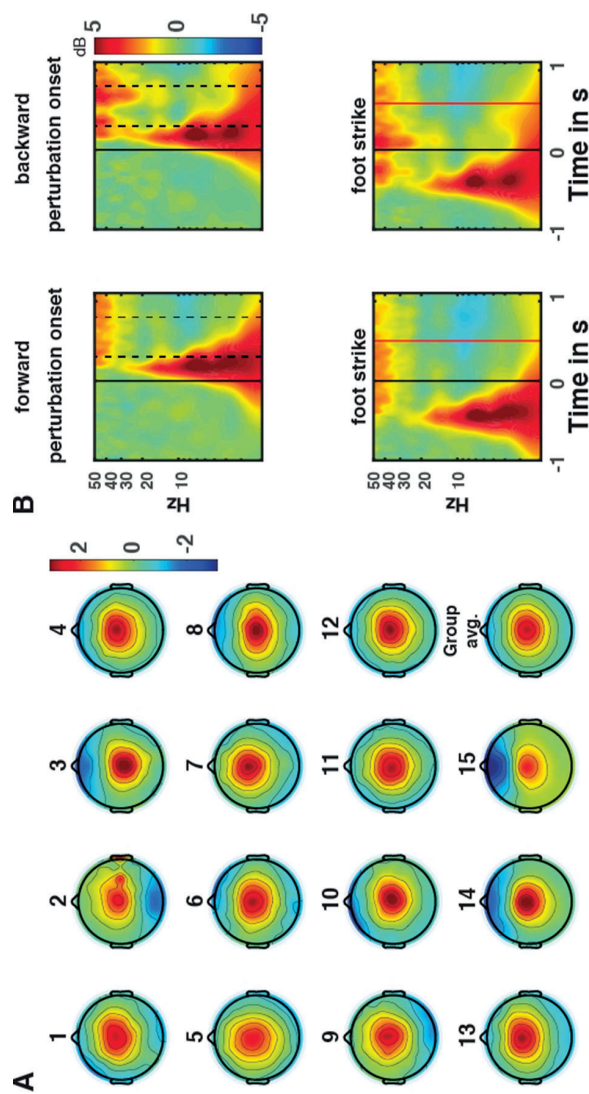
Figure 3. Characteristics of midfrontal GED component data. (A) Participant-specific scalp topographies of the spatial filter with the largest eigenvalue and a midfrontal topography (normalized scale). The group average (Group avg.) scalp topography is presented in the bottom right figure. (B) Group averaged time–frequency results. Top row illustrates forward and backward time–frequency analysis of perturbation time locked EEG data, with the vertical solid line indicating perturbation onset. The vertical dashed lines indicate the start of platform constant velocity (0.3 s) and the end of the constant velocity phase (0.8 s). Bottom row illustrates time–frequency analysis of foot strike event time locked EEG data. The black vertical line at 0 s indicates the moment of foot strike and the vertical red line represents the average end of platform motion relative to foot strike in the forward or backward direction. Figures were created with the EEGlab toolbox.

compared to baseline for both forward and backward directions (top panels Figure 3B). In addition to theta, delta (0.5–4 Hz), alpha (9–12 Hz) and low-gamma (40–50 Hz) band power increase is observed following perturbation onset. Time locked to foot strike we observe a theta power increase (bottom panels of figure 3B). Note that because of our focus on balance monitoring and a priori hypothesis, we here restrict our analyses to the theta band. In the backward direction, we also observed a longer-lasting theta power increase that was not evident in the forward direction.

Theta power following foot strike event

Average theta power during backward stepping trials was significantly stronger compared to baseline over 0–540 ms post foot strike (see thick black line figure 4A). Theta power following foot strike over 0–540 ms was $Mean_{forward} = 0.1$ dB, $std_{forward} = 1.36$ dB, $mean_{backward} = 0.97$ dB, $std_{backward} = 1.39$ dB. Forward stepping trials did not show differences in theta dynamics relative to baseline. In addition, we found significantly stronger foot-strike related theta power for backward compared to forward stepping over 280–550 ms post foot strike (see figure 4).

Time series correlation between theta power and margin of stability

The average theta power in the backward direction per participant showed a significant positive correlation with the average MoS at foot strike (see figure 4B). This indicates that stronger theta power was observed in individuals with comparatively large margins of stability at foot strike. These correlations were significant between 110 to 340 ms following foot strike. We did not find a significant correlation for the MoS at foot strike and theta power in the forward stepping direction.

Foot strike time locked theta dynamics may facilitate performance adaptation

We had expected to find *negative* correlations between the MoS at foot strike and theta power, as our previous study demonstrated that theta dynamics scale with the intensity of a balance perturbation (i.e. platform acceleration) as well as with its anticipated impact on postural stability (7,8), suggesting that theta dynamics play a role in balance monitoring. However, contrary to our hypothesis and previous findings, we found a significant *positive* correlation between MoS and theta power in the backward stepping direction. To further investigate this unexpected finding, we performed an explorative post hoc analysis to evaluate the potential role of the observed midfrontal theta dynamics at foot strike. Importantly, the observed MoS values at foot strike were all well above zero (see figure 5A), suggesting that stability was not threatened at foot strike. Therefore, we considered other cognitive roles of foot strike related theta dynamics that may potentially explain our findings.
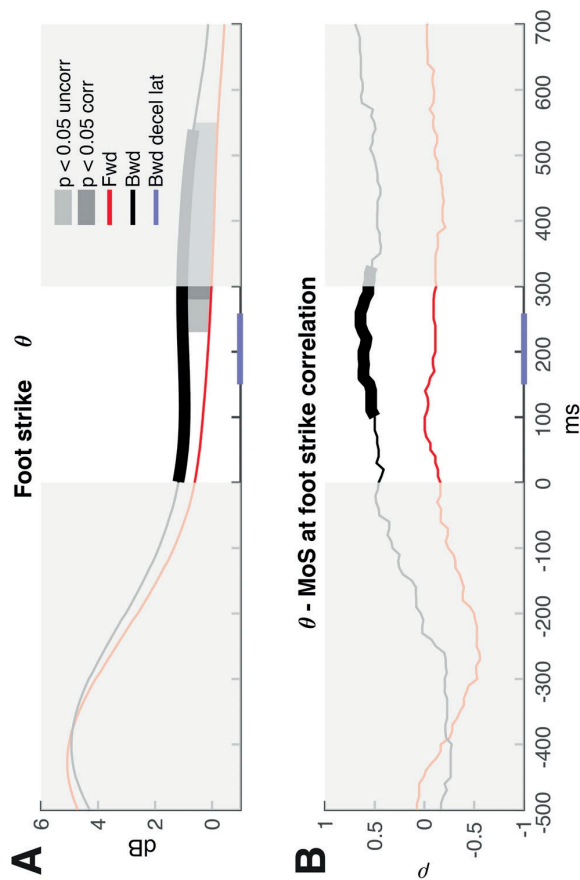
Figure 4. Foot strike time-locked theta time series. (A) Average theta time series for both stepping directions, with forward (Fwd) stepping indicated in red and backward (Bwd) stepping indicated in black. The highlighted white background indicates the temporal window where platform deceleration effects on theta dynamics are minimal. Significant difference in theta power between backward foot strikes relative to baseline with corrected false detection rate (fdr) is presented with a thicker line. Significant differences in theta power dynamics between stepping directions are indicated with dark grey (fdr corrected, 'corr') and light grey (uncorrected, 'uncorr'). The horizontal blue line on the x-axis represents the average latency of platform deceleration onset (Bwd decel lat) relative to the instant of foot strike and standard deviation during backward stepping trials. (B) Spearman correlation over time of margin of stability (MoS) at foot strike with theta power. Significant correlation time window for backward foot strikes is indicated with a thicker line.

Theta dynamics have commonly been studied in simplified cognitive control and feedback paradigms (button press response performance), indicating that theta dynamics facilitate feedback processing and adaption of response performance during learning (23,24,25). The positive correlation between theta and MoS may indicate that participants who initially take too large steps (as a function of greater MoS values) adjust their step lengths towards the end of the experiment in a feedback-based optimization process (indicated with high theta values). Thus, we investigated whether we could identify any participants who adapted their MoS at foot strike (that is, they saved energy by making smaller steps to successfully recover balance), with repeated perturbations and whether there would be a relation with theta dynamics. In particular, we investigated whether stronger theta power would be present in participants who adapted their stepping performance, thus gradually changing their MoS values at foot strike across repeated perturbations of equal and predictable intensity in the backward direction. Although generating smaller MoS may imply bringing balance at risk, MoS values were always large enough to achieve stability and thus may suggest that smaller MoS was generated to save energy rather than generating greater MoS. We labeled participants as "adapters" if MoS at foot strike decreased over trials (that is, they used smaller steps to successfully recover balance), or as "non-adapters" if their MoS was not significantly different over the course of the experiment (figure 5A). There were 7 adapters that individually showed significant and moderately strong negative correlations between MoS at foot strike and trial progression ($\rho = [-0.66: -0.55]$, $p < 0.01$), and 8 non-adapters with non-significant correlations between MoS and trial number ($\rho = [-0.29: 0.1]$, all $p > 0.05$). Of note, the segregation of adapters and non-adapters through significant correlations, resulted in a median split based on correlation magnitude as observed in figure 5B.

We averaged the MoS over the first five trials to investigate whether the MoS in the beginning differed between adapters and non-adapters. Similarly, we checked whether the MoS at foot strike differed between the two groups over average of the last five trials. We found that over the first five trials, adapters generated greater MoS compared to non-adapters ($p = 0.01$, ranksum 43, median$_{adapters} = 0.22$ m, IQR$_{adapters} = 0.03$ m, median$_{non\text{-}adapters} = 0.17$ m, IQR$_{non\text{-}adapters} = 0.04$ m). MoS values averaged over the last five trials did not differ between adapters and non-adapters ($p = 0.7$, ranksum 45, median$_{adapters} = 0.16$ m, IQR$_{adapters} = 0.05$ m, median$_{non\text{-}adapters} = 0.16$ m, IQR$_{non\text{-}adapters} = 0.06$ m). In addition, foot strike MoS values averaged over the first five trials negatively correlated with the slope of adaptation ($\rho = -0.58$, $p = 0.03$).
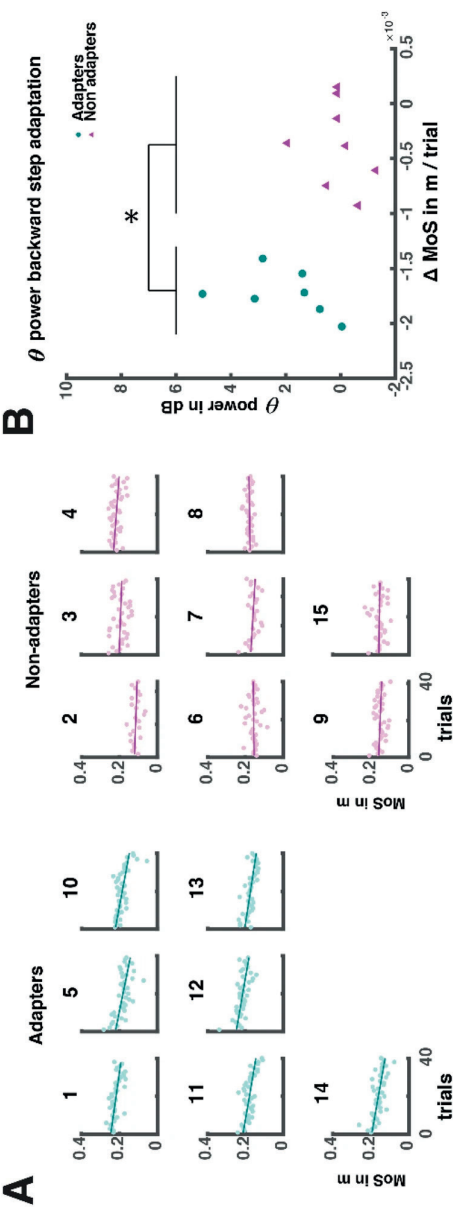
Figure 5. Adaptation of margin of stability at foot strike over the experimental time course for backward perturbations. (A) Participant specific margins of stability (MoS) are presented on the y-axis in meters and the trial order is presented on the x-axis. Adapters and non-adapters were classified based on significant correlations of MoS (in meters) change over trials. Numbers above plots represent the participant number. (B) Theta power as a function of adaptation slope in change of MoS in meters per trial. Significant difference in average theta power between adapters and non-adapters is indicated with *, p=0.02.

4

For each participant, we averaged the theta power time series that was also used for the time series in figure 4. The start of the window was chosen to match the earliest time point where the correlation of MoS at foot strike with theta power reached significance, and the end of the window corresponded to ~ 900 ms post perturbation. As evident changes in theta dynamics are observed as early as 100 ms post event onset (5,7,26), this time window limits the influence of possible theta dynamics induced by the platform deceleration (800 ms after perturbation onset; see "Methods").

We observed stronger theta modulations at foot strike in adapters compared to non-adapters (Wilcoxon rank sum test median$_{adapters}$ = 1.40 dB, IQR$_{adapters}$ = 2.16 dB, median$_{non-adapters}$ = 0.12 dB, IQR$_{non-adapters}$ = 0.73 dB, ranksum = 44, p = 0.02), indicating that participants who adapted their MoS over the time course of the experiment showed stronger theta power following foot strike. The correlation of theta with adaptation slope (the change in MoS with trial count) did not reach significance (Spearman ρ = − 0.43, p = 0.11; Pearson r = − 0.48, p = 0.07) see figure. 5B).

Discussion

The goal of our study was to clarify the balance monitoring role of the theta dynamics following foot strike of a reactive stepping response. We expected that the foot strike event requires a cognitive balance monitoring assessment, which would manifest as an increase of midfrontal theta power. Our results indicate that midfrontal theta power increased following a foot strike for the backward direction only. In addition, we hypothesized that these theta dynamics represent the balance monitoring of the new postural state after foot strike and predicted that stronger theta dynamics scale with postural threat (i.e. lower MoS) at foot strike. Interestingly and opposite to our hypothesis, the correlation analysis of theta power with the MoS at foot strike revealed *greater* stability related to stronger theta power following foot strike, which contradicts previous findings of midfrontal theta and its relation to postural stability. In a post hoc analysis we explored whether midfrontal theta dynamics related to response adaptation by distinguishing between individuals who adapted their MoS during stepping responses over the experimental duration and those who did not (i.e., adapters vs non-adapters). The results of this analysis showed that cortical theta power of adapters was significantly stronger post foot strike compared to non-adapters.

Cortical theta dynamics following foot strike

The finding of a significantly increased theta power following foot strike of a reactive backward step may seem in agreement with its proposed role in stability monitoring, yet the observed positive correlation of theta power with MoS argues against such a role in this phase of the balance recovery response. For the interpretation of balance monitoring related cortical dynamics, it is important to note that the increased theta power reported here already presented itself in the constant velocity phase of the perturbation profile, thus excluding a potential confounding effect of platform deceleration on theta power, at least for the initial ~ 300 ms post foot strike.

The presently observed positive correlation between MoS and theta power is inconsistent with previous literature that reported negative correlations between theta power and postural stability, suggesting that theta indexes to what extent stability is at risk (5,27). It must be mentioned, though, that in our experiment the participants' stability was never at risk once the stepping foot had landed, as the observed MoS values were well above zero (~ 17.5 cm on average) and participants never needed a second step to recover balance. This lack of challenge to stability following foot strike in response to our relatively low-intensity perturbations may (at least partly) explain the discrepancies with previous findings. Yet, the significant *positive* correlation that we found raised the question whether the theta dynamics following foot strike may have facilitated a different cognitive process. This led us to conduct a secondary explorative analysis, the results of which will be elaborated on below.

Foot strike direction and theta

Our results indicate differences in cortical theta dynamics for foot strike directionality with greater theta power dynamics after backward compared to forward steps. It is interesting that we only observed a significant increase of midfrontal theta in the backward direction, which suggests that there may be a greater need for cortical involvement following foot strike in this direction. Despite the fact that the perturbation intensity was not very challenging in either direction, backward reactive steps may still have been perceived as more difficult than forward reactive steps, with MoS values in the latter direction being larger by ~ 4 cm on average. While the imposed perturbation intensities in this study were higher than the stepping thresholds in either direction, stepping thresholds also differ across direction, with lower thresholds in the backward (0.66 m/s2) compared to forward direction (1.09 m/s2) for the presently used perturbation waveform (13). Yet, the perturbation intensities where young participants need more than one step to recover balance are substantially higher than those used in the present study (1.5 m/s2), as previous

work has reported multiple stepping thresholds of 4.5 m/s2 (forward) and 3.5 m/s2 backward (28,29). Hence, while in the present study stability was never at risk following foot strike, the relative challenge was slightly larger in the backward than the forward direction.

Another possible explanation for the directional differences may be sought in the role of visual input that differs between stepping directions. Theta dynamics have been shown to increase in walking with eyes closed compared to eyes open (30), suggesting that differences in theta dynamics arise from cortical engagement of sensory areas when visual input is present to a lower extent or missing at all. During forward stepping we can rely on visual input of where we will place our foot while stepping, whereas in the backward stepping direction this information is not available to us. Therefore, the lack of visual input in the backward direction may result in an increase of theta dynamics during backward stepping.

Theta power time locked to foot strike may facilitate monitoring of step performance

Cognitive control and feedback processes are facilitated by the theta frequency band, suggesting that theta dynamics are involved in feedback processing and adaptation of response performance during task learning (23,24,31). Therefore, we explored whether a similar process may have been at work in our experiment by identifying whether theta dynamics differed between participants who did and those who did not adapt their postural stability at foot strike over the time course of the experiment.

We reasoned that naïve participants would gradually become more familiar with the platform perturbations—which intensities were kept constant throughout the experiment—and learn to optimize their step responses. Successful stepping with incrementally smaller MoS (i.e. taking smaller steps) may have reflected learning throughout the course of the experiment that enabled participants to maintain stability while adopting a more energetically favorable strategy. We did not instruct participants to adapt their behavior, and thus the adaptation effects reflected a spontaneous strategy that approximately half of the participants deployed.

We expected this gradual step adaptation to be most evident in those participants who took (unnecessary) large steps at the start of the experiment with, consequently, a higher *average* MoS value across the experiment. We reasoned that this may explain the unanticipated *positive* correlation between theta power and MoS in our experiment. The explorative post hoc analysis indeed revealed that adapters showed stronger theta modulations following foot strike than did non-adapters. These findings are in line with

previous studies reporting stronger theta modulations in participants who adapted their task performance in other types of tasks (23-25) In addition, adapters showed greater theta dynamics compared to weak adapters in a performance feedback task (32). Our present results may therefore hint towards a role of midfrontal theta power representing performance monitoring post foot strike for optimizing the reactive stepping response, rather than monitoring whether balance is at risk, at least for the particular perturbation protocol that we used. Future studies may further address this by systematically investigating trial to trial changes in theta dynamics and adaptation of step performance in response to balance perturbations to investigate whether the correlation between MoS and theta changes over time as a function of adaptation.

Limitations

We identified some limitations that should be considered for future studies investigating cortical dynamics time locked to reactive balance steps. Importantly, we identified that theta dynamics may facilitate different monitoring roles throughout the postural response and therefore the experimental design should be carefully considered with regard to the specific role of interest.

Perturbations used in our experimental paradigm may not have been challenging enough to study the monitoring of postural stability at foot strike in healthy young participants. In our study, we used fixed intensities that were well below their multiple stepping threshold in both directions. Yet, it must be mentioned that the presently used experimental protocol was devised for comparing reactive stepping behavior across multiple groups, including people with stroke. Because people with stroke experience substantial difficulties in reactive stepping, we purposely selected a relatively low perturbation intensity of 1.5 m/s^2, which roughly corresponds to the 25% percentile of multiple stepping thresholds in people with stroke as reported by (28). It would therefore be of interest to evaluate whether the anticipated negative correlation between theta dynamics and MoS may be present in people with stroke or other clinical populations with impaired reactive stepping responses. Yet, for future studies in young adults we suggest to use higher perturbation intensities that challenge the participants' postural stability at foot strike.

In addition, balance perturbations of similar intensities are experienced as more difficult in the backward than the forward direction. Thus, our results may be biased to finding stronger theta dynamics in the backward direction. Therefore, we suggest future studies to use equally challenging perturbations in either direction, for instance by tailoring these to the individual's direction-specific multiple stepping threshold, to allow better comparison of cortical markers.

While it would have been of interest to study trial-to-trial MoS adaptions, the randomized perturbation directions only allowed us to focus on long term adaptation over the course of the experiment. Future studies on trial-to-trial adaptations should include sequences of multiple perturbations in the same direction. In addition, such studies may want to use shorter ITI durations than those used in the present study (8 s), as it was previously shown that a potential learning effect in a Stroop task paradigm, was reduced when the inter-trial interval (ITI) was greater than 2 s (33). Yet, it remains to be studied whether a similar decay is also applicable to short-term adaptations in balance responses.

Clinical implications

Many neurological conditions cause balance impairments that drastically reduce the quality of life of people affected. In addition to the aforementioned studies of reactive stepping related cortical dynamics in people with stroke, our present results may also inform future studies in people with Parkinson's disease. It is known that the dopaminergic pathway, involving the striatum and the rostral cingulate zone are affected in Parkinson's disease (34). These brain areas are also involved in learning and action adaptation from response outcomes, through theta dynamics (and the event related negativity, ERN/ N1) representing reinforcement-learning to optimize task performance (For an extensive review on performance monitoring, see (35). Therefore, clarification of foot strike related cognitive underpinnings are an interesting area of study for gaining novel insight into mechanistic underpinnings of balance control deficits in people with PD.

Conclusion

We aimed to investigate the balance monitoring role of midfrontal theta dynamics following foot strike during reactive stepping. The positive correlation between theta dynamics following backward foot strikes and postural stability contradicts previous literature on the relation of theta dynamics and stability. Based on our post hoc analysis results we speculate that the observed increase of theta power following foot strike was not related to stability monitoring but instead may indicate cortical dynamics related to performance monitoring of the response outcome. It is an interesting question for future studies whether theta dynamics following foot strike may reflect the anticipated balance monitoring role by studying young adults at higher perturbation intensities, or balance-impaired individuals at the presently used intensities. When selecting the experimental protocol, these future studies should carefully consider the possible cognitive roles theta may facilitate at foot strike.

Data availability

The datasets generated and/or analyzed during the current study are not publicly available due to ongoing data collection and analysis for the "*Roads to recovery*" study. Data from this study are available from the corresponding author on reasonable request.

Abbreviations

CoM: Center of mass
BoS: Boundary of the base of support
MoS: Margin of stability
xCoM: Extrapolated center of mass
EEG: Electroencephalogram
EOG: Electrooculogram
ERN: Event related negativity
ICA: Independent component analysis
**GED:** Generalized eigendecomposition
FDR: False discovery rate
PD: Parkinson's disease

4

References

1. Rogers, M. W., Hedman, L. D., Johnson, M. E., Cain, T. D. & Hanke, T. A. Lateral stability during forward-induced stepping for dynamic balance recovery in young and older adults. *J. Gerontol. A Biol. Sci. Med. Sci.* 56(9), M589–M594 (2001).

2. Mansfield, A., Inness, E. L., Wong, J. S., Fraser, J. E. & McIlroy, W. E. Is impaired control of reactive stepping related to falls during inpatient stroke rehabilitation?. *Neurorehabil. Neural Repair* 27(6), 526–533 (2013).

3. Varghese, J. P., McIlroy, R. E. & Barnett-Cowan, M. Perturbation-evoked potentials: Significance and application in balance control research. *Neurosci. Biobehav. Rev.* 83, 267–280 (2017).

4. Solis-Escalante, T. *et al.* Cortical dynamics during preparation and execution of reactive balance responses with distinct postural demands. *Neuroimage* 188, 557–571 (2019).

5. Hülsdünker, T., Mierau, A., Neeb, C., Kleinöder, H. & Strüder, H. K. Cortical processes associated with continuous balance control as revealed by EEG spectral power. *Neurosci. Lett.* 10(592), 1–5 (2015).

6. Mierau, A. *et al.* Cortical correlates of human balance control. *Brain Topogr.* 30(4), 434–446 (2017).

7. Solis-Escalante, T., Stokkermans, M., Cohen, M. X. & Weerdesteyn, V. Cortical responses to whole-body balance perturbations index perturbation magnitude and predict reactive stepping behavior. *Eur. J. Neurosci.* 54(12), 8120–8138 (2021).

8. Stokkermans, M., Solis-Escalante, T., Cohen, M. X. & Weerdesteyn, V. Midfrontal theta dynamics index the monitoring of postural stability. *Cereb. Cortex.* https://doi.org/10.1093/cercor/bhac283 (2022).

9. Torres-Oviedo, G. & Ting, L. H. Muscle synergies characterizing human postural responses. *J. Neurophysiol.* 98(4), 2144–2156 (2007).

10. Henry, S. M., Fung, J. & Horak, F. B. EMG responses to maintain stance during multidirectional surface translations. *J. Neurophysiol.* 80(4), 1939–1950 (1998).

11. Lee, P.-Y., Gadareh, K. & Bronstein, A. M. Forward–backward postural protective stepping responses in young and elderly adults. *Hum. Mov. Sci.* 34, 137–146 (2014).

12. McIlroy, W. E. & Maki, B. E. Age-related changes in compensatory stepping in response to unpredictable perturbations. *J. Gerontol. A Biol. Sci. Med. Sci.* 51(6), M289–M296 (1996).

13. de Kam, D., Kamphuis, J. F., Weerdesteyn, V. & Geurts, A. C. H. The effect of weight-bearing asymmetry on dynamic postural stability in healthy young individuals. *Gait Posture.* 45, 56–61 (2016).

14. Oostenveld, R., & Oostendorp, T. F. (2002). Validating the boundary element method for forward and inverse EEG computations in the presence of a hole in the skull. *Human Brain Mapping*, 17, 179– 192. https://doi.org/10.1002/hbm.10061

15. Nonnekes, J. *et al.* Are postural responses to backward and forward perturbations processed by different neural circuits?. *Neuroscience* 15(245), 109–120 (2013).

16. Carpenter, M. G., Thorstensson, A. & Cresswell, A. G. Deceleration affects anticipatory and reactive components of triggered postural responses. *Exp. Brain Res.* 167(3), 433–445 (2005).

17. Hof, A. L., Gazendam, M. G. J. & Sinke, W. E. The condition for dynamic stability. *J. Biomech.* 38(1), 1–8 (2005).

18. Delorme, A. & Makeig, S. EEGLAB: An open source toolbox for analysis of single-trial EEG dynamics including independent component analysis. *J. Neurosci. Methods* 134(1), 9–21 (2004).

19. Cohen MX. A tutorial on generalized eigendecomposition for source separation in multichannel electrophysiology. arXiv:210412356v1 [q-bioQM] [Internet]. 2021 Apr 26 [cited 2021 May 27]. Available from: https://arxiv.org/pdf/2104.12356.pdf.

20. Blankertz, B., Tomioka, R., Lemm, S., Kawanabe, M. & Muller, K. Optimizing spatial filters for robust EEG single-trial analysis. *IEEE Signal Process. Mag.* 25(1), 41–56 (2008).

21. Haufe, S. *et al.* On the interpretation of weight vectors of linear models in multivariate neuroimaging. *Neuroimage* 15(87), 96–110 (2014).

22. Benjamini, Y. & Yekutieli, D. The control of the false discovery rate in multiple testing under dependency. *Ann. Stat.* 29(4), 1165–1188 (2001).

23. Cavanagh, J. F., Frank, M. J., Klein, T. J. & Allen, J. J. B. Frontal theta links prediction errors to behavioral adaptation in reinforcement learning. *Neuroimage* 49(4), 3198–3209 (2010).

24. Cohen, M. X. & Donner, T. H. Midfrontal conflict-related theta-band power reflects neural oscillations that predict behavior. *J. Neurophysiol.* 110(12), 2752–2763 (2013).

25. Cohen, M. X. Midfrontal theta tracks action monitoring over multiple interactive time scales. *Neuroimage* 1(141), 262–272 (2016).

26. Payne, A. M., Hajcak, G. & Ting, L. H. Dissociation of muscle and cortical response scaling to balance perturbation acceleration. *J. Neurophysiol.* 121(3), 867–880 (2019).

27. Slobounov, S., Cao, C., Jaiswal, N. & Newell, K. M. Neural basis of postural instability identified by VTC and EEG. *Exp. Brain Res.* 199(1), 1–16 (2009).

28. de Kam, D., Roelofs, J. M. B., Bruijnes, A. K. B. D., Geurts, A. C. H. & Weerdesteyn, V. The next step in understanding impaired reactive balance control in people with stroke: The role of defective early automatic postural responses. *Neurorehabil. Neural Repair* 31(8), 708–716 (2017).

29. van Duijnhoven, H. J. R. *et al.* Perturbation-based balance training to improve step quality in the chronic phase after stroke: A proof-of-concept study. *Front. Neurol.* 22(9), 980 (2018).

30. Oliveira, A. S., Schlink, B. R., Hairston, W. D., König, P. & Ferris, D. P. Restricted vision increases sensorimotor cortex involvement in human walking. *J. Neurophysiol.* 118(4), 1943–1951 (2017).

31. Cavanagh, J. F. & Frank, M. J. Frontal theta as a mechanism for cognitive control. *Trends Cogn. Sci. (Regul. Ed.)* 18(8), 414–421 (2014).

32. Rawls, E. *et al.* Feedback-related negativity and frontal midline theta reflect dissociable processing of reinforcement. *Front. Hum. Neurosci.* 13, 452 (2019).

33. Egner, T., Ely, S. & Grinband, J. Going, going, gone: Characterizing the time-course of congruency sequence effects. *Front. Psychol.* 16(1), 154 (2010).

34. Holroyd, C. B. & Coles, M. G. H. The neural basis of human error processing: Reinforcement learning, dopamine, and the error-related negativity. *Psychol. Rev.* 109(4), 679–709 (2002).

35. Ullsperger, M. Genetic association studies of performance monitoring and learning from feedback: The role of dopamine and serotonin. *Neurosci. Biobehav. Rev.* 34(5), 649–659 (2010).
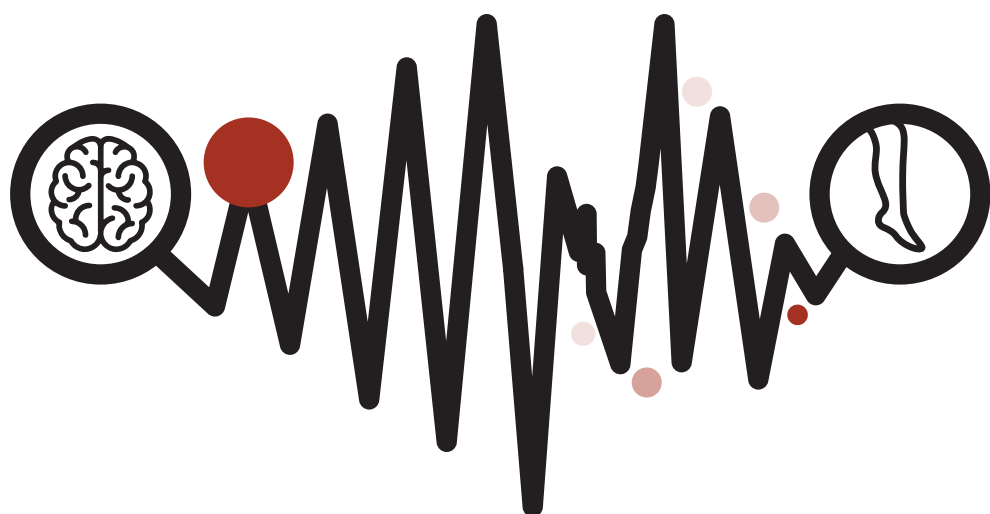
4

Distinct cortico-muscular coherence between step and stance leg during reactive stepping responses

Abstract

Balance recovery often relies on successful stepping responses, which presumably require precise and rapid interactions between the cerebral cortex and the leg muscles. Yet, little is known about how cortico-muscular coupling (CMC) supports the execution of reactive stepping. We conducted an exploratory analysis investigating time-dependent CMC with specific leg muscles in a reactive stepping task. We analyzed high density EEG, EMG, and kinematics of 18 healthy young participants while exposing them to balance perturbations at different intensities, in the forward and backward directions. Participants were instructed to maintain their feet in place, unless stepping was unavoidable. Muscle-specific Granger causality analysis was conducted on single step- and stance-leg muscles over 13 EEG electrodes with a midfrontal scalp distribution. Time-frequency Granger causality analysis was used to identify CMC from cortex to muscles around perturbation onset, foot-off and foot strike events. We hypothesized that CMC would increase compared to baseline. In addition, we expected to observe different CMC between step and stance leg because of their functional role during the step response. In particular, we expected that CMC would be most evident for the agonist muscles while stepping, and that CMC would precede upregulation in EMG activity in these muscles. We observed distinct Granger gain dynamics over theta, alpha, beta and low/high-gamma frequencies during the reactive balance response for all leg muscles in each step direction. Interestingly, between-leg differences in Granger gain were almost exclusively observed following the divergence of EMG activity. Our results demonstrate cortical involvement in the reactive balance response and provide insights into its temporal and spectral characteristics. Overall, our findings suggest that higher levels of CMC do not facilitate leg-specific EMG activity. Our work is relevant for clinical populations with impaired balance control, where CMC analysis may elucidate the underlying pathophysiological mechanisms.

Introduction

Performing daily activities (e.g. standing or walking) constantly challenges postural balance. With different postures and activities, continuous adaptation through contraction and relaxation of specific muscles allows the control of balance and the execution of corrective steps whenever these are needed. In the past decade, many studies using mobile EEG have provided evidence that the cortex plays an important role in postural control (1–3). This notion is in line with studies investigating postural control in people with cortical lesions (e.g. stroke), which reported deficient recruitment of the muscles involved in perturbation-evoked responses, including delayed onset latencies, lower response amplitudes, and aberrant coordination patterns across muscles (4,5).

Postural perturbations are known to elicit several event-related potentials, suggesting cortical involvement in the ensuing balance recovery responses. The initial P1 response (30-90 ms) is thought to represent proprioceptive sensory afferents (6), followed by the N1 (90 – 200 ms), which is suggested to reflect monitoring of postural stability (1,7–11). The N1 perturbation-related response is accompanied by a transient power increase of the theta (3-8 Hz) rhythm (12). Interestingly, the N1 and theta rhythm have been shown to predict the response outcome to a balance perturbation with stronger cortical dynamics for stepping responses compared to feet-in-place responses at similar perturbation intensities (12). Yet, little is known about the temporal evolution of cortical interaction with specific leg muscles that contribute to the generation of the balance correcting response (either directly or indirectly through cortico-cortical coupling with the motor areas).

Cortico-muscular coupling (CMC) is a powerful analysis tool to investigate functional connectivity between the cerebral cortex and muscles across the body. CMC is known to take place with the Tibialis Anterior (TA) and Soleus (SO) muscles at beta (15-25 Hz) frequencies during isometric contraction and gamma (40-80 Hz) frequencies during isotonic contraction (13,14). In addition, several studies reported beta frequency coupling with the medial Gastrocnemius (MG) and TA muscles during cyclic ankle movements (15). These findings suggest that multiple cortical frequency bands may couple to similar muscles during different muscle exercises. Until today, only a few studies have investigated CMC of dynamic human behavior related to postural control and gait. Moreover, studies investigating gait reported an increase in theta, alpha, and beta band CMC after foot strike with TA, Vastus Medialis (VM), Biceps Femoris (BF), Peroneus longus (PL), MG and SO muscles (16–18). Cortical involvement in the balance response is thought to occur during later phases of the balance recovery response

5

(19,20), which suggests that reactive step responses may coincide with strong CMC time locked to perturbation onset. Only a few studies investigated CMC during walking and standing balance (17,21). Muscle synergies showed strong coherence with cortical activity over the Piper rhythm (~40 Hz) during lateral balance perturbation of unipedal stance that led to feet-in-place responses (21). In addition, strong theta and alpha (8-13 Hz) band CMC dynamics were observed from cortex to MG, TA and PL muscles during physical standing perturbations leading to feet-in-place responses compared to visual perturbations while standing (17). This indicates that physical perturbations require more cortical control. Yet, their experimental setup only focused on the theta and alpha frequency bands averaged over a window of 1 second, thus lacking information on the temporal evolution of cortical interaction with the muscles during the balance response. In addition, beta and gamma frequency bands are motor task related rhythms, which may also be involved in the recruitment of balance responses.

The aim of this study was to investigate CMC from cortex to muscle through spectral Granger causality coupled to key events of the stepping response in balance. We hypothesized that CMC would occur over multiple frequency bands during stepping responses**.** In addition, we expected CMC to differ between the step and stance leg according to their differential muscle recruitment patterns inherent in executing the step response. In particular, we expected that stronger CMC would be most evident for the muscles involved in generating the greatest biomechanical contribution for the stepping movement (depending on the step and stance leg), and that an increase in CMC would precede changes in EMG activity in these muscles relative to foot off and foot strike event. Therefore, we conducted separate CMC analyses time-locked to perturbation onset, foot-off and foot strike event.

Materials & Methods

Twenty young healthy adults participated in this study. We analyzed a total of 18 datasets (8 female; age mean 23.9 years, sd 3.6 years) due to technical issues in two other datasets. All participants received ample information about the experiment and signed an informed consent document prior to the start of the experiment. Participants were financially compensated after completion of the study. None of the participants had a history of neuromuscular disease or any other impairment that could affect their performance in the experiment. The experimental procedure was approved by the Research Ethics Committee of the Radboud University Medical Center (Nijmegen, The Netherlands; Dossier 2018-4970). The experiments were conducted in line with the Declaration of Helsinki.

Experimental paradigm

Data used in this study were derived from a protocol to investigate theta power modulations related to balance monitoring by imposing leaning angles prior to perturbation (22). Participants were familiarized with the balance platform through a series of 28 forward and backward perturbations with increasing acceleration, delivered by the Radboud Falls Simulator (2,12,23,24). Participants stood barefoot on the movable platform with their feet at shoulder width and their arms crossed in front of the body and had to maintain three different initial leaning postures prior to a balance perturbation. At the beginning of each sequence, the participants were instructed about which leaning posture to maintain throughout the series of perturbations. Participants were instructed and encouraged to respond with feet-in-place responses following balance perturbations. A real-time 3D-motion data stream monitored the participants' posture and performance (Vicon motion systems, United Kingdom), such as maintaining leaning angle, excessive knee flexion and changes in leg weight bearing (which may indicate whether specific strategies to counteract balance perturbations were used).

Balance perturbation profiles consisted of 300 ms platform acceleration, 500 ms constant velocity and 300 ms deceleration (figure 1 B). Platform accelerations were randomized and ranged from 0.25 m/s^2 to 1.9 m/s^2 with a higher resolution at lower accelerations in both forward and backward sway direction (0.25,0.4,0.7,1.0,1.3,1.6,1.9 m/s^2). The initial experiment contained 15 sequences with 29 balance perturbations each (435 total). The first perturbation of a sequence always consisted of a low-intensity dummy trial and was not included in the analyses. For the analysis of the present study, we only considered the neutral stance conditions with forward and backward perturbation directions (i.e. 140 trials per participant).

Participants took a small break of five minutes after three consecutive sequences and were seated on a chair to prevent fatigue. After nine perturbation sequences, participants were given a twenty-minute resting break. The active experiment time was 2.5 hours and the preparation time was 2.5 hours, the complete lab visit lasted a maximum of 6 hours (including resting breaks).
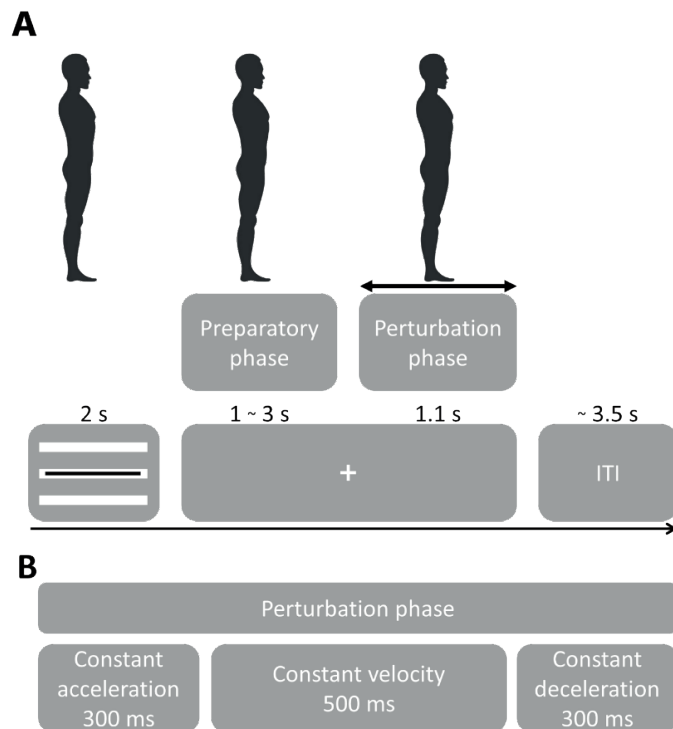
Figure 1. Experimental procedure. A, Participants were instructed to maintain a straight posture during the sequence of perturbations. Perturbation onset times were randomized as well as direction and acceleration. A visual cue tracking the participant's posture was presented for 2 s, followed by a fixation cross. Platform onset was randomized from 1~3 s followed by a perturbation that lasted 1.1 s. Following a perturbation, the platform returned to the initial position. At platform return, the visual feedback of the leaning posture was presented. Feedback for the leaning posture (important for the experimental setup in Stokkermans et al 2022) was presented through three white bars representing forward leaning (top bar), neutral stance (middle bar) and backward leaning (bottom bar). The black bar presented on top of the white bars, indicated the participant's real-time leaning angle. Participants were instructed to maintain the black bar on the white bar corresponding to the instructed leaning posture. The initial leaning posture had to be maintained while the fixation cross was presented ensuring that postural stability was controlled at platform perturbation. B, Platform perturbation profiles.

Data acquisition

We recorded high-density EEG using a cap with 126 Ag-AgCl electrodes (WaveGuard, ANT Neuro, The Netherlands). The electrodes were fixed in the cap and distributed across the scalp according to the five percent electrode system (25). The EEG data were referenced to the common average during acquisition. The ground electrode was placed on the left mastoid. A biosignal amplifier (REFA System, TMSi, The Netherlands) recorded the EEG at 2048 Hz without any filters, except for a hardware low-pass filter at 552 Hz. To monitor physiological activity that could present artifacts

in the EEG, we also recorded electrical activity of the left eye in the vertical and horizontal direction (electrooculogram, EOG) using adhesive Ag-AgCl electrodes. The EOG was recorded from electrodes placed slightly under the left eye (vertical eye movement) and at the outer canthus of the left eye (horizontal eye movement).

We recorded electrical activity bilaterally from five leg muscles (see figure 2; soleus (SO), tibialis anterior (TA), rectus femoris (RF), biceps femoris (BF), semitendinosus (ST)), using surface EMG electrodes (Mini Wave, Cometa systems, Italy). Muscle sites were shaved to remove hair, and the skin was scrubbed with skin preparation gel (Nuprep, MedCat) to improve skin conduction and cleaned with alcohol. The EMG amplifier (Wave plus wireless, Cometa, Italy) recorded muscle activity at 2000 Hz. Before the start of the experimental paradigm, the EMG signals of the muscles were carefully checked. This was done through observation of the EMG signal following instructions to contract the individual muscles during specific exercises.
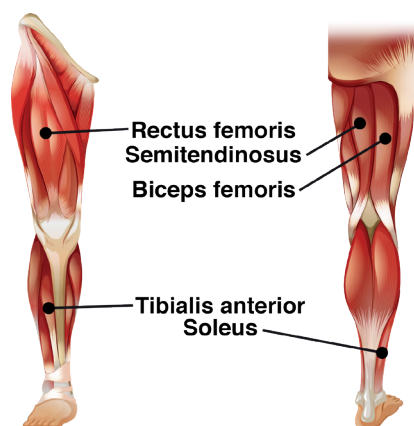
Figure 2. EMG electrode locations

Body movement was recorded using an 8-camera 3D motion analysis system (Vicon motion systems, United Kingdom) at a sample rate of 100 Hz. For this purpose, a total of 23 reflective markers (PlugInGait Full-body AI model excluding the head and arm markers; Vicon Nexus software 2.7.1) were attached to anatomical landmarks on the participants' body.

Ground reaction forces were recorded from two force plates (AMTI Custom 6 axis composite force platform, USA; size: 60 x 180 cm each; sampling rate: 2000 Hz) embedded in the moveable platform. Trials were recorded from -2 s to +5 s relative to the platform perturbation. Synchronization triggers were generated by the platform controller and recorded for post-hoc alignment of EMG, EEG and motion data.

EMG processing

The EMG signal was preprocessed in MATLAB using low-pass filtering with the 'filtfilt.m' function (125 Hz low-pass filtered 5th order Butterworth IIR filters, zero-phase shift), and downsampling to 250 Hz. EMG was separately preprocessed for EMG envelope visualization and Granger causality.

For EMG envelope visualization, the data were band-pass filtered (20-120 Hz band-pass 5th order Butterworth IIR filters, zero-phase shift), full-wave rectified, low-pass filtered (40 Hz low-pass 5th order Butterworth IIR filters, zero-phase shift), and normalized per muscle per subject to the maximum muscle activation at 0.7 m/s2 for feet-in-place responses. This normalization allowed us to evaluate the difference in activation between step and stance legs during stepping trials since both legs contributed equally in the feet-in-place trials. The acceleration of 0.7 m/s2 was the maximum platform acceleration where all participants were able to respond with feet-in-place in either direction.

Prior to Granger causality computation, we downsampled and normalized (z-score) the EMG activity. Then we subtracted the ensemble average rectified EMG from the single-trial EMG data per participant and muscle. This procedure is necessary for Granger causality analyses involving an event related potential to facilitate model-fitting and reduce non-stationarities (26; see figure 3C for an example on removing non-stationarities from EEG data).

EEG processing

For the preprocessing of EEG and EOG data, MATLAB functions of the EEGLAB toolbox were used (27). Continuous data were epoched into intervals of -2 to +3 s relative to perturbation onset. Data were bandpass filtered using the 'filtfilt.m' function (2-200 Hz, consecutive high-pass and low-pass 5th order Butterworth IIR filters, zero-phase shift) and common average re-referenced. Noisy channels were flagged for rejection based on a kurtosis >3 and a variance >3 and rejected based on visual inspection. In addition, epochs were visually inspected for noise. Independent components analysis (Infomax ICA) with a minimum of 90 and maximum of 125 principal components (depending on the rank of the EEG data) was run, and independent components were rejected based on being excessively noisy and of non-brain origin (mean = 91, sd = 16 rejected components; two data sets showed excessive noise resulting in a large mean). Back-projection of the retained independent components resulted in artifact-reduced EEG data. Noise rejected channels were interpolated.

Our and other studies indicated that midfrontal cortical activity plays a major role during the initial phase of the balance response regarding the monitoring and cortical control of the balance response (2,17,22). In addition, cortical (pre-)motor regions are located around the midfrontal head location. Therefore we chose a substantial amount of midfrontal electrodes, resulting in the 13 selected electrodes (FCz, Cz, CPz, C1, C2, CCP3h, CCP1h, CCP2h, CCP4h, FCC3h, FCC1h, FCC2h and FCC4h; see figure 3A for topographical locations) centered over the midfrontal scalp location for CMC analysis. Prior to the Granger causality computation, the ERP was subtracted from the single-trial data for both EMG and EEG. This process maintains spectral information of the data and reduces the non-stationarities in the signal (figure 3C).

5
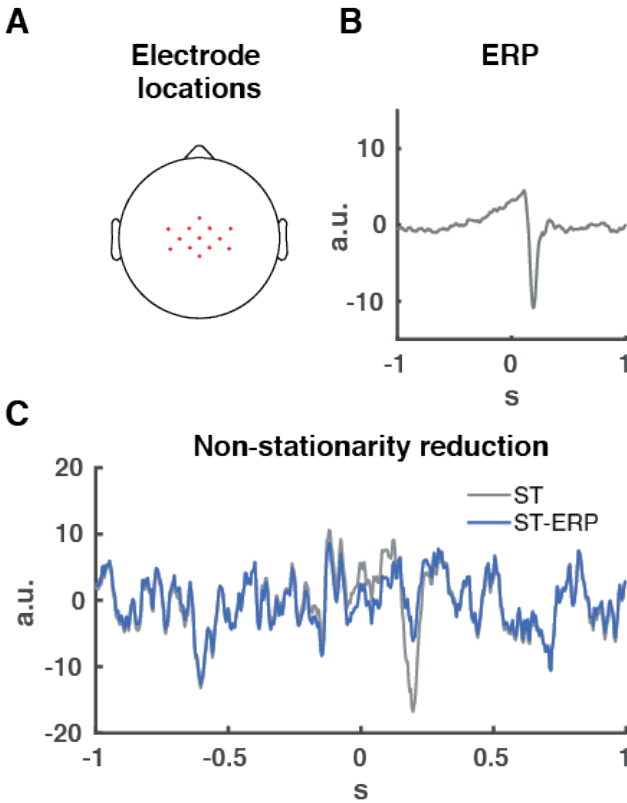
Figure 3. EEG electrode locations and ERP signal removal. A) 13 midfrontal electrode scalp locations averaged together for the Granger causality analysis. B) Participant EEG average event related potential (ERP) from midcentral electrode location CZ time-locked to perturbation onset. C) signal non-stationarity reduction. Time series of single trial (ST) EEG data from midcentral electrode location CZ time-locked to perturbation onset indicated in grey. Time series of ERP subtraction from single trial time series data (ST-ERP) in blue.

Data inclusion

We collected a total of 2491 trials and rejected 149 trials, based on flat lines and artifacts in EEG and EMG data. Of the remaining 2342 trials (mean = 130, sd = 19 trials per subject), 1177 were forward and 1165 were backward perturbations. In the forward direction there were 675 feet-in-place responses versus 502 step responses. In the backward direction, we recorded 565 feet-in-place responses and 600 step responses.

Granger causality analysis

We applied Granger causality analysis to compute the directional coupling from the cerebral cortex to the muscles between individual EEG channels and EMG data over 1 to 100 Hz with a resolution of 0.05 Hz. For the analysis we used the spectral Granger causality Matlab MVGC toolbox (28,29). We applied a sliding window of 400 ms to predict EMG activity from the EEG signal (using a smaller window would collapse the frequency interpretation of lower frequencies, whereas a larger window would diminish temporal accuracy). We used a model order of 100 ms, meaning we predicted muscle activity up to 100 ms ahead of the current EEG sample. This 100 ms model order was visually determined through time domain Granger causality tests of multiple participants, identifying a clear Granger causality increase relative to baseline (-1.4 to -0.75 s relative to perturbation onset) and a stationary baseline Granger causality. The time domain Granger causality analysis determined the Granger gain of cortical interaction averaged over all muscles. According to these parameters, Granger causality temporal data should be interpreted as a prediction of EMG from EEG over the past 400 ms window where EEG signal of sample t_0 predicts EMG activity up to sample t_{100} (up to 100 ms ahead).

Granger Causality analysis benefits from a large amount of data. To optimize the Granger causality outcome we conducted the analysis over a time interval of 4 seconds with a consistent amount of data for all frequency bands and individual muscles. Second, we included all step trials per participant, which resulted in a substantial number of 500 (forward) and 600 backward) trials (see 2.5 Data inclusion). In addition, we removed the ERP from both the EMG and EEG data to improve the signal stationarity (see 2.4 EEG processing). The sliding window approach of the Granger causality analysis provided by the MVGC toolbox (28,29) also improves analysis of non-stationary signals. The sliding window was sufficiently large to interpret low frequency (3-8Hz) data similar to the Peterson study (17). Lastly, the data was averaged over 13 midfrontal electrodes (see 2.4 EEG processing and figure 3C), which further increased the midfrontal Granger causality signal to noise ratio.

We conducted spectral Granger causality relative to three time-locking events to get a good alignment with the EMG activity. Due to the temporal sliding window of the Granger causality analysis, between-signal comparisons can only be made at specific time locked events. Therefore, we time-locked to three specific events at which we can temporally accurately compare EMG with Granger causality at time 0s. First, perturbation onset time-locked Granger causality analysis was done to investigate coupling with muscles immediately after perturbation. Secondly, Granger causality time-locked to foot-off event was computed to investigate CMC prior to step initiation and during stepping response. Finally, Granger causality time-locked to foot strike was done to investigate CMC prior to and after foot landing. For each time-locking event we averaged the Granger causality data over all 13 EEG electrodes, meaning that we analyzed one average cortical Granger causality time-frequency map for each muscle.

Statistical analysis

For EMG and CMC time series data, statistical tests were done over all time windows of the time-locked events. Interquartile range latencies were used to determine the upper temporal boundaries for statistical testing. Participant average foot off event latencies did not significantly differ between directions (Ranksum= 391, Z=1.8, p=0.07; median$_{forward}$ = 451 ms, IQR$_{forward}$ = 210ms, median$_{backward}$= 400 ms, IQR$_{backward}$ =202ms). In addition, foot strike latencies did not differ between step direction (Ranksum= 362, Z=0.9, p=0.23; median$_{forward}$ = 641 ms, IQR$_{forward}$ = 214ms, median$_{backward}$ = 629ms, IQR$_{backward}$=225ms). For convenience, we rounded the 75th percentile values up to foot off = 600 ms, foot strike = 800 ms. This resulted in the following analysis time windows; perturbation onset to 600 ms, -200 ms to 250 ms relative to foot off and -250 ms to 200 ms relative to foot strike. Please note that there is temporal overlap between these time windows. To determine whether significant EMG activity and CMC occurred relative to baseline activity in response to balance perturbations, multiple sample-wise t-tests were conducted time-locked to perturbation onset for each muscle per step and stance leg separately. Given the multiple tests computed in the time domain, the corresponding *p*-values were corrected for false discovery rate (FDR; 30). Statistical significance was assessed for critical α = 0.05. For EMG activity, an activity duration threshold of 100 ms and mean baseline activity +1SD (-500ms to 0ms relative to perturbation onset) was used to eliminate premature false positive significance results.

To determine differences between step and stance leg, significant differences between muscle specific step and stance leg EMG activity were computed using a sample-wise t-test. Differences in Granger gain for muscle-specific step and stance

legs were computed with sample-wise t-tests (p<.05, FDR correction). Temporal windows for significance testing were determined by foot-off and foot strike latencies.

Results

Corticomuscular coupling

Time-frequency analysis averaged over all 13 midfrontal EEG electrodes and muscles in the forward and backward direction revealed increases in Granger causality over multiple frequency bands in response to perturbation onset (figure 4). The frequencies of interest for further analysis were in the theta (θ: 3-8 Hz), alpha (α: 10-13 Hz), beta (β: 15-22 Hz), low gamma (γ_{lo}: 25-40 Hz) and high gamma (γ_{hi}: 50-85 Hz) ranges, and are indicated with dashed boxes.
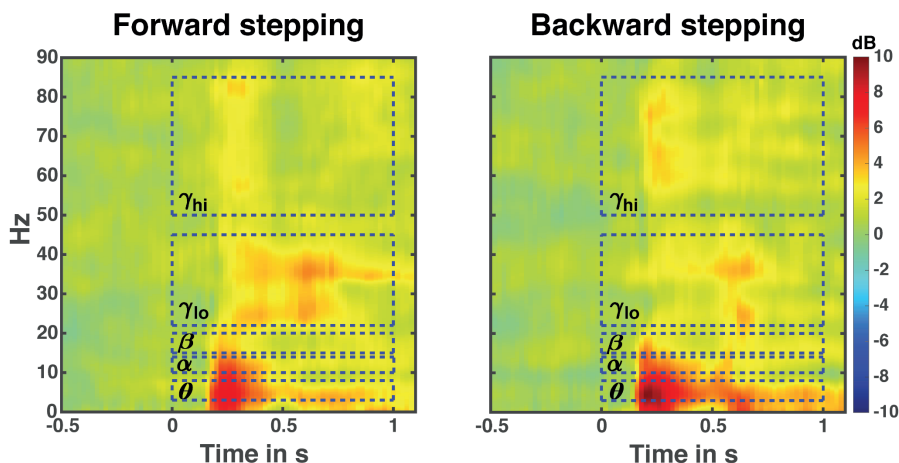
Figure 4. Perturbation time-locked time frequency granger gain. Illustrated data are averaged over all leg muscles in either the forward (left figure) or backward (right figure) stepping direction. The dashed boxes indicate frequency bands of interest for the time course analyses. Note that the temporal boundaries are illustrative; the actual time windows for analysis differed based on stepping times and time-locking events.

EMG envelopes and frequency-specific CMC

Overall, EMG activity significantly increased compared to baseline in both perturbation directions (forward average EMG onset latency = 152 ms, SD = 37ms; backward average EMG onset latency = 145 ms, SD = 30 ms; seen in table 1), indicating that all leg muscles were actively engaged during the stepping responses. All muscles exhibited significant increases in CMC relative to baseline during the

reactive step task, though the specific frequency band dynamics varied over time-locking events and muscles (forward average CMC onset latency = 186 ms, SD = 85 ms; backward average CMC onset latency = 171 ms , SD = 83 ms; seen in table 1). In addition, the onset of significant CMC dynamics following perturbation onset lagged the transient increase in EMG activity. Note that the end of the perturbation onset time window may include some foot-off-related activity. The next sections separately describe for both perturbation directions whether a muscle functions as agonist or antagonist during the specific time locked events. In addition, the next section reports simultaneous muscle frequency specific CMC dynamics per time locked event. For an illustrative summary of the EMG and CMC data and observed significance values, please see the supplementary figures S1 and S2.

Table 1. Onset of significant EMG and CMC dynamics following perturbation onset relative to baseline. Presented data are in ms.

Forward

Muscles	SO		TA		ST		BF		RF		*M*	*SD*
	Step	Stance	Step	Stance	Step	Stance	Step	Stance	Step	Stance		
EMG	112	116	152	160	144	144	172	176	184	172	152	26
CMC												
Theta	160	180	160	180	160	180	220	200	280	180	190	37
Beta	160	180	180		20					260	160	87
Low gamma	300				200		0	260	260		204	119
Hi gamma	0	160	180	220		300		240		240	191	96
										CMC onset	186	85

Backward

| Muscles	SO		TA		ST		BF		RF		*M*	*SD*
	Step	Stance	Step	Stance	Step	Stance	Step	Stance	Step	Stance		
EMG	164	184	96	100	176	156	148	156	136	136	145	30
CMC												
Theta	180	180	160	160	220	180	240	160		180	184	28
Beta		180								180		
Low gamma		80	200	220	340		0	140			163	118
Hi gamma	100	0	120	200			320	220		140	157	102
										CMC onset	171	83

5

Forward reactive stepping

Time-locked to perturbation onset, all muscles showed bilateral increase of EMG activity in the initial 150 ms following perturbation onset as steps have not yet been initiated (i.e. both step and stance leg showed similar increased activity; figure 5). A similar significant increase of CMC was observed across different muscles and over different frequencies. In the theta range, CMC increase was observed in all muscles. Alpha band CMC dynamics were most abundant in both SO,TA ,ST and RF muscles, though not significant for the step leg TA. In addition, we observed symmetrically increased beta coupling for all but RF muscles (i.e. similar CMC dynamics between step and stance leg). In the low-gamma frequency band, a gradually and symmetrically increased CMC was observable in the ST and BF muscles. In the high-gamma band CMC increased symmetrically but not significantly across muscles.

Time-locked to foot off, all muscles showed increased EMG activity relative to baseline. Prior to foot off, symmetric EMG activity was observed in both ST and BF muscles. Asymmetric activity was observed in SO (larger in stance leg), TA and RF (larger in stepping leg), consistent with their differential roles in the stance and stepping leg. Observed CMC dynamics did not follow similar patterns to EMG activity within time locked events. Theta dynamics were mainly increased for stance leg muscles and the lower leg muscles of the step leg. Alpha band CMC only increased bilaterally in the SO and ST muscles. In the beta frequency, increased CMC compared to baseline was observed in the step leg SO and ST. Increased CMC in the low-gamma frequency band is observed around the foot off event for all but the TA muscles. The high-gamma band dynamics are overall symmetrical for all muscles and mostly not significantly increased relative to baseline.

Time-locked to the foot strike event, all muscles showed elevated muscle activity relative to baseline. We observed greater EMG activity in step leg TA compared to the stance-leg TA muscle and the other stance leg muscles show increased EMG activity relative to the step-leg.

Although significant CMC dynamics are observed, these did not follow similar activity patterns from the EMG activity. Significant increase in theta CMC was observed prior to foot strike in the step-leg SO and following foot strike event in the stance-leg ST and BF. Alpha band CMC dynamics were limited to both SO muscles. In the beta frequency, step-leg SO and both ST leg muscles showed increased CMC prior to foot strike. In addition, all but the BF muscles showed asymmetrical beta CMC increase following the foot strike event. Low-gamma CMC dynamics were mostly increased symmetrically prior to foot strike in the posterior leg muscles. In addition,
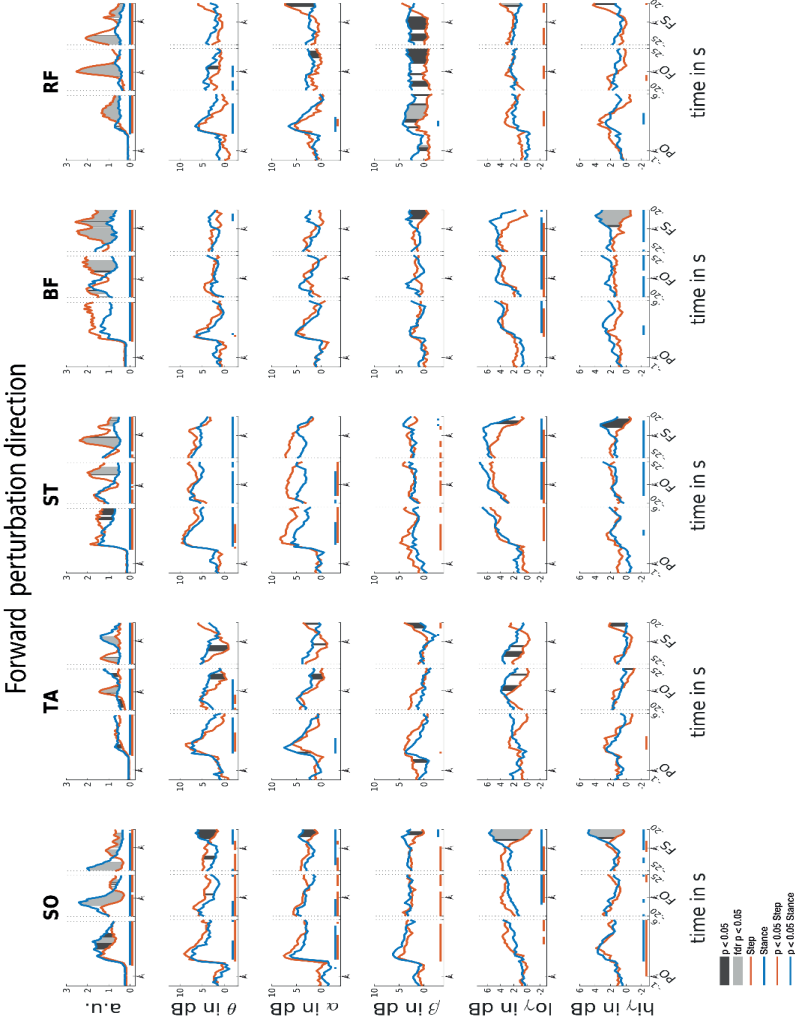
Figure 5. Forward reactive stepping muscle specific EMG and frequency specific CMC. Top row columns contain normalized EMG muscle activity, below are frequency-specific CMC dynamics. Figure columns are leg muscles Soleus (SO), Tibialis anterior (TA), Semitendinosus (ST) , Biceps Femoris (BF), Rectus Femoris (RF). Statistically significant differences relative to baseline are indicated using horizontal lines, and differences between step and stance are indicated with grey shaded patches between the time courses. Note that there is temporal overlap between the different temporal windows of interest. Perturbation onset (PO), Foot off (FO), Foot Strike (FS). Foot off latency: Median = 451 ms, IQR = 210ms. Foot strike latency: median = 641 ms, IQR = 214 ms.

5

both low and high gamma showed asymmetric activation patterns for all except the TA muscles following foot strike.

Backward reactive stepping

In the backward perturbation direction, EMG activity of all muscles was increased relative to baseline, yet only modestly so in SO. This increased EMG activity is sustained throughout all time-locked events (figure 6).

Time-locked to perturbation onset, EMG activity transiently and symmetrically increased for all muscles over the initial 200ms. Similar transient and symmetrical CMC dynamics are observed in the theta range for all muscles. Only stance leg ST and RF showed significant Alpha CMC increase following perturbation onset. Beta CMC dynamics followed a corresponding transient and symmetrical pattern in the lower leg muscles which only resulted in a significant increase for the stance-leg SO. Gradual and modest increase of low-gamma dynamics are observed in posterior leg muscles, albeit not always reaching significance. High-gamma band dynamics overall show similar symmetrical transient cortical interaction patterns as the theta band in all muscles.

Time-locked to the foot off event, all muscles showed increased EMG activity relative to baseline. Prior to foot off, a symmetrical increase in muscle activity was observed in all lower leg muscles. However, upper leg muscles show greater EMG activity in the step leg hamstring and stance leg RF muscles, in line with their agonist roles in backward step initiation. Overall, CMC theta dynamics follow similar symmetrical patterns for the lower leg muscles in comparison to the EMG activity. Yet, dissimilar theta band CMC dynamics compared to EMG were observed in the upper leg muscles. Only increased alpha CMC was observed in the stance leg TA. Please note that the alpha CMC seems elevated for the RF throughout the foot off event while a significant effect remains absent. However, this is caused by strongly increased CMC in one participant specific for this muscle and frequency band. Removal of this participant's data did not influence the observation of additional significant difference effects. Little significant CMC dynamics were observed in the beta band. In the low-gamma band, almost all leg muscles, except for the RF, showed a gradual increase in CMC activity. In the high-gamma frequency band, all lower leg muscles show similar CMC patterns compared to the EMG activity. However, the upper leg muscles overall show little dynamics in comparison to the EMG activity during foot-off event with only slight high-gamma band CMC increases over stance-leg RF and BF muscles.
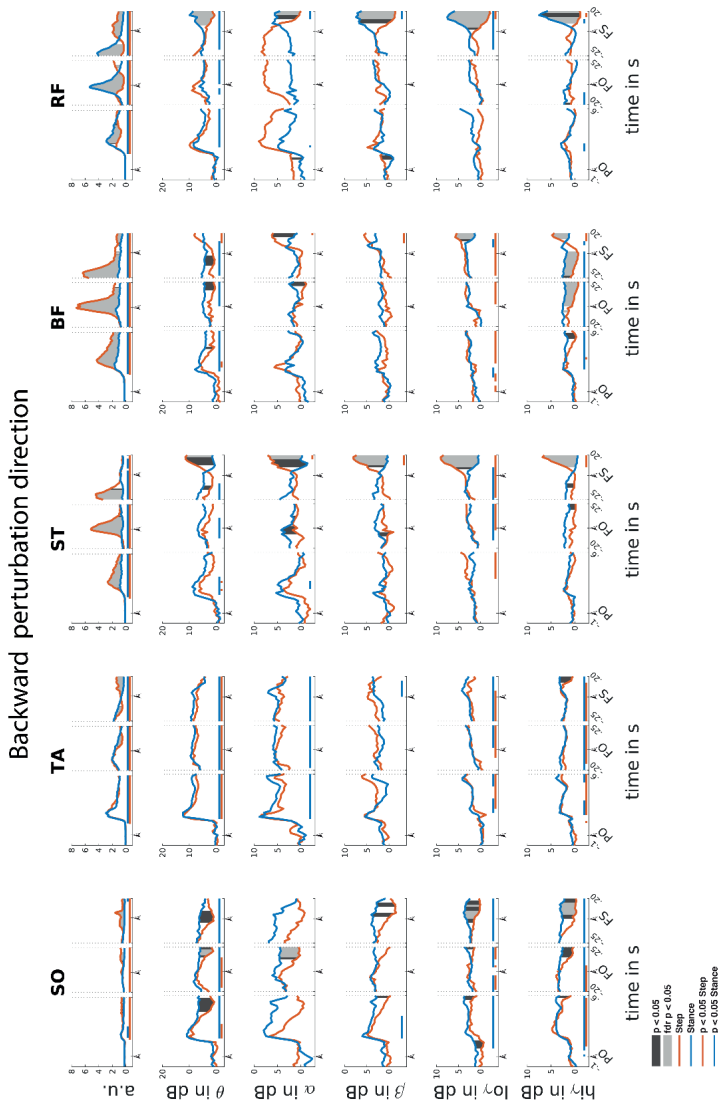
Figure 6. Backward reactive stepping muscle specific EMG and frequency specific CMC. Top row columns contain normalized EMG muscle activity, below are frequency band specific CMC dynamics. Figure columns are leg muscles Soleus (SO), Tibialis anterior (TA), Semitendinosus (ST) , Biceps Femoris (BF), Rectus Femoris (RF). Differences relative to baseline are indicated using horizontal lines, and differences between step and stance are indicated with grey shaded patches between the time courses. Note that there is temporal overlap between the different time-locking events. Perturbation onset (PO), Foot off (FO), Foot Strike (FS). Foot off latency: median = 400 ms, IQR =202 ms. Foot strike latency: median = 629 ms, IQR=225 ms.

Time-locked to the foot strike event, all muscles show increased EMG activity and step leg muscles show greater muscle activation. In

addition, all muscles showed CMC over multiple frequency bands, yet the observed asymmetrical EMG activation patterns are not mirrored in the CMC patterns in the various frequency bands. All stance leg muscles except the ST muscle show increased CMC in the theta frequency. In addition, the step leg ST and BF showed increased theta CMC following foot strike. Alpha band CMC dynamics were limited to the stance leg SO and the upper leg muscles that showed increased EMG activity prior to the foot strike event. CMC dynamics in the beta band were primarily observed following foot strike for the upper leg muscles that showed increased EMG activity prior to foot strike. Overall, relatively similar CMC dynamics were observed over both the low and high gamma bands.

Differences between step and stance leg

Overall, asymmetrical activation patterns in EMG and CMC between step and stance leg were observed time locked to foot off and foot strike events in both stepping directions. Following a brief symmetrical recruitment of the various muscles shortly after perturbation onset (consistent with an automatic postural response), the activation patterns of stance- and stepping leg muscles started to differ depending on their differential functional roles. Time locked to foot strike, all muscles show difference in CMC activity primarily over beta and gamma frequency bands. Only the RF muscles show similar asymmetrical activity over beta and gamma frequencies compared to the EMG activity following foot strike.

In the backward perturbation direction (figure 6), the lower leg muscles showed significant EMG activity increases in the step leg during the foot strike time-locked phase of the step response. Whereas, in the upper leg muscles the posterior step leg muscles and stance leg anterior muscles showed consistent increases throughout all three time-locked events of the step response. Prior to foot strike time-locked event, EMG activity in anterior stance leg muscles was lower compared to the step leg EMG activity. Yet following foot strike, EMG activity in these anterior step leg muscles increases relative to the stance leg. Following foot strike, all but the TA muscle show greater EMG activity in the step leg. With respect to the CMC, all but the TA muscle showed distinct differences over all frequency bands following the foot strike event.

Discussion

Our aim was to identify cortical interactions with various leg muscles through spectral Granger causality during a reactive balance task. We hypothesized that CMC

would occur during reactive stepping responses, indicating the contributions of the cerebral cortex to the execution of these responses. In line with our hypothesis, our results illustrated significant CMC increase relative to baseline over multiple muscles and frequency bands following balance perturbations in both directions. In addition, we expected CMC dynamics to differ between step and stance leg. In particular, we expected that stronger CMC would be most evident for the agonist muscles involved in generating the stepping movements, and that an increase in CMC would precede an upregulation of EMG activity in these muscles. Contrary to our expectations, our data illustrated that step and stance leg CMC generally did not show similarity with EMG data (i.e. increases in CMC did not align with increases in EMG activity). Our findings shed new light on cortical involvement of dynamic postural responses with implications for future studies involving clinical populations with deficient CMC (such as stroke).

Increase in CMC during reactive balance stepping
Granger causality analysis during reactive step responses revealed cortical interaction over multiple frequency bands for all muscles in both stepping directions, showing that on average the cortex becomes actively involved in the execution of reactive stepping response at ~180 ms post perturbation. Overall, we observed significant CMC increases in the theta, beta and both gamma frequency bands relative to baseline for individual muscles in either perturbation direction and throughout the three time locked events. In the backward direction, notable broadband interaction was present in upper leg muscles following the foot strike event. Although such broadband CMC following foot strike may suggest that observed dynamics were caused by an artifact, increased broadband CMC in the stance leg muscles during forward stepping and the absence of similar broadband CMC in other step leg muscles (the leg that receives most movement impact that may cause artifacts) support the interpretation of a causal cortical interaction that spanned multiple canonical frequency bands. We propose that the broadband interaction with specific muscles may emphasize the importance of these respective muscles in maintaining a stable posture following the stepping response and we will elaborate on our arguments below. As multiple studies investigated distinct functional roles of cortical rhythms, we will separately discuss their potential roles during the reactive stepping response.

Theta band coupling
Strong transient cortico-muscular interactions in the theta frequency band were observed following perturbation onset in both perturbation directions for almost all leg muscles, indicating that theta dynamics may play a general role in the initial reactive stepping response. Interestingly, after the foot strike event in the backward

stepping direction CMC in the theta frequency band mostly involved the muscles that showed increased muscle activity around foot off (i.e. stance-leg RF and step-leg BF), suggesting that the leg muscles that primarily showed increased EMG activation also require relatively more cortical interaction in the later phase of the response. Our findings are in agreement with an increase in CMC in the theta frequency band observed in lateral pull perturbations while standing, which was speculated to facilitate muscle recruitment of the feet-in-place balance response (17). Thus, the increase of CMC in the theta frequency band in the current study may emphasize the importance of the theta rhythm in muscle control following the perturbation onset and termination of the stepping response.

Alpha band coupling

Increased dynamics in the alpha band has been coupled to sensorimotor processes and motor readiness, and it may facilitate a similar role during the reactive balance response. Several studies reported increased alpha coupling during standing compared to walking (17,31,32). Although not all muscles showed increased CMC in the alpha band, most dynamics were primarily observed following perturbation onset and time locked to foot off event. These events require specific muscle activation to initially respond to the balance perturbation and initiate the stepping response. Therefore, our results may hint that the alpha frequency signals for muscle readiness in the reactive balance response.

Beta band coupling

The cortical beta frequency band is known for its close relation with voluntary muscle recruitment in a wide variety of tasks (33) and we reasoned that it may play a similar role during the muscle recruitment to facilitate the reactive stepping response. Although relatively few muscles showed significant beta coupling, beta CMC dynamics were most evident following perturbation onset and after foot strike. During these phases, muscle activity was elevated compared to baseline and yet relatively little changes in EMG dynamics occurred, suggesting a rather isometric (semi-static) muscle contraction. Previous studies investigated isometric leg muscle contractions, observing increased CMC in the beta frequency band (14,34,35), suggesting that beta dynamics play a role in leg muscle control. In addition, CMC in the beta band has been demonstrated during quiet standing postural control (36) and during feet-in-place balance responses following small lateral perturbations in unipedal stance (21). Interestingly, *increase* in beta band CMC is linked to increase in muscle activity, while a simultaneous power *decrease* of the cortical beta rhythm (note: cortical beta power should not be confused with cortical beta coupling) is observed during sustained muscle contraction (37). Yet, although a decrease in

beta power has been reported following perturbation onset for either feet-in-place and step response (2,12,17,22), no consistent increase in beta CMC dynamics was observed in the present study and that of Peterson (17). As beta CMC has mainly been observed during muscle activity in (semi-)static postures, we speculate that the general lack of significant beta CMC may be due to the dynamic nature of the reactive stepping response, with beta CMC becoming somewhat more evident when participants maintained a (semi-)static posture following foot strike. Therefore, we propose that the observed beta CMC in our study may relate to relatively isometric muscle recruitment facilitating stability in this phase of the reactive step response.

Gamma band coupling
Gamma coupling dynamics scale with increased muscle contraction and coordination (14,38), and may facilitate a similar increased muscle recruiting role during reactive balance stepping. The cortical gamma rhythm covers a wide frequency range and although we analyzed two distinct frequency bands, cortical coupling in either band occurred mostly between foot off and foot strike. Therefore, we will discuss these results as general gamma dynamics (for an extensive review on gamma oscillations and CMC during the control of movements see (38)). Interestingly, we observed gamma rather than beta coupling throughout the reactive step response. Relative increase over CMC dynamics in the gamma band compared to beta band coupling has been linked to an increase in force and muscle coordination during isotonic compared to isometric muscle contraction of ankle and knee joints (14). Therefore, we speculate that the greater need for coordinated muscle recruitment during the step response may result in greater gamma CMC dynamics.

No evidence that lateralized EMG activity is driven by lateralized cortical coupling
Distinct cortical interactions with step or stance leg mainly occurred with respect to the foot off and foot strike events in either direction, suggesting that although the cortex was initially engaged following perturbation onset (as evidenced by the increased coupling relative to baseline; see figure 5 & 6), surprisingly little leg-specific interactions were observed under the hypothesis that transcortical loops are involved in facilitating the reactive stepping response (20,39). Interestingly, distinct CMC between step and stance leg in both stepping directions were also not mirrored in similar asymmetric EMG activity, contrasting with our expectation that distinct cortical interaction would precede a distinct increase in EMG activity. Previous studies did find a correlation between CMC and EMG (13,15,34), but these studies concerned voluntary movements and thus involved intentional top-down regulation of muscle activity. In contrast, the stepping responses in the present study were executed in response to an unexpected balance perturbation

and were thus *reactive* in nature. We speculate that the difference between feedforward and feedback control may explain these discrepant findings regarding the relationships between CMC and EMG patterns. While the initial phase of the balance recovery response (i.e. automatic postural response) is known to be mediated by subcortical circuits (20), the present study may hint at these circuits also playing a greater-than-expected role during leg specific muscle activations of the stepping response.

Clinical implications

Our results demonstrate CMC throughout the reactive stepping response, indicating that impairments in any of the cortico-muscular communication circuitry may lead to dysfunctional cortico-muscular interaction underlying the impaired balance response. Indeed, impaired stepping responses have been reported for a variety of conditions of the central nervous system (e.g. stroke and Parkinson's disease; 40,41), which may in turn contribute to their elevated risk of falling (42,43). Yet, the specific mechanisms underlying reactive stepping impairments are still poorly understood. Our work indicates that the application of Granger causality analysis for studying muscle and frequency specific deviations may help provide valuable insights in the underlying pathophysiology of impaired balance response in these clinical populations.

Limitations and strengths

The current study is exploratory and there are some limitations to consider. An important limitation is the sliding window approach used in the Granger causality analysis, meaning that observed effects are smeared over time. Yet, while peak activity is not systematically biased by the windowing, temporal comparison between EMG and CMC timeseries needs to be done with care, as events time locked to foot-off and foot strike contain a signal mixture related to other events due to the large sliding window and the heterogeneity of response latencies.

The experiment involved balance perturbations of different intensities resulting in stepping responses. As perturbation intensity is known to affect the amplitude of the perturbation evoked potential, the ERP contains the average of all perturbation intensities (i.e. low and high intensities and thus small and large amplitudes). While subtracting the ERP from the single trial data, we may have induced minor non-stationarities. Therefore, we recommend future studies to include perturbation intensities of a single intensity that is strong enough to elicit step responses.

On the other hand, our study shows novelty and strengths in several aspects. First of all, CMC at key events throughout the stepping response elicited temporal

evolution of distinct spectral dynamics with respect to EMG. Future studies may further investigate the specific role of the spectral dynamics with respective muscles throughout the balance response. In specific, it is of interest to investigate the role of each frequency band with respect to the functional muscular role during the reactive step response. In addition, the current study is the first to conduct separate analysis of step- and stance-leg CMC in comparison to the temporal evolution of EMG activity. The surprising dissimilarity that we observed in CMC and EMG patterns between the legs indicates that the cortex does not appear to facilitate EMG recruitment for executing the balance recovery step in a refined leg- and muscle specific manner.

Conclusion

We conclude that reactive balance responses require direct interactions from the cortex with the individual muscles, yet without substantial leg-specific differences in CMC patterns. Our work is relevant for clinical populations with impaired balance control, where CMC analysis may elucidate the underlying pathophysiological mechanisms.

5

References

1.   Sipp AR, Gwin JT, Makeig S, Ferris DP. Loss of balance during balance beam walking elicits a multifocal theta band electrocortical response. J Neurophysiol. 2013 Nov;110(9):2050–60.

2.   Solis-Escalante T, van der Cruijsen J, de Kam D, van Kordelaar J, Weerdesteyn V, Schouten AC. Cortical dynamics during preparation and execution of reactive balance responses with distinct postural demands. Neuroimage. 2019 Mar;188:557–71.

3.   Varghese JP, McIlroy RE, Barnett-Cowan M. Perturbation-evoked potentials: Significance and application in balance control research. Neurosci Biobehav Rev. 2017 Dec;83:267–80.

4.   Mansfield A, Inness EL, Wong JS, Fraser JE, McIlroy WE. Is impaired control of reactive stepping related to falls during inpatient stroke rehabilitation? Neurorehabil Neural Repair. 2013 Aug;27(6):526–33.

5.   de Kam D, Geurts AC, Weerdesteyn V, Torres-Oviedo G. Direction-Specific Instability Poststroke Is Associated With Deficient Motor Modules for Balance Control. Neurorehabil Neural Repair. 2018 Jun 29;32(6–7):655–66.

6.   Dietz V, Quintern J, Berger W, Schenck E. Cerebral potentials and leg muscle e.m.g. responses associated with stance perturbation. Exp Brain Res. 1985;57(2):348–54.

7.   Slobounov S, Cao C, Jaiswal N, Newell KM. Neural basis of postural instability identified by VTC and EEG. Exp Brain Res. 2009 Oct;199(1):1–16.

8.   Payne AM, Ting LH. Worse balance is associated with larger perturbation-evoked cortical responses in healthy young adults. Gait Posture. 2020 Jul;80:324–30.

9.   Hülsdünker T, Mierau A, Strüder HK. Higher Balance Task Demands are Associated with an Increase in Individual Alpha Peak Frequency. Front Hum Neurosci. 2015;9:695.

10. Varghese JP, Staines WR, McIlroy WE. Activity in Functional Cortical Networks Temporally Associated with Postural Instability. Neuroscience. 2019 Mar 1;401:43–58.

11. Varghese JP, Marlin A, Beyer KB, Staines WR, Mochizuki G, McIlroy WE. Frequency characteristics of cortical activity associated with perturbations to upright stability. Neurosci Lett. 2014 Aug 22;578:33–8.

12. Solis-Escalante T, Stokkermans M, Cohen MX, Weerdesteyn V. Cortical responses to whole-body balance perturbations index perturbation magnitude and predict reactive stepping behavior. Eur J Neurosci. 2020 Dec;54(12):8120–38.

13. Glories D, Soulhol M, Amarantini D, Duclay J. Specific modulation of corticomuscular coherence during submaximal voluntary isometric, shortening and lengthening contractions. Sci Rep. 2021 Mar 18;11(1):6322.

14. Gwin JT, Ferris DP. Beta- and gamma-range human lower limb corticomuscular coherence. Front Hum Neurosci. 2012 Sep 11;6:258.

15. Yoshida T, Masani K, Zabjek K, Chen R, Popovic MR. Dynamic Increase in Corticomuscular Coherence during Bilateral, Cyclical Ankle Movements. Front Hum Neurosci. 2017 Apr 4;11:155.

16. Artoni F, Fanciullacci C, Bertolucci F, Panarese A, Makeig S, Micera S, et al. Unidirectional brain to muscle connectivity reveals motor cortex control of leg muscles during stereotyped walking. Neuroimage. 2017 Oct 1;159:403–16.

17. Peterson SM, Ferris DP. Group-level cortical and muscular connectivity during perturbations to walking and standing balance. Neuroimage. 2019 Sep;198:93–103.

18. Roeder L, Boonstra TW, Kerr GK. Corticomuscular control of walking in older people and people with Parkinson's disease. Sci Rep. 2020 Feb 19;10(1):2980.

19. Taube W, Schubert M, Gruber M, Beck S, Faist M, Gollhofer A. Direct corticospinal pathways contribute to neuromuscular control of perturbed stance. J Appl Physiol. 2006 Aug;101(2):420–9.

20. Jacobs JV, Horak FB. Cortical control of postural responses. J Neural Transm. 2007 Mar 29;114(10):1339–48.

21. Zandvoort CS, van Dieën JH, Dominici N, Daffertshofer A. The human sensorimotor cortex fosters muscle synergies through cortico-synergy coherence. Neuroimage. 2019 Oct 1;199:30 7.

22. Stokkermans M, Solis-Escalante T, Cohen MX, Weerdesteyn V. Midfrontal theta dynamics index the monitoring of postural stability. Cereb Cortex. 2022 Sep 6;

23. Nonnekes J, de Kam D, Geurts ACH, Weerdesteyn V, Bloem BR. Unraveling the mechanisms underlying postural instability in Parkinson's disease using dynamic posturography. Expert Rev Neurother. 2013 Dec;13(12):1303–8.

24. Nonnekes J, Scotti A, Oude Nijhuis LB, Smulders K, Queralt A, Geurts ACH, et al. Are postural responses to backward and forward perturbations processed by different neural circuits? Neuroscience. 2013 Aug 15;245:109–20.

25. Oostenveld R, Praamstra P. The five percent electrode system for high-resolution EEG and ERP measurements. Clin Neurophysiol. 2001 Apr;112(4):713–9.

26. Wang X, Chen Y, Ding M. Estimating Granger causality after stimulus onset: a cautionary note. Neuroimage. 2008 Jul 1;41(3):767–76.

27. Delorme A, Makeig S. EEGLAB: an open source toolbox for analysis of single-trial EEG dynamics including independent component analysis. J Neurosci Methods. 2004 Mar 15;134(1):9–21.

28. Barnett L, Seth AK. The MVGC multivariate Granger causality toolbox: a new approach to Granger-causal inference. J Neurosci Methods. 2014 Feb 15;223:50–68.

29. Barnett L, Seth AK. Granger causality for state-space models. Phys Rev E Stat Nonlin Soft Matter Phys. 2015 Apr 23;91(4):040101.

30. Benjamini Y, Yekutieli D. The control of the false discovery rate in multiple testing under dependency. Ann Statist. 2001 Aug;29(4):1165–88.

31. Lau TM, Gwin JT, Ferris DP. Walking reduces sensorimotor network connectivity compared to standing. J Neuroeng Rehabil. 2014 Feb 13;11:14.

32. Wagner J, Solis-Escalante T, Neuper C, Scherer R, Müller-Putz G. Robot assisted walking affects the synchrony between premotor and somatosensory areas. Biomed Tech (Berl). 2013 Aug;58 Suppl 1.

5

33. Khanna P, Carmena JM. Neural oscillations: beta band activity across motor networks. Curr Opin Neurobiol. 2015 Jun;32:60–7.

34. Kilner JM, Baker SN, Salenius S, Hari R, Lemon RN. Human cortical muscle coherence is directly related to specific motor parameters. J Neurosci. 2000 Dec 1;20(23):8838–45.

35. Dal Maso F, Longcamp M, Cremoux S, Amarantini D. Effect of training status on beta-range corticomuscular coherence in agonist vs. antagonist muscles during isometric knee contractions. Exp Brain Res. 2017 Oct;235(10):3023–31.

36. Jacobs JV, Wu G, Kelly KM. Evidence for beta corticomuscular coherence during human standing balance: Effects of stance width, vision, and support surface. Neuroscience. 2015 Jul 9;298:1–11.

37. Echeverria-Altuna I, Quinn AJ, Zokaei N, Woolrich MW, Nobre AC, van Ede F. Transient beta activity and cortico-muscular connectivity during sustained motor behaviour. Prog Neurobiol. 2022 May 9;102281.

38. Ulloa JL. The control of movements via motor gamma oscillations. Front Hum Neurosci. 2021;15:787157.

39. Bolton DAE. The role of the cerebral cortex in postural responses to externally induced perturbations. Neurosci Biobehav Rev. 2015 Oct;57:142–55.

40. de Kam D, Nonnekes J, Oude Nijhuis LB, Geurts ACH, Bloem BR, Weerdesteyn V. Dopaminergic medication does not improve stepping responses following backward and forward balance perturbations in patients with Parkinson's disease. J Neurol. 2014 Dec;261(12):2330–7.

41. de Kam D, Roelofs JMB, Bruijnes AKBD, Geurts ACH, Weerdesteyn V. The next step in understanding impaired reactive balance control in people with stroke: the role of defective early automatic postural responses. Neurorehabil Neural Repair. 2017 Aug;31(8):708–16.

42. Mansfield A, Wong JS, McIlroy WE, Biasin L, Brunton K, Bayley M, et al. Do measures of reactive balance control predict falls in people with stroke returning to the community? Physiotherapy. 2015 Dec;101(4):373–80.

43. Paul SS, Allen NE, Sherrington C, Heller G, Fung VSC, Close JCT, et al. Risk factors for frequent falls in people with Parkinson's disease. J Parkinsons Dis. 2014;4(4):699–703.

Supplementary material

Manuscript: Distinct cortico-muscular coherence between step and stance leg during reactive stepping responses

To summarize our time series EMG and CMC observations, we provide the data averaged over time. For this figure we took the following ROI's per event. 100-300ms for the perturbation onset time window. 0 - 200ms for both the foot off and foot strike events.

5
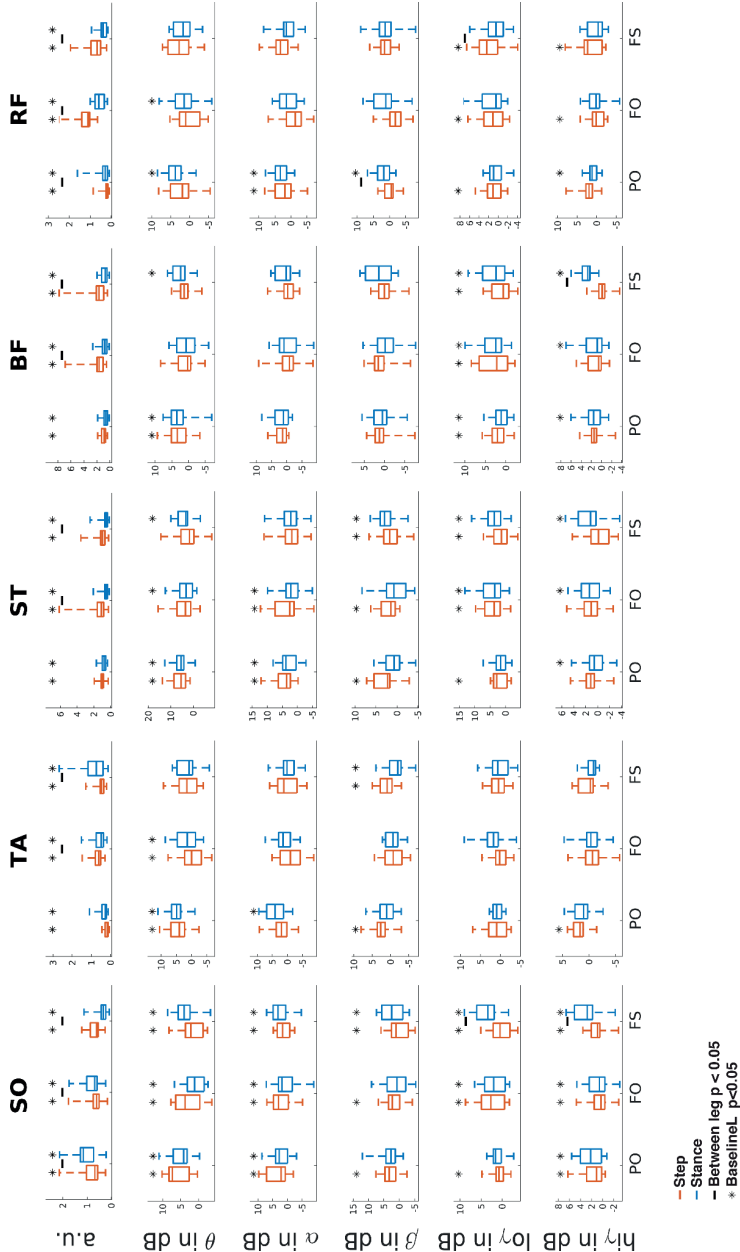
Figure S1. Top row columns contain normalized EMG muscle activity, below are frequency band specific CMC dynamics. Figure columns are leg muscles Soleus (SO), Tibialis anterior (TA), Semitendinosus (ST), Biceps Femoris (BF), Rectus Femoris (RF). Statistically significant differences relative to baseline are indicated using an asterisk, and differences between step and stance leg are indicated with a horizontal dash. Perturbation onset (PO), Foot off (FO), Foot strike (FS).
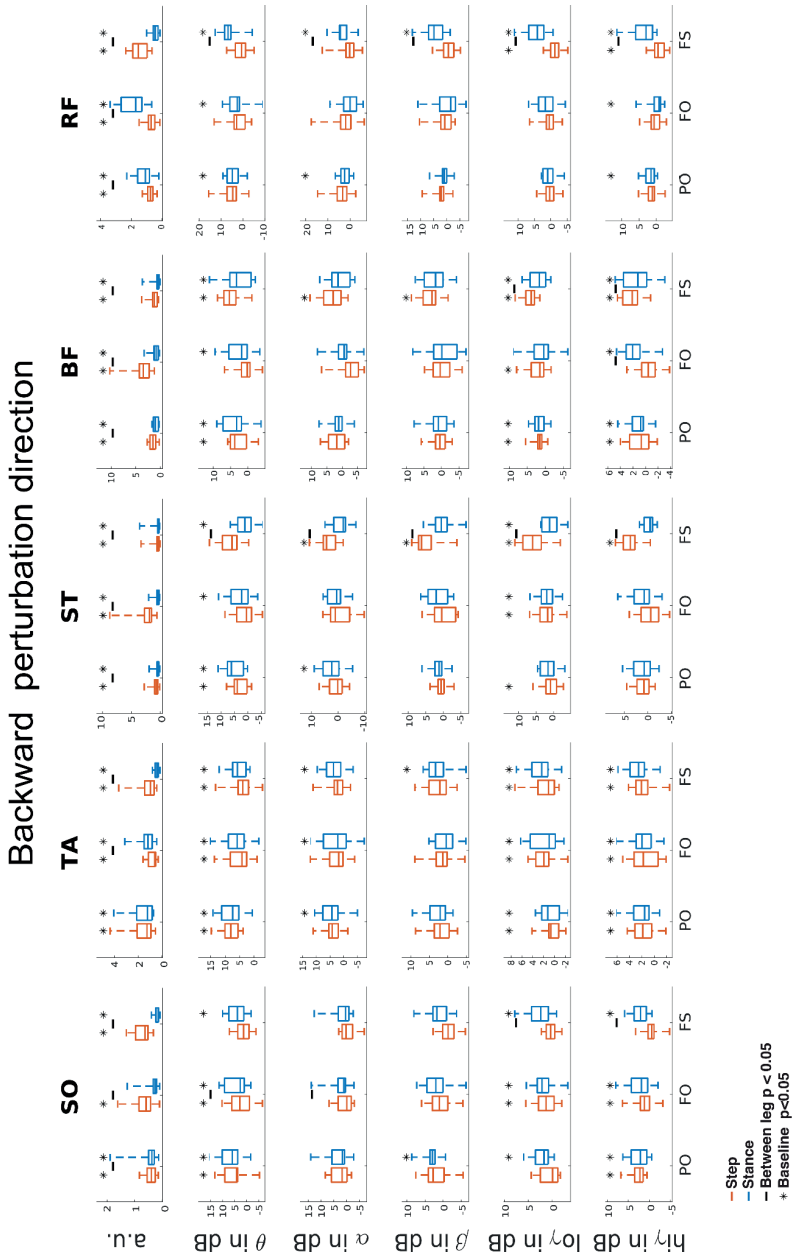
Figure S2. Top row columns contain normalized EMG muscle activity, below are frequency band specific CMC dynamics. Figure columns are leg muscles Soleus (SO), Tibialis anterior (TA), Semitendinosus (ST) , Biceps Femoris (BF), Rectus Femoris (RF). Statistically significant differences relative to baseline are indicated using an asterisk, and differences between step and stance leg are indicated with a horizontal dash. Perturbation onset (PO), Foot off (FO), Foot strike (FS).
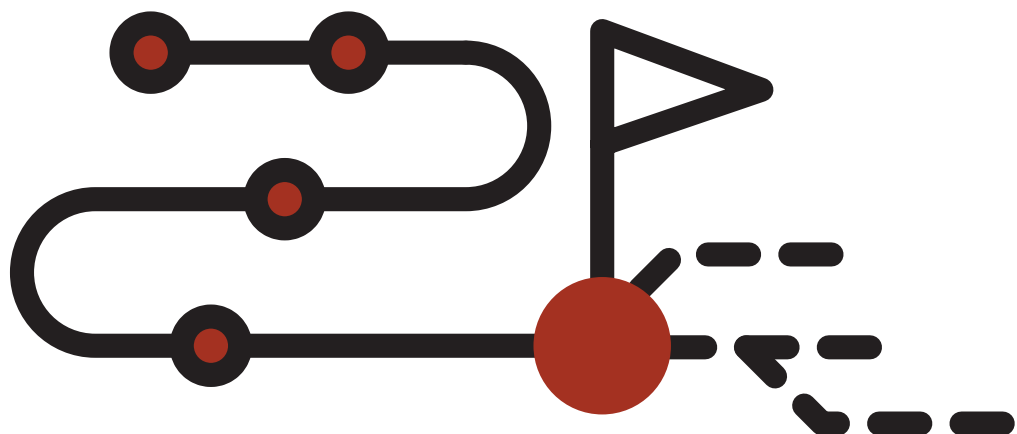
Chapter 6

Summary and general discussion

Summary and general discussion

On a daily basis we humans are exposed to postural threats requiring active cognitive control to maintain a stable upright posture. Yet, most of the time we are not actively aware of these cognitive processes taking place. There is limited understanding of the cortical role in postural balance control in the healthy brain, while balance impairments in certain clinical populations with cortical lesions (such as people after stroke) indicate that cortical involvement is necessary for a proper balance response. In this thesis, I investigated cortical correlates of balance monitoring throughout the different phases of the balance response. The chapters in this thesis describe a critical part of human postural control and provide novel evidence on the functional role of cortical dynamics during the reactive balance response, which I will summarize and discuss in a broader perspective in this chapter. In addition, I will address methodological considerations and open questions remaining from my work which may provide opportunities for future studies. Lastly, I will present my views on how to approach investigating balance impairments in clinical populations and close this thesis with concluding remarks.

In **chapter 2** of this thesis we determined whether the cortical responses elicited by balance perturbations were similar to established cortical markers of action monitoring. Action monitoring is considered a cognitive function where the timely detection of errors leads to the initiation of corrective adjustments. We confirmed that cortical responses to balance perturbations scale with the magnitude of the perturbation intensity and additionally indicate whether a step response is required. We proposed that the cortical control during reactive balance responses may represent the cognitive control mechanisms (i.e., action monitoring) that facilitate the monitoring of balance to maintain postural stability. Yet, the relation of the theta rhythm with perturbation intensity and response outcome does not imply a monitoring role *per se* since perturbations with greater intensity are more likely to lead to step responses and, accordingly, may only reflect the scaling of sensory information up to the threshold where perturbations always result in stepping responses.

Therefore, in **chapter 3** I investigated the potential monitoring role of theta dynamics during reactive balance performance by manipulating this relation of theta dynamics with perturbation intensity by imposing different states of postural stability prior to perturbation. I observed a change in slope of theta power over perturbation intensity with leaning posture during forward feet-in-place responses which indicated that midfrontal theta dynamics subserve action monitoring during forward reactive

balance responses in humans. These findings suggest that midfrontal theta dynamics likely facilitate balance monitoring during postural control.

Chapter 4 investigated the balance monitoring role of cortical midfrontal theta dynamics at foot strike, following reactive balance stepping responses. I hypothesized that the foot strike event may require a balance assessment on whether the step sufficiently restored balance, characterized by an increased theta modulation following foot strike. In agreement with my expectations, I demonstrated that foot strike events evoke a midfrontal theta power increase, though only in the backward stepping direction. Contrary to my expectations, theta dynamics following foot strike positively correlated with the margin of stability, meaning that greater theta power was observed with greater achieved stability. This suggested a different role of foot-strike related theta from monitoring whether stability is at risk. In a post-hoc analysis, I investigated whether theta dynamics following foot strike may instead facilitate adaptation of postural stability at subsequent stepping responses. This additional analysis indicated that theta dynamics were increased for participants that reduced their MoS at foot strike throughout the course of the experiment. Therefore, I speculate that foot strike related theta dynamics may represent a step performance monitoring process rather than monitoring whether stability is threatened.

In **Chapter 5** I conducted an exploratory analysis investigating cortical interaction with leg muscles through spectral Granger causality during a reactive stepping task. Here I observed broadband corticomuscular interaction following perturbation onset. In addition, distinct corticomuscular interactions for step and stance leg muscles following the foot strike event were observed. Contrary to my expectations, between-leg differences in Granger gains did not drive divergence of between-leg differences in EMG activity in all muscles in the foot strike time-locked analysis. This indicated that the traditional observations of CMC driving muscle activity do not seem to apply to lateralized muscle recruitment during reactive balance stepping responses. The results of this chapter demonstrate cortical involvement in the later phases of reactive balance responses and provide insightful information on its temporal and spectral aspects. In specific, the cortex interacted with individual muscles over multiple frequency bands following perturbation onset. However, the absence of lateralized cortical interactions with individual muscles, indicated that subcortical brain regions may be more involved in the stepping response than previously expected.

Discussion

The overarching goal of this thesis was to investigate the cortical role during the reactive balance response. In particular, I aimed to investigate theta dynamics underlying the balance monitoring process of reactive balance responses. In addition, I explored the spectral dynamics of cortico-muscular interactions following perturbations. Here I will reflect on how my findings have contributed to gaining a better understanding of the cortical role during reactive balance responses.

Midfrontal theta dynamics monitor postural stability following perturbation onset

Prior to this thesis the N1 and theta dynamics were known cortical markers involved in postural balance control, but little was known about their exact role. Studies investigating the role of the N1 during reactive balance responses, reported task-related modulations that suggest a cortical role during balance control. The N1 is influenced by manipulations of perturbation intensity (1), attention (2) and onset predictability (3,4). In addition, only one of these studies reported that the N1 amplitude scaled with response outcome (5); however, perturbation intensities also differed between responses, making it impossible to compare whether responses would indeed elicit different cortical dynamics. Further, time-frequency analysis illustrated that losing balance while walking on a treadmill resulted in increased theta dynamics, indicating the involvement of the theta rhythm during balance control (6). In addition, balance perturbations were known to elicit theta power increase during both feet-in-place (7) and stepping trials (8).

In **chapter 2** of this thesis, we contribute to this body of literature with the observation that cortical midfrontal N1 and theta dynamics scale with perturbation intensity and the ensuing behavioral response. Moreover, the effect of stepping on the N1 amplitude and latency as well as theta power indicates that at a similar acceleration, the N1 and theta scale with the response outcome. Yet, higher perturbation intensities were more likely to elicit step responses and therefore would confound the interpretation of greater theta dynamics signaling the monitoring of balance. Therefore, a definitive conclusion on whether theta dynamics reflect the action monitoring of postural balance could not be drawn from the findings in **chapter 2** alone. To address this research question, the interaction of theta dynamics with acceleration had to be manipulated. I chose to manipulate the interaction of theta dynamics with perturbation intensity by changing the initial postural stability prior to perturbation onset. On that account, **chapter 3** provided an additional piece of evidence, which indicated that during the forward reactive balance response, the

theta rhythm may facilitate the monitoring of postural balance only when being able to respond with feet-in-place responses. Similarly to the observations in **chapter 2**, an effect of response outcome indicated that theta indexes whether a step is required or not.

Interestingly, previous studies have observed similar theta dynamics scaling with monitoring behavior in other tasks besides balance control. For instance, in a target tracking paradigm, theta dynamics were greater when the distance between the target and the actual position increased (and accompanying corrective behavior; (9). Altogether, these findings suggest that the magnitude of the observed midfrontal theta increase may represent the mismatch between the expected and real afferent sensory information. Theta dynamics scale with the mismatch between expected sensory information and true sensory information, according to the feed forward model for stability (10). In the paradigms of action monitoring and predictive feedback control it is assumed that to maintain an upright posture, an execution of motor commands yields a representation of expected sensory information of the response outcome. When being perturbed while maintaining an upright posture, real afferent sensory information is being compared with the expected sensory information (arising from the task of steady-state balance maintenance) resulting in a mis-match between the expected and real afferent sensory representation (11). Hence, it is likely that theta dynamics index the monitoring of the expected impact of the perturbation on postural stability (i.e. postural threat) through an action monitoring process during the initial 100-300ms of the reactive balance responses.

Theta dynamics during distinct phases of the balance response may facilitate monitoring of different cognitive processes

Findings in **chapters 2 & 3** of this thesis emphasized that theta dynamics index the monitoring of postural threat. Similarly, previous studies indicated that theta dynamics increased with greater postural threat (12,13). Therefore, in **chapter 4**, we investigated whether theta dynamics would follow up on foot strike as a reassessment of balance and whether these would similarly resemble the monitoring of balance. Although we observed a general theta increase following backward foot strike events, we did not anticipate that higher theta power would signal for *greater* achieved stability as previous literature indicated that theta signaled for *poorer* stability (12,13). This suggests a different monitoring role for midfrontal theta dynamics following foot strike of the reactive postural response compared to the observations following perturbation onset in **chapters 2 & 3** and other literature.

6

Theta dynamics following foot strike may correspond with performance monitoring of the response outcome in a role of monitoring whether the balance response may require adaptation. Post-hoc analysis in **chapter 4** revealed that people who showed greater theta dynamics adjusted their stability throughout the experiment (generating smaller MoS over the time course of the experiment), suggesting a step performance monitoring role. Similar monitoring-related theta dynamics have been studied in simplified cognitive control and feedback paradigms (button press response performance), indicating that theta dynamics facilitate feedback processing and adaptation of response performance during learning (14–16). Although these findings hint towards a performance monitoring role of theta at foot strike, further investigation is necessary to provide conclusive evidence.

The cortex actively interacts with muscles during the reactive stepping response

Prior to this thesis, little was known about cortical interactions with leg muscles during the execution of reactive balance response. Previous studies already illustrated cortico-muscle interactions during voluntary isometric and isotonic contractions of leg muscles (17,18). In addition, cortico-muscle interactions were illustrated during muscle contractions of dynamic ankle movements (19) and gait (20), suggesting that the cortex directly interacts with muscles during muscle recruitment. Interestingly, only a few studies investigated cortical interaction with leg muscles in response to balance perturbations during standing and walking (7,21), illustrating cortical interaction with leg muscles during the reactive balance response. Yet, the temporal evolution of the cortical interaction with specific leg muscles, in specific for stepping responses, remained unexplored.

In **chapter 5** I report distinct broadband cortical interactions between the cortex and leg muscles throughout three key events of the stepping response. Contrary to my expectations, cortical interactions did not appear to drive leg-specific EMG activity throughout the stepping response, suggesting that the cortex does not have a direct muscle recruiting role during the reactive balance response. This observation raises the question whether subcortical rather than cortical brain regions may facilitate the distinct lateralized muscle recruitment during the step response. Although this work justifies the involvement of cortico-muscular interactions during the reactive stepping response, further investigation is necessary to understand the exact role of frequency band specific cortico-muscular interaction during postural control.

Clinical implications

Balance impairments are a key risk factor for falling which is specifically observed in clinical populations (22–32). With the insights gained through the chapters of this thesis, interesting questions can be answered in patient groups with central neurological disorders regarding the role of monitoring and muscle control during their impaired postural balance responses.

People with Parkinson's disease experience omnidirectional balance impairments, though these tend to be the worst in the backward direction, even when medicated with Levodopa (33–35). Interestingly, people with Parkinsons typically show unaffected muscle onset latencies during balance paradigms (36). Yet, the balance response seems impaired due to a combination of abnormalities. First of all, overall underscaling of the muscle response during feet-in-place and stepping responses are observed (37). Secondly, abnormal prolonged antagonist muscle activations, cause the inability to appropriately inhibit muscle activity underlying a proper biomechanical step response (37) often leading to a reactive balance response of multiple small steps (3 or more) that fail to result in a stable posture. Therefore, studies investigating the cortico-muscular interaction of people with parkinson's disease during balance paradigms may shed light on the underlying impaired neural mechanisms of these abnormal muscle contraction symptoms. In addition, studies investigating the cortical representation of perturbation directionality in people with Parkinson's disease (as was done for people with stroke by (38) may provide insights on a potential deficient cortical directional representation in the backward direction and indicate why the step response in the backward direction often remains absent (39).

People after stroke show impaired muscle recruitment to facilitate a balance-correcting stepping response. These impairments are characterized by delayed muscle recruitment, reduced muscle recruitment amplitude and deficient coordination of muscle recruitment in both feet-in-place and step responses (40). Interestingly, preliminary evidence indicated that cortical encoding for the directionality of postural perturbations remained preserved in people post stroke (38), suggesting that the cause of the impaired balance response may rather lie in the execution of the reactive balance response. Findings in *chapter 5* of this thesis illustrate the cortico-muscular dynamics of healthy human subjects during the reactive balance stepping response. These results may provide insights for cortico-muscular analysis in people with chronic stroke and help clarify the deficits in neural circuitry underlying the impaired balance response. Previous studies indicated that perturbation-based balance training in people post stroke (41–43) may improve the reactive stepping capacity of individuals. This indicates that although cortical

6

structures facilitating the stepping response may be affected, necessary structures of the nervous system remain preserved to facilitate this response that may be susceptible to training. In addition, these findings may shed light on the working mechanisms involved in perturbation based training in clinical populations.

Methodological considerations

Although we used state of the art technology to investigate the cortical involvement during the reactive balance response these studies were not without limitations. In this section I will discuss some important methodological considerations.

Balance perturbations in daily life rarely involve static quiet standing circumstances resulting in an instantaneous loss of balance. Instead, it is more likely to happen that we stumble over an object (44). However, this introduces multiple variable factors such as gait speed, and tracking when in the gait cycle a perturbation is induced, leading to complication for interpretation of the cortical dynamics. The balance response that we induced using a sophisticated perturbation platform, the 'Radboud Falls Simulator' (8,39) allowed for rigorous standardization of perturbations, which facilitated the investigation of cortical control during postural balance control. This simulator induces standardized sudden displacements of the CoM relative to the BoS, to simulate a loss of balance. Therefore, we chose to perturb balance from quiet standing and we anticipated that these insights are equally relevant to dynamic balance perturbations such as during walking (6).

On a more practical note, The Radboud falls simulator is a sophisticated piece of equipment which won't easily fit in every research or rehabilitation facility regarding budget and physical space. Alternatively, balance perturbations may be delivered using smaller devices such as treadmills (45–47). The advantage of treadmill based perturbations is that these devices are more affordable and occupy less space. In addition, these devices allow consecutive perturbations at a faster rate (because the platform requires an initialization period to return to the initial position) and perturbations during dynamic tasks (walking), compared to the platform movements of the Radboud falls simulator. Yet, an advantage of the Radboud falls simulator is the multi-directionality of perturbations, whereas a treadmill can only perturb in two directions.

On a similar note, the application of reflective markers for 3D-motion capture may become redundant in the near future. Advances in motion capture methods using deep learning computer vision techniques, such as the python OPENCV library (48) can identify body landmarks and joints without the use of markers. These

developments require fewer cameras compared to the expensive eight infrared camera setup currently used. Several studies investigated the reliability of alternative motion tracking techniques compared to established methods, reporting similar levels of accuracy between the different techniques (47,49). Therefore, availability of affordable and reliable 3D-motion capture methods may eventually lead to more rapid advances in the field of mobile-brain imaging as more research groups will be able to utilize these resources.

Whilst the findings in this thesis indicate that midfrontal theta dynamics index the monitoring of postural balance control, action monitoring of postural stability cannot be dissociated from changes of sensory inflow. In the experimental setup I could only indirectly assess the monitoring of stability through the MoS. Yet, in addition to altering stability, the leaning conditions likely also altered the proprioceptive information arising from the perturbations, due to the relative slack or tension in the ankle muscles. Therefore, action monitoring of more destabilizing perturbations cannot be dissociated from changes in sensory inflow. For that reason, I could only speculate on how destabilizing perturbations would cause reweighting of sensory information which in turn may modulate the relation of theta dynamics during balance monitoring. With the current technologies it is practically impossible to measure such changes of sensory inflow in humans.

EEG is infamous for its sensitivity to artifacts and although advances in equipment and data cleaning methods improve data quality, explained variance of single trial data remained low. **Chapters 2 & 3** of this thesis, focused on single trial data analysis of theta dynamics. Such analyses require an extensive amount of trials to improve the signal to noise ratio. Yet, similar to other studies (1,50), explained variance remained low.

This raises the question of which internal and/or external factors cause the substantial amount of noise underlying the theta signal. Although external sources of noise have been shown to be removable (51,52), chances are that residual externally induced noise remains in the data after preprocessing (53). With respect to internal factors, a possible clarification may be the brain containing multiple sources that contribute to the cumulative measured signal at the scalp. Although extensive analysis methods were used to preprocess the data and identify independent components that contributed to the measured signal, there is no silver bullet for perfectly isolating balance monitoring related cortical activity.

Preprocessing steps vary between studies, resulting in analysis of individual independent components following ICA (8,54,55). In this thesis, I chose to analyze a combination of independent component data rather than individual components, followed by spatiotemporal filtering of the data in the theta frequency band. The advantage of this approach was that little brain-component data was lost in the ICA process. Yet, this process introduced more sources of midfrontal theta power which may have increased the observed variance in the data (56). These findings illustrated that response conflict midfrontal theta is multidimensional, meaning that multiple sources may contribute to the same midfrontal scalp topography). As mentioned earlier, cortical theta dynamics have been linked to a wide range of cortical tasks (14–16) and therefore interference of concurrent cortical roles in the same frequency band may cause additional noise to the signal when investigated during balance monitoring. In addition, this begs the question whether it would be ecologically valid to rule out the majority of cortical independent components in the endeavor to find cortical activity solely scaling with the expectations. Here, I advocate that although single component analysis may reduce the explained variance of the data, including more components may result in a more valid understanding of cortical dynamics compared to individual component analysis. Yet, analysis of individual components may shed more light on behavioral correlates of certain cortical source activities. Ultimately, this emphasizes that although extensive cleaning steps of EEG data and specialized filtering of frequency band specific dynamics still yield very low explained variance of the data.

Advances in neuroimaging methods may address these restrictions and change the way we investigate cortical activity during mobile brain imaging paradigms. For instance, optically pumped magnetometer (OPM) magnetoencephalogram (MEG) OPM-MEG is a mobile setup of the MEG method, which measures the magnetic field of the cortical brain activity with optical sensors (57). In comparison to MEG, OPM-EMG is not restrained to a fixed setup and allows measuring cortical activity during ambulatory paradigms. The sensors of OPM-MEG are fixed to the head, making this method less sensitive to movement artifacts and increasing the signal to noise ratio. In addition, OPM-MEG does not have to cope with the surface conductance of electrical activity compared to EEG (58), improving source localization limitations of EEG. Lastly, OPM-MEG does not require an extensive application procedure compared to high-density EEG, allowing shorter duration of experimental setups, which will significantly benefit the burden on clinical populations.

Although OPM-MEG has a lot of potential, there are some challenges to overcome. One major challenge is the heat generated by the OPM sensors. Current MEG systems

are designed such that the heat is isolated from the participants' head scalp. Yet, in a OPM-MEG setup, sensor temperatures may rise to uncomfortable temperatures at the scalp of the participants head, requiring development of proper cooling systems. Advances in systems involving Helium-4 may provide a suitable solution to these heat issues (59). Although OPM-MEG seems promising for mobile brain imaging, the applicability of OPM-EMG has not yet been investigated in combination with experimental setups involving movements. Movements can induce low frequency artifacts that may obscure the interpretation of low frequency brain activity. Therefore, development of coils that reduce such low frequency artifact sensitivity is necessary. Once these challenges are overcome OPM-MEG may become a preferential method for future mobile brain imaging studies.

Future studies

The findings in this thesis led to answers of our research questions, yet, these often lead to multiple new questions. In this section, I will address some of these questions I encountered as recommendations for future studies.

6

Task-dependent relations of theta dynamics with stability monitoring requires careful a priori determination of the study's purpose with regard to the behavior they aim to investigate. The reactive balance response is a complex behavioral response that can be divided into different phases. This division has important implications on the interpretation of cortical dynamics. In this thesis we investigated the postural balance response in three different phases, I) following perturbation, II) around foot off and III) around foot strike. Similarly, studies investigating the gait cycle, also identify key events such as foot-off and foot strike events to investigate event specific cortical dynamics (50,60). These phases each come with different biomechanical challenges with corresponding behavior and, as discussed in the previous paragraphs, theta dynamics may facilitate different roles of action monitoring based on the behavior required in a specific phase of the postural balance response. In addition, our findings regarding cortico-muscle coherence in **chapter 5** indicate that the cortex actively interacts with specific muscles during the execution of the reactive balance response, indicating that aligning data to specific events within the reactive balance response helps to illustrate dynamics best for each event rather than these results being canceled out due to interference (and trial-to-trial variations; as may have been the case in the perturbation intensity binning in chapter 5). Therefore, it is of great importance to a priori determine what exact action monitoring role is the focus of the study and which response phase would be the most suitable to study it.

Secondly, little is understood about balance recovery responses in different perturbation directions. In **chapters 2 & 3** of this thesis we did not observe similar cortical dynamics between forward and backward reactive balance responses, suggesting differences in the monitoring of balance with directionality. A previous study already showed that low frequency cortical dynamics may decode directionality (38). It is likely that visual input delivers distinct contributions to the monitoring of balance, yet, we do not fully understand whether and how a distinction between different sensory modalities is made and which sensory modality is prioritized. Future studies may investigate this by delivering perturbations in the forward and backward direction with and without visual occlusion or by delivering congruent and incongruent optic flow. In addition, we suggest future studies use equally challenging perturbations in either direction, for instance by tailoring these to the individual's direction-specific single or multiple stepping threshold (61), to allow more accurate comparison of cortical markers. These findings are particularly of interest to understand the underlying deficits in backward balance impairments in clinical populations.

Concluding remarks

The human postural balance response involves cortical processing on deciding whether balance is at risk and what response strategy is required. In this thesis, I investigated the cortical role of midfrontal theta dynamics during reactive balance responses. This thesis extends on the involved cortical dynamics during postural control and the knowledge of midfrontal theta dynamics facilitating action monitoring behavior. In addition, I demonstrated the temporal evolution of direct cortico-muscle interactions during the reactive balance stepping response. I demonstrated that midfrontal theta dynamics facilitate a monitoring role of balance following perturbations. In addition, I illustrated that midfrontal theta dynamics facilitate a performance monitoring role following the foot strike of the stepping response, indicating that theta subserves different cognitive processes during the balance response. Lastly, I showed the temporal evolution of cortical interaction with multiple leg muscles throughout key events of the stepping response.

I hope that the knowledge in this thesis contributes to the understanding of the balance impairments of clinical populations and that readers may find motivation in further investigating the complex but fascinating role of the cortex during balance control.

References

1. Payne AM, Hajcak G, Ting LH. Dissociation of muscle and cortical response scaling to balance perturbation acceleration. J Neurophysiol. 2019 Mar 1;121(3):867–80.

2. Adkin AL, Quant S, Maki BE, McIlroy WE. Cortical responses associated with predictable and unpredictable compensatory balance reactions. Exp Brain Res. 2006 Jun;172(1):85–93.

3. Mochizuki G, Sibley KM, Esposito JG, Camilleri JM, McIlroy WE. Cortical responses associated with the preparation and reaction to full-body perturbations to upright stability. Clin Neurophysiol. 2008 Jul;119(7):1626–37.

4. Mochizuki G, Sibley KM, Cheung HJ, McIlroy WE. Cortical activity prior to predictable postural instability: is there a difference between self-initiated and externally-initiated perturbations? Brain Res. 2009 Jul 7;1279:29–36.

5. Payne AM, Ting LH. Worse balance is associated with larger perturbation-evoked cortical responses in healthy young adults. Gait Posture. 2020 Jul;80:324–30.

6. Sipp AR, Gwin JT, Makeig S, Ferris DP. Loss of balance during balance beam walking elicits a multifocal theta band electrocortical response. J Neurophysiol. 2013 Nov;110(9):2050–60.

7. Peterson SM, Ferris DP. Group-level cortical and muscular connectivity during perturbations to walking and standing balance. Neuroimage. 2019 Sep;198:93–103.

8. Solis-Escalante T, van der Cruijsen J, de Kam D, van Kordelaar J, Weerdesteyn V, Schouten AC. Cortical dynamics during preparation and execution of reactive balance responses with distinct postural demands. Neuroimage. 2019 Mar;188:557–71.

9. Pereira M, Sobolewski A, Millán JDR. Action monitoring cortical activity coupled to submovements. eNeuro. 2017 Oct 24;4(5).

10. Yao Li, Levine WS. An optimal control model for human postural regulation. 2009 American Control Conference. IEEE; 2009. p. 4705–10.

11. Rasman BG, Forbes PA, Tisserand R, Blouin J-S. Sensorimotor Manipulations of the Balance Control Loop-Beyond Imposed External Perturbations. Front Neurol. 2018 Oct 26;9:899.

12. Slobounov S, Cao C, Jaiswal N, Newell KM. Neural basis of postural instability identified by VTC and EEG. Exp Brain Res. 2009 Oct;199(1):1–16.

13. Hülsdünker T, Mierau A, Neeb C, Kleinöder H, Strüder HK. Cortical processes associated with continuous balance control as revealed by EEG spectral power. Neurosci Lett. 2015 Apr 10;592:1 5.

14. Cavanagh JF, Frank MJ, Klein TJ, Allen JJB. Frontal theta links prediction errors to behavioral adaptation in reinforcement learning. Neuroimage. 2010 Feb 15;49(4):3198–209.

15. Cohen MX, Donner TH. Midfrontal conflict-related theta-band power reflects neural oscillations that predict behavior. J Neurophysiol. 2013 Dec;110(12):2752–63.

16. Cohen MX. Midfrontal theta tracks action monitoring over multiple interactive time scales. Neuroimage. 2016 Nov 1;141:262–72.

17. Glories D, Soulhol M, Amarantini D, Duclay J. Specific modulation of corticomuscular coherence during submaximal voluntary isometric, shortening and lengthening contractions. Sci Rep. 2021 Mar 18;11(1):6322.

18. Gwin JT, Ferris DP. Beta- and gamma-range human lower limb corticomuscular coherence. Front Hum Neurosci. 2012 Sep 11;6:258.

19. Yoshida T, Masani K, Zabjek K, Chen R, Popovic MR. Dynamic Increase in Corticomuscular Coherence during Bilateral, Cyclical Ankle Movements. Front Hum Neurosci. 2017 Apr 4;11:155.

20. Artoni F, Fanciullacci C, Bertolucci F, Panarese A, Makeig S, Micera S, et al. Unidirectional brain to muscle connectivity reveals motor cortex control of leg muscles during stereotyped walking. Neuroimage. 2017 Oct 1;159:403–16.

21. Zandvoort CS, van Dieën JH, Dominici N, Daffertshofer A. The human sensorimotor cortex fosters muscle synergies through cortico-synergy coherence. Neuroimage. 2019 Oct 1;199:30–7.

22. Weerdesteyn V, de Niet M, van Duijnhoven HJR, Geurts ACH. Falls in individuals with stroke. J Rehabil Res Dev. 2008;45(8):1195–213.

23. Belgen B, Beninato M, Sullivan PE, Narielwalla K. The association of balance capacity and falls self-efficacy with history of falling in community-dwelling people with chronic stroke. Arch Phys Med Rehabil. 2006 Apr;87(4):554–61.

24. Harris JE, Eng JJ, Marigold DS, Tokuno CD, Louis CL. Relationship of balance and mobility to fall incidence in people with chronic stroke. Phys Ther. 2005 Feb;85(2):150–8.

25. Hyndman D, Ashburn A. Stops walking when talking as a predictor of falls in people with stroke living in the community. J Neurol Neurosurg Psychiatr. 2004 Jul;75(7):994–7.

26. Jørgensen L, Engstad T, Jacobsen BK. Higher incidence of falls in long-term stroke survivors than in population controls: depressive symptoms predict falls after stroke. Stroke. 2002 Feb;33(2):542–7.

27. Lamb SE, Ferrucci L, Volapto S, Fried LP, Guralnik JM. Risk Factors for Falling in Home-Dwelling Older Women With Stroke. Stroke. 2003 Feb;34(2):494–501.

28. Mackintosh SFH, Hill K, Dodd KJ, Goldie P, Culham E. Falls and injury prevention should be part of every stroke rehabilitation plan. Clin Rehabil. 2005 Jun;19(4):441–51.

29. Mackintosh SF, Hill KD, Dodd KJ, Goldie PA, Culham EG. Balance score and a history of falls in hospital predict recurrent falls in the 6 months following stroke rehabilitation. Arch Phys Med Rehabil. 2006 Dec;87(12):1583–9.

30. Suzuki T, Sonoda S, Misawa K, Saitoh E, Shimizu Y, Kotake T. Incidence and consequence of falls in inpatient rehabilitation of stroke patients. Exp Aging Res. 2005 Dec;31(4):457–69.

31. Teasell R, McRae M, Foley N, Bhardwaj A. The incidence and consequences of falls in stroke patients during inpatient rehabilitation: factors associated with high risk. Arch Phys Med Rehabil. 2002 Mar;83(3):329–33.

32. Pickering RM, Grimbergen YAM, Rigney U, Ashburn A, Mazibrada G, Wood B, et al. A meta-analysis of six prospective studies of falling in Parkinson's disease. Mov Disord. 2007 Oct 15;22(13):1892–900.

33. Carpenter MG, Allum JHJ, Honegger F, Adkin AL, Bloem BR. Postural abnormalities to multidirectional stance perturbations in Parkinson's disease. J Neurol Neurosurg Psychiatr. 2004 Sep;75(9):1245–54.

34. Curtze C, Nutt JG, Carlson-Kuhta P, Mancini M, Horak FB. Levodopa Is a Double-Edged Sword for Balance and Gait in People With Parkinson's Disease. Mov Disord. 2015 Sep;30(10):1361–70.

35. de Kam D, Nonnekes J, Oude Nijhuis LB, Geurts ACH, Bloem BR, Weerdesteyn V. Dopaminergic medication does not improve stepping responses following backward and forward balance perturbations in patients with Parkinson's disease. J Neurol. 2014 Dec;261(12):2330–7.

36. Nonnekes J, de Kam D, Geurts ACH, Weerdesteyn V, Bloem BR. Unraveling the mechanisms underlying postural instability in Parkinson's disease using dynamic posturography. Expert Rev Neurother. 2013 Dec;13(12):1303–8.

37. Lang KC, Hackney ME, Ting LH, McKay JL. Antagonist muscle activity during reactive balance responses is elevated in Parkinson's disease and in balance impairment. PLoS ONE. 2019 Jan 25;14(1):e0211137.

38. Solis-Escalante T, De Kam D, Weerdesteyn V. Classification of Rhythmic Cortical Activity Elicited by Whole-Body Balance Perturbations Suggests the Cortical Representation of Direction-Specific Changes in Postural Stability. IEEE Trans Neural Syst Rehabil Eng. 2020 Nov 6;28(11):2566–74.

39. Nonnekes J, Scotti A, Oude Nijhuis LB, Smulders K, Queralt A, Geurts ACH, et al. Are postural responses to backward and forward perturbations processed by different neural circuits? Neuroscience. 2013 Aug 15;245:109–20.

40. de Kam D, Geurts AC, Weerdesteyn V, Torres-Oviedo G. Direction-Specific Instability Poststroke Is Associated With Deficient Motor Modules for Balance Control. Neurorehabil Neural Repair. 2018 Jun 29;32(6–7):655–66.

41. Mansfield A, Inness EL, Mcilroy WE. Stroke. Handb Clin Neurol. 2018;159:205–28.

42. van Duijnhoven HJR, Roelofs JMB, den Boer JJ, Lem FC, Hofman R, van Bon GEA, et al. Perturbation-Based Balance Training to Improve Step Quality in the Chronic Phase After Stroke: A Proof-of-Concept Study. Front Neurol. 2018 Nov 22;9:980.

43. Schinkel-Ivy A, Huntley AH, Aqui A, Mansfield A. Does Perturbation-Based Balance Training Improve Control of Reactive Stepping in Individuals with Chronic Stroke? J Stroke Cerebrovasc Dis. 2019 Apr;28(4):935–43.

44. Okubo Y, Sturnieks DL, Brodie MA, Duran L, Lord SR. Effect of reactive balance training involving repeated slips and trips on balance recovery among older adults: A blinded randomized controlled trial. J Gerontol A Biol Sci Med Sci. 2019 Aug 16;74(9):1489–96.

45. Steib S, Klamroth S, Gaßner H, Pasluosta C, Eskofier B, Winkler J, et al. Perturbation During Treadmill Training Improves Dynamic Balance and Gait in Parkinson's Disease: A Single-Blind Randomized Controlled Pilot Trial. Neurorehabil Neural Repair. 2017 Aug;31(8):758–68.

46. Gaßner H, Steib S, Klamroth S, Pasluosta CF, Adler W, Eskofier BM, et al. Perturbation treadmill training improves clinical characteristics of gait and balance in parkinson s disease. J Parkinsons Dis. 2019;9(2):413 26.

47. Roelofs J. Static and dynamic standing balance in the chronic phase after stroke: how to recover? [Doctoral dissertation]. Radboud University; 2019.

48. Bradsky G. The OpenCV Library. Dr Dobb's Journal of Software Tools. 2000;120:122–5.

49. Lee K-D, Park H-S. Real-Time Motion Analysis System Using Low-Cost Web Cameras and Wearable Skin Markers. Front Bioeng Biotechnol. 2021;9:790764.

6

50. Wagner J, Martinez-Cancino R, Delorme A, Makeig S, Solis-Escalante T, Neuper C, et al. High-density EEG mobile brain/body imaging data recorded during a challenging auditory gait pacing task. Sci Data. 2019 Oct 17;6(1):211.

51. Gwin JT, Gramann K, Makeig S, Ferris DP. Removal of movement artifact from high-density EEG recorded during walking and running. J Neurophysiol. 2010 Jun;103(6):3526–34.

52. Kline JE, Huang HJ, Snyder KL, Ferris DP. Isolating gait-related movement artifacts in electroencephalography during human walking. J Neural Eng. 2015 Aug;12(4):046022.

53. Gorjan D, Gramann K, De Pauw K, Marusic U. Removal of movement-induced EEG artifacts: current state of the art and guidelines. J Neural Eng. 2022 Feb 28;19(1).

54. Makeig S, Gramann K, Jung T-P, Sejnowski TJ, Poizner H. Linking brain, mind and behavior. Int J Psychophysiol. 2009 Aug;73(2):95–100.

55. Gramann K, Ferris DP, Gwin J, Makeig S. Imaging natural cognition in action. Int J Psychophysiol. 2014 Jan;91(1):22–9.

56. Zuure M. The origins of response conflict theta, an adventure in source separation [Doctoral dissertation]. Donders Institute for Brain, Cognition and Behaviour, Nijmegen, Radboud University; 2021.

57. Brookes MJ, Leggett J, Rea M, Hill RM, Holmes N, Boto E, et al. Magnetoencephalography with optically pumped magnetometers (OPM-MEG): the next generation of functional neuroimaging. Trends Neurosci. 2022 Aug;45(8):621–34.

58. van den Broek SP, Reinders F, Donderwinkel M, Peters MJ. Volume conduction effects in EEG and MEG. Electroencephalogr Clin Neurophysiol. 1998 Jun;106(6):522–34.

59. Labyt E, Corsi M-C, Fourcault W, Palacios Laloy A, Bertrand F, Lenouvel F, et al. Magnetoencephalography with optically pumped 4he magnetometers at ambient temperature. IEEE Trans Med Imaging. 2019 Jan;38(1):90–8.

60. Roeder L, Boonstra TW, Kerr GK. Corticomuscular control of walking in older people and people with Parkinson's disease. Sci Rep. 2020 Feb 19;10(1):2980.

61. de Kam D, Roelofs JMB, Bruijnes AKBD, Geurts ACH, Weerdesteyn V. The next step in understanding impaired reactive balance control in people with stroke: the role of defective early automatic postural responses. Neurorehabil Neural Repair. 2017 Aug;31(8):708–16.

6
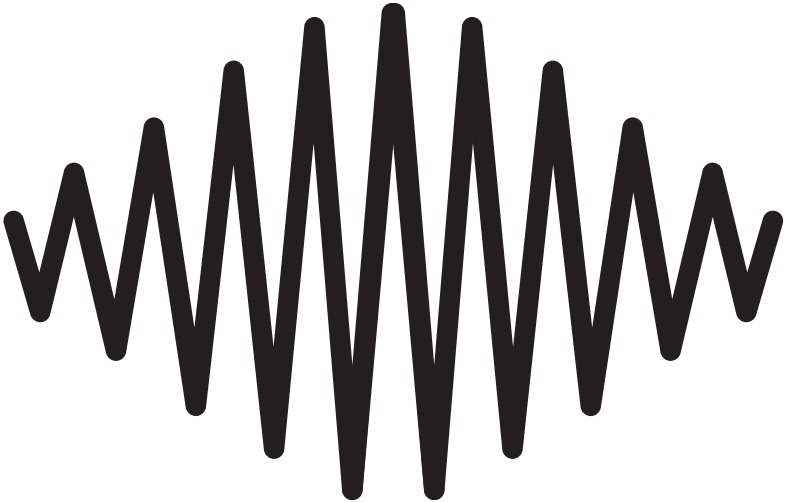
Chapter 7

Nederlandse samenvatting

Dit hoofdstuk geeft een beknopte Nederlandse samenvatting van de wetenschappelijke hoofdstukken in dit proefschrift. Een uitgebreidere samenvatting met discussie is te vinden in hoofdstuk 6 'Summary and General discussion' (Engelstalig).

Er is momenteel weinig bekend over de corticale mechanismen in het menselijk brein die balanscontrole mogelijk maken. Het is van groot belang hier meer over te weten, want controle van de balans is één van de belangrijkste functies die het voor de mens mogelijk maakt om rechtop te staan en zich vrij te bewegen. Daarnaast is deze kennis belangrijk omdat het verduidelijking kan scheppen over de verminderde evenwichtscontrole bij bijvoorbeeld personen met de ziekte van Parkinson of personen die een beroerte hebben gehad (m.a.w. klinische populaties met een aangedane functionaliteit van het centrale zenuwstelsel).

Corticale reacties van balansverstoringen op het lichaam geven een indicatie van de intensiteit van de balansverstoringen en voorspellen of reactief stap gedrag nodig is

In hoofdstuk 2 is onderzocht of de corticale respons die veroorzaakt wordt door een balansverstoring vergelijkbaar is met de al bekende corticale respons van cognitieve controle en het monitoren van acties. Veranderingen van onze lichamelijke stabiliteit door externe balansverstoringen veroorzaken een robuust negatief potentiaal (N1) gemeten met elektro-encefalografie (EEG). Ook is een sterke toename in activiteit in de theta frequentie (3-8Hz) waar te nemen over de midfrontale hersengebied. Het monitoren van acties is een cognitieve functie van ons brein, bestaande uit foutdetectie en het initiëren van corrigerende aanpassingen. Daarom stelden wij de hypothese dat deze corticale respons die acties tijdens balanscontrole monitort (N1 en theta frequentie) zich verhoudt tot de intensiteit van de balansverstoring. Daarnaast verwachten we dat de uiteindelijke staprespons een sterker corticaal signaal afgeeft in vergelijking tot het vermogen om op de plaats te blijven staan. Wij hebben dit onderzocht door middel van een EEG onderzoek (met een hoge dichtheid van 128 elektroden) bij 11 gezonde jongvolwassen die deelnamen aan een balansexperiment. De deelnemers kregen de opdracht om zonder een stap te zetten hun balans te herstellen als reactie op een onverwachte balansverstoring in de voor- en achterwaartse richting met verschillende intensiteiten. Uit de gemeten EEG data hebben we door middel van een onafhankelijke componenten analyse de midfrontale corticale activiteit geïsoleerd. Met behulp van een tijd-frequentie analyse en general linear modeling van individuele trials hebben we een significante interactie tussen de intensiteit van de balansverstoring en het stapgedrag over verschillende midfrontale corticale signalen aangetoond, zoals het N1 Potentiaal en de theta-, alpha- en beta frequenties. Onze bevindingen suggereerden dat de

sterkte van de corticale respons op balansverstoringen zowel de magnitude van de afwijking tot de stabiele status weerspiegeld alsmede voorspeld of een corrigerende stap nodig is. Daarom vermoeden we dat balanscontrole door middel van een corticaal controlemechanisme wordt gefaciliteerd die lichamelijke acties monitort voor het behoud van stabiliteit.

Midfrontale theta modulaties duiden op het monitoren van onze lichamelijke stabiliteit

Het zetten van een stap is een bekende strategie om de lichamelijke stabiliteit te behouden. Balansverstoringen staan erom bekend dat ze neuro-elektrische signalen als de N1 en veranderingen in de theta frequentie genereren. In *hoofdstuk 3* onderzochten we de rol van corticale midrontale theta frequenties in het monitoren van balans tijdens balansverstoringen met verschillende initiële stabiele houdingen. Hiervoor hebben we EEG, elektromyografie (EMG) en de 3D kinematische data van het lichaam gemeten terwijl deelnemers op een platform stonden dat balansverstoringen in de voor- en achterwaartse richting met verschillende intensiteiten simuleerde. De stabiliteit van de deelnemers werd vooraf gemanipuleerd door ze de instructie te geven om naar voren of achteren te leunen. De mate van het leunen werd gecontroleerd door middel van de real-time kinematische data die als feedback op het scherm werd geprojecteerd voor de deelnemer. Alle deelnemers kregen de instructie om geen stap te zetten in respons op de balansverstoringen. Door middel van de kinematische data reconstrueerden we de stabiliteitsmarge van de proefpersoon gedurende de hele balansverstoring. We stelden de hypothese dat midfrontale theta modulatie de participatie van een monitoringsysteem weerspiegeld en dat daarom de magnitude van de theta modulatie, als gevolg van de balansverstoring, zou veranderen door de initiële stabiele houding voorafgaand aan de balansverstoring. Met andere woorden, sterkere theta modulaties wanneer de balans het meeste bedreigd wordt. Door middel van een doelgerichte spatiële filtering in combinatie met een generalized linear mixed effects model analyse hebben we onze hypothese bevestigd en dus aangetoond dat theta modulaties zich verhouden tot lichamelijke stabiliteit. Deze resultaten bieden het nieuwe inzicht dat midfrontale theta modulaties het monitoren van onze staande balans faciliteren. Het begrijpen van de corticale mechanismen die betrokken zijn bij de balanshuishouding is van groot belang voor het ontrafelen van de problematiek in de balanshuishouding bij ouderen en mensen met aandoeningen aan het centrale zenuwstelsel, zoals bij mensen na een beroerte.

7

Corticale midfrontale theta modulaties na voetlanding van een reactieve staprespons indexeren mogelijk de adaptatie van de staprespons

Na een onverwachte verstoring van je balans is het vaak nodig om een stap te zetten om je balans te behouden. Het monitoren van onze balans wordt gekenmerkt door neuro-elektrische signalen zoals de N1 en midfrontale theta modulaties. In *hoofdstuk 4* onderzochten we de rol van deze corticale midfrontale theta modulaties gedurende het monitoren van de balans tijdens de voetlanding na een staprespons als gevolg op externe balansverstoringen. Onze hypothese stelde dat midfrontale theta modulaties de activatie van een balansmonitorendsysteem reflecteert en als mede dat theta modulaties zouden toenemen na de voetlanding van de staprespons. Hierbij nemen we aan dat op het moment van voetlanding een herbeoordeling van de lichamelijke stabiliteit plaatsvindt te bepalen of een additionele stap nodig is. Hiervoor hebben we EEG en kinematische data gemeten van 15 gezonde jongvolwassenen terwijl zij op een platform stonden die balansverstoringen leverde in verschillende richtingen. De marge van stabiliteit werd voor de gehele balansrespons vastgesteld aan de hand van de kinematische data. Deelnemers kregen de instructie om de verstoorde balans te herstellen met een enkele stap van het geïnstrueerde linker of rechter been. Door middel van doelgerichte spatiële filtering (generalized eigen decomposition) in combinatie met een tijd-frequentie analyse van de EEG data onderzochten we of theta modulaties toenamen na de voetlanding van de staprespons. Onze resultaten kwamen overeen met onze hypothese dat de theta frequentie toenam na de voetlanding van de staprespons, echter, observeerden we dit enkel in de achterwaartse stap richting. Daarnaast vonden we in tegenstelling tot onze verwachtingen een positieve correlatie van theta modulaties en de marge van stabiliteit net na de voetlanding. Om deze onverwachte correlatie van theta modulaties met de stabiliteitsmarge nader te onderzoeken hebben we een post-hoc analyse uitgevoerd. De uitkomst van deze post-hoc analyse suggereerde dat theta modulaties na de voetlanding mogelijk de adaptatie van de stabiliteitsmarge bij volgende stapreacties faciliteren. We observeerden namelijk sterkere theta modulaties bij proefpersonen die hun stabiliteitsmarge succesvol verkleinen bij het maken van een stap. Bij aanvang van het experiment namen deze proefpersonen onnodig grote stappen om de balans zeker te stellen. Echter leidden de kleinere stappen die zij over de tijd van het experiment namen ook tot de gewenste stabiliteit. Daarom speculeerden wij dat de toename in theta modulaties zich niet verhield tot het monitoren van de stabiliteit, maar in plaats daarvan zou kunnen duiden op een corticale dynamiek gerelateerd aan het monitoren van de prestatie van de balansrespons.

Specifieke cortico-musculaire interactie tussen stap en standbeen tijdens de reactieve staprespons

Het herstellen van onze balans berust op het succesvol uitvoeren van een staprespons, welke waarschijnlijk een snelle en precieze interactie vergt tussen de cerebrale cortex en de beenspieren. Toch is er weinig bekend over hoe cortico-musculaire koppeling de uitvoering van de staprespons faciliteert. Daarom voerden wij een exploratief onderzoek uit door middel van tijdsafhankelijke cortico-musculaire koppeling met individuele beenspieren gedurende de reactieve staprespons. Hiervoor analyseerden wij EEG, EMG en kinematische data van 18 gezonde jongvolwassen deelnemers terwijl zij werden blootgesteld aan balansverstoringen met verschillende intensiteiten in de voor- en achterwaartse richting. De deelnemers kregen de instructie om de balans te herstellen zonder een stap te zetten tenzij niet anders mogelijk was. De spier-specifieke Granger causaliteit analyse werd toegepast tussen vijf individuele spieren van zowel het stap- als standbeen en 13 EEG elektroden verdeeld over de midfrontale positie van het hoofd. Middels een tijd-frequentie Granger causaliteitsanalyse identificeerden we de cortico-musculaire interactie tijdens de balansperturbatie, voetheffing en voetlanding. Onze initiële hypothese was een toename van cortico-musculaire interactie te observeren ten opzichte van rust. Daarnaast verwachtten we een verschil in cortico-musculaire interactie te observeren tussen de stap- en standbeen spieren vanwege hun functionele rol tijdens het maken van een stap. In het bijzonder verwachtten we dat de cortico-musculaire interactie het meest aanwezig zou zijn in de agonistische spieren tijdens de stap, en dat de cortico-musculaire interactie vooraf zou gaan aan de toename van EMG activiteit in deze spieren. We observeerden specifieke toename in Granger causaliteit over theta, bèta en lage/hoge gamma frequenties gedurende de reactieve staprespons in alle beenspieren voor beide stap richtingen. Interessant was dat verschillen in Granger causaliteit tussen de specifieke beenspieren vrijwel uitsluitend werden waargenomen na de divergentie van EMG-activiteit. Onze resultaten demonstreren de betrokkenheid van cortico-musculaire interactie tijdens de reactieve balansrespons en voorzien ons tevens van inzichten in zowel de de temporele en spectrale karakteristieken. Over het algemeen suggereren onze bevindingen dat hogere niveaus van corticale-musculaire koppeling de beenspecifieke EMG-activiteit niet faciliteren. Hier spelen subcorticale regio's van het centrale zenuwstelsel een grotere rol dan voorheen gedacht. Ons werk is relevant voor klinische populaties met verminderde evenwichtscontrole (zoals mensen na een beroerte), waar analyse van de cortico-musculaire interactie de onderliggende pathofysiologische mechanismen kan verduidelijken.
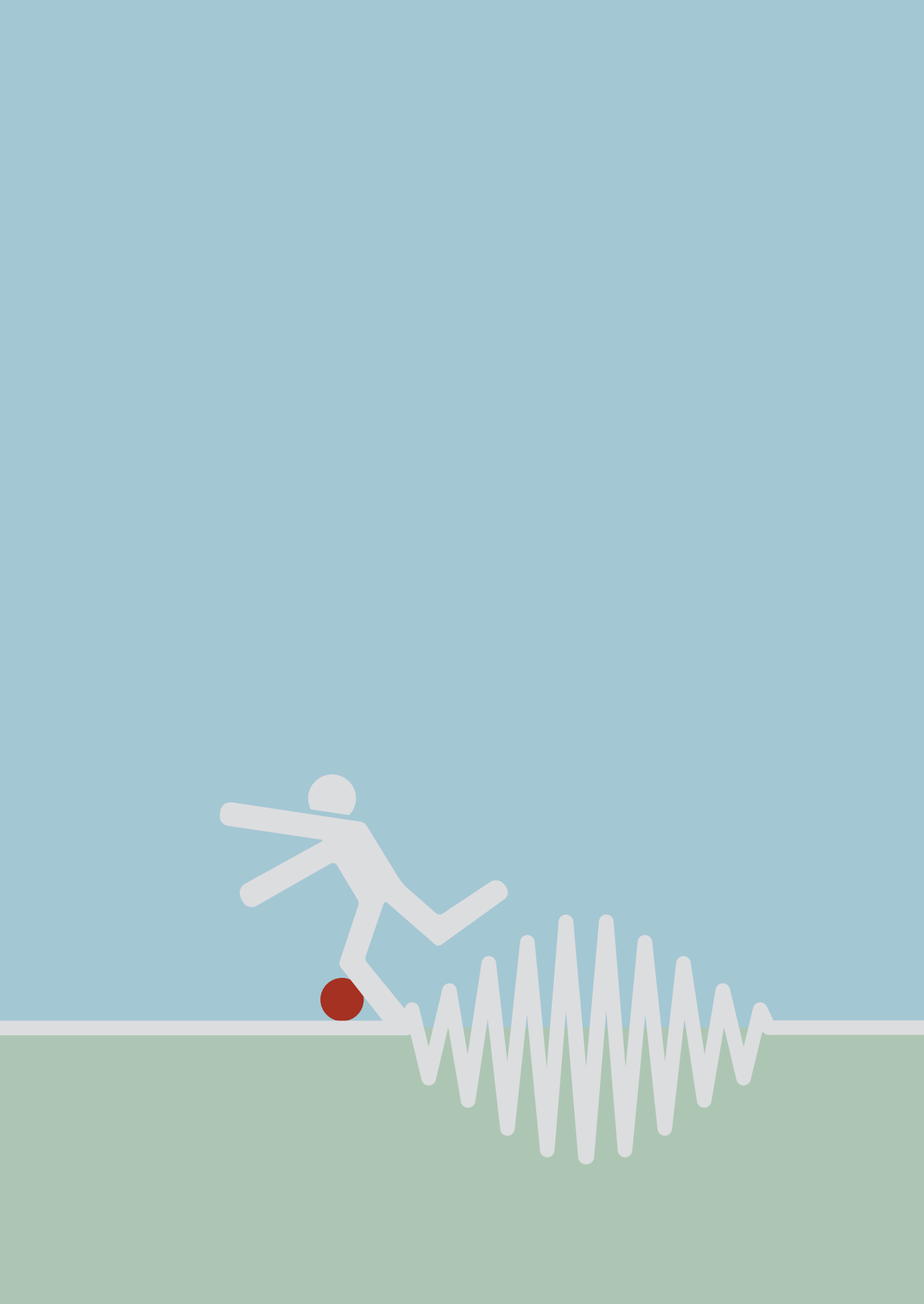
Chapter 8

Appendices

- List of Publications
- Research data management according to FAIR principles
- Portfolio
- Donders Graduate School for Cognitive Neuroscience
- Curriculum Vitae
- Dankwoord

List of Publications

1. **Mitchel Stokkermans**, Teodoro Solis-Escalante, Michael X Cohen, Vivian Weerdesteyn, Midfrontal theta dynamics index the monitoring of postural stability, Cerebral Cortex, 2022;, bhac283, https://doi.org/10.1093/cercor/bhac283

2. **Stokkermans, M.**, Staring, W., Cohen, M.X. et al. Cortical midfrontal theta dynamics following foot strike may index response adaptation during reactive stepping. Sci Rep 12, 17748 (2022). https://doi.org/10.1038/s41598-022-22755-3

3. **Stokkermans M.**, Solis-Escalante T., Cohen M.X., Weerdesteyn V., Distinct cortico-muscular coherence between step and stance leg during reactive stepping responses. Frontiers in Neurology (2023). https://doi.org/10.3389/fneur.2023.1124773

4. Solis-Escalante, T, **Stokkermans, M**, Cohen, MX, Weerdesteyn, V. Cortical responses to whole-body balance perturbations index perturbation magnitude and predict reactive stepping behavior. *Eur J Neurosci*. 2021; 54: 8120– 8138. https://doi.org/10.1111/ejn.14972

5. Joan Duprez, **Mitchel Stokkermans**, Linda Drijvers, Michael X. Cohen; Synchronization between Keyboard Typing and Neural Oscillations. *J Cogn Neurosci* 2021; 33 (5): 887–901. doi: https://doi.org/10.1162/jocn_a_01692

6. Manuel R, Gorissen M, **Stokkermans M,** Zethof J, Ebbesson LO, van de Vis H, Flik G, van den Bos R. The effects of environmental enrichment and age-related differences on inhibitory avoidance in zebrafish (Danio rerio Hamilton). Zebrafish. 2015 Apr;12(2):152-65. https://doi.org/10.1089/zeb.2014.1045

*

Research data management according to FAIR principles

General information about data collection

All chapters of this thesis are based on the results of human studies, which were conducted in accordance with the principles of the Declaration of Helsinki, including informed consent of all participants. Data in all chapters were collected at the Radboudumc. The study protocols of *chapters 2, 3 and 5* were approved by The Research Ethics Committee of the Radboud University Medical Center (Nijmegen, The Netherlands; Dossier 2018-4970). The study protocol of *chapter 4* was approved by the Research Ethics Committee of the Radboud University Medical Center (Nijmegen, The Netherlands; Dossier NL67690.091.18).

The participant's privacy was warranted in all cases by use of unique individual subject numbers. No direct or indirect identifiers exist in the anonymized data.

FAIR principles

Findability & accessibility

Data from chapter 2 is available upon reasonable request from the Radboud university medical center via secretariaat-staf.reval@radboudumc.nl under reference of 'the AP study'.

The data and research documentation for chapters 3 & 5 can be retrieved on the Donders Repository (https://data.donders.ru.nl/) via di.dccn.DSC_4220000.06_843, '*EEG of human balance control*'. Data specific to chapter 3 is found in the 'Balance monitoring study' folder. Data of chapter 5 will be added to this DSC in the folder 'CMC study' upon publication. All data archived as a Data Sharing Collection (DSC) remain available for at least 10 years after the DSC publishing date accompanied by the analysis code.

Data from chapter 4 could not yet be made publicly available due to an ongoing study. The data of this study is available upon reasonable request from the Radboud university medical center via secretariaat-staf.reval@radboudumc.nl under reference of 'The foot strike study of the ROADS study data'

Interoperability: Documentation is attached to the datasets in Readme.txt files ensuring interpretability. Stepwise explanation of preprocessing and analysis scripts are attached to the specific data collections. The shared data was stored in the .mat (Matlab, Mathworks, USA) format.

Reusable: For the reusability of the data, data will be stored for at least 10 years. There is no embargo in the accessibility of the data.

*

Portfolio

Courses & workshops	Organizer	Year	EC
Introduction Day	Radboudumc	2018	0.2
Graduate school Introduction Day	Donders Graduate School	2018	0.3
Basiscursus regelgeving en Organisatie voor Klinisch Onderzoekers (BROK)	NFU BROK academie	2018	1.5
Writing week	Department of Rehabilitation, Radboudumc	2018, 2022	4
Management for promovendi	Radboud University	2018	2
Mindfulness for promovendi	Radboud University	2018	1.5
Designing a PhD project	Radboud University	2018	3
Linear algebra for Neuroscientists	Radboud University	2018	2
Analysis of neural time series	Radboud University	2018	2
Scientific Integrity course	Donders Graduate school	2018	0.3
Personal development week	Radboudumc	2018	2
Internship supervision course	Donders Institute, Radboud University	2020	0.5
Brok herregistratie	NFU BROK academie	2022	0.2
Master Math by coding in Python	Michael Cohen, Udemy	2023	1.5
Deep Learning: Convolutional Neural Networks in Python	Lazy Programmer Inc, Udemy	2023	0.5
Master statistics & Machine learning	Michael Cohen, Udemy	2023	2
Totaal			**23.5**

Conferences & Symposia

Conferences & Symposia	Role	Location	Year	EC
Mobile brain Imaging conference (MoBi)	attendee	Berlin	2018	1.5
International Society of Posture & Gait Research (ISPGR)	attendee	Edinburgh	2019	1.5
NeuroControl Summer School	attendee	Chicago	2019	1.5
Dutch Neuroscience Meeting	Poster presentation	Tiel	2022	0.3
International Society of Posture & Gait Research (ISPGR)	Poster presentations	Montreal	2022	1.5

Teaching

Role	Program	Year	Duration
Daily supervisor	Master Biomedical sciences Internship	2020	6 months

*

Donders Graduate School for Cognitive Neuroscience

For a successful research Institute, it is vital to train the next generation of young scientists. To achieve this goal, the Donders Institute for Brain, Cognition and Behaviour established the Donders Graduate School for Cognitive Neuroscience (DGCN), which was officially recognised as a national graduate school in 2009. The Graduate School covers training at both Master's and PhD level and provides an excellent educational context fully aligned with the research programme of the Donders Institute.

The school successfully attracts highly talented national and international students in biology, physics, psycholinguistics, psychology, behavioral science, medicine and related disciplines. Selective admission and assessment centers guarantee the enrolment of the best and most motivated students.

The DGCN tracks the career of PhD graduates carefully. More than 50% of PhD alumni show a continuation in academia with postdoc positions at top institutes worldwide, e.g. Stanford University, University of Oxford, University of Cambridge, UCL London, MPI Leipzig, Hanyang University in South Korea, NTNU Norway, University of Illinois, North Western University, Northeastern University in Boston, ETH Zürich, University of Vienna etc.. Positions outside academia spread among the following sectors: specialists in a medical environment, mainly in genetics, geriatrics, psychiatry and neurology. Specialists in a psychological environment, e.g. as specialist in neuropsychology, psychological diagnostics or therapy. Positions in higher education as coordinators or lecturers. A smaller percentage enters business as research consultants, analysts or head of research and development. Fewer graduates stay in a research environment as lab coordinators, technical support or policy advisors. Upcoming possibilities are positions in the IT sector and management position in pharmaceutical industry. In general, the PhDs graduates almost invariably continue with high-quality positions that play an important role in our knowledge economy.

For more information on the DGCN as well as past and upcoming defenses please visit: http://www.ru.nl/donders/graduate-school/phd/

*

Curriculum Vitae

Mitchel Stokkermans was born on the 3rd of August 1990, in Tilburg, the Netherlands. He followed his secondary education at the Rooi Pannen (VMBO), followed by graduating from the Beatrix college in Tilburg at the level of Havo and eventually VWO.

He pursued his Bachelor degree in Medical biology at the Radboud university in Nijmegen, the Netherlands. During his bachelor internship he cooperated with dr. Remy Manuel and Prof. dr. Gert Flik, investigating The effects of environmental Enrichment and Age-Related Differences on Inhibitory avoidance in Zebrafish, published in Zebrafish.

After graduation, Mitchel proceeded his education at the Radboud University, attending the Medical Biology Master program with a specialization in Neuroscience. During this program, he investigated multi-sensory stimulation in chronic stroke populations in cooperation with dr. Ahmed Gardoh, Prof. dr. Richard van Wezel and Prof. dr. Raymond van Ee. In the same period, Mitchel was an ambassador of Start up Mix Nijmegen as an event-manager to encourage and guide students in their pursuit of entrepreneurship.

During the second year of his Masters' program, Mitchel joined the lab 'Synchronization in Neural Systems' of dr. Mike X Cohen, where he was supervised by dr. Linda Spaak Drijvers. He investigated midfrontal theta increase during keyboard typing error corrections. To finalize his Masters' program, Mitchel wrote his thesis under supervision of Prof. dr. Vivian Weerdesteyn entitled 'Neural oscillatory mechanisms of human balance control', a project which he later continued as part of his PhD.

Mitchel Carried out all the work that led to this PhD thesis at the Donders Centre for Cognitive Neuroimaging and the Donders centre for Medical Neuroscience as part of the Radboudumc department of Rehabilitation. During his PhD he was supervised by dr. Teodoro Solis-Escalante, dr. Mike X Cohen and Prof. dr. Vivian Weerdesteyn. In addition to the fundamental research, Mitchel was involved in the PhD council, where he contributed to PhD policy making and organizing events in support of the Donders PhD's well being and skill development. For the department of Rehabilitation he organized the personal development week in cooperation with dr. Mariska Janssen and dr. Renee Lustenhouwer. Mitchel will continue his career in data science to apply his analytical skills and experience outside of academia.

*

Dankwoord

I could not have succeeded in this promotion on my own. My thanks go out to the support of a great promotion team, participants for experiments, colleagues, friends and family. In this chapter, I would like to thank each one of you for your involvement.

To start off, I would like to thank all the people who participated in my experiment. Thank you for your participation and perseverance during the measurements. Without you, I would not have been able to conduct any of my work. Thanks to your participation we are a 'step' closer to understanding the role of the cerebral cortex in human postural balance control.

In addition, I would like to thank my promoters and co-promotor. First of all, **Mike**, thank you for your great supervision. You were always straightforward and knew how to keep me engaged in the project even when I was struggling to comprehend some complex analyses. I really appreciate your way of working and giving me enough space to figure things out by myself and when necessary jumping in to guide me in the right direction. This always kept me engaged and motivated while working through the projects we collaborated on throughout the years. You made me a more confident scientist than I was before.

Vivian thank you for guiding me through the PhD like you did. I have learned a lot of your talented writing skills and endless knowledge database stored in your brain. If I ever struggled with phrasing a section, you could pinpoint the sentence and exact word that required changing. You have a fine eye for details and I always highly valued your criticism and feedback. Not only did you make me a more critical scientist, you also taught me to have more patience rather than dashing directly for my goal.

Last but not least**,** my co-promotor **Teo.** I would like to thank you for your excellent supervision, and patience. On a daily basis we discussed mostly regarding preprocessing and analyzing the data. You were always available to brainstorm about my ideas and help me back on track when I was floundering. To me it was also valuable that we could get along very well and were able to sometimes grab a drink or even go see a movie together. Thanks for the great support!

I would like to thank the members of the manuscript committee Prof. dr. Ir Natasha Maurits, Prof. dr. Richard van Wezel and Prof. dr. Pieter Medendorp for critically reading and approving my manuscript.

Further I'd like to thank my fellow members of the DCMN PhD council, **Dewi**, **Tomasz**, **Mariana**, **Boyd** & **Martin.** Thank you all for the great and pleasant cooperation. Although most of our meetings were online due to Covid-19, we did manage to make the most of it. I had a lot of fun during our online meetings with drinks, food and games!

The colleagues of the Trigon office 02.270 **Tim**, **Sophie**, **Mats**, **Anneloes**, **Mariana** & **Martin.** Although some of you only knew me for a year as you finished your PhD, you did manage to teach me some lessons in PhD planning and expectation management skills as a PhD. Besides that, a common denominator of us is being able to have good conversations and every now and then go for a drink together at the Aesculaaf or cultuur cafe. I'd like to thank **Mats** in specific, as we spent most time together in the office. It was great to have a good colleague around with whom I could level and talk about women, motorbikes and music. I always looked forward to the trance music in the office on Fridays!

Of course there are the colleagues of the SINS lab **Marrit**, **Ashutosh**, **Arthur, Nader, Paul**, **Jordi** & **Sjef.** Although I sometimes felt like the odd one out who was researching humans compared to the rats you guys were studying, you did make me feel like a member of the team. I felt like I connected with each one of you and it was fun to go out together for drinks or a team activity. **Arthur**, thanks for the great conversations and letting me beat you at sports except for tennis. **Nader** with you I could write a whole separate thesis, but to keep it short, I want to thank you for your energy and gratitude. I hope to see you again soon habibi! **Jordy,** we also share a lot such as fish and camper vans. It was always great to talk about these topics and drink a beer, thanks!

Of course I want to thank **Betty** & **Mora**, **Lorenzo** and **Max** for the great food & coffee. Your presence is valuable to the Trigon, you guys truly are the beating heart of the building!

Niet te vergeten mijn collega's aan de andere zijde van de Radboud campus in het Radboudumc. **Bas**, **Frank**, **Milou**, **Lotte Heutinck**, **Jolanda**, **Renee**, **Jamie**, **Vera**, **Wouter**, **Marian**, **Anouk**, **Lucas**, **Lotte van de Venis**, **Lotte Hagedoorn**, **Marielle**, **Rosanne**, **Digna**, **Mariska**, **Joris, Sarah, Jorik** & **Geert**. We hebben veel tijd samen doorgebracht, niet alleen op kantoor maar ook met verschillende schrijfweken, een personal development week en conferenties in Edinburgh, Chicago & Montreal. Een grote diverse groep waarmee er altijd wel een goed gesprek te voeren was en wat te lachen viel.

*

Specifiek wil ik nog mijn paranimfen **Vera** & **Wouter** bedanken. **Vera** ik waardeer je enorm voor de fijne collega die je bent. Ik heb altijd het gevoel gehad dat we goed konden levelen en we hebben regelmatig (telefoon)gesprekken gehad om te sparren over hoe we beter konden omgaan met bepaalde situaties. Ik bewonder hoe je jezelf er doorheen werkt en nu ook bezig bent met het afronden van je PhD! Je bent er bijna!

Wouter, samen hebben we heel wat steden afgereisd voor congressen of een summer school. Het was tof om op die manier samen in Chicago wat plekken te verkennen en uit eten te gaan of naar een wedstrijd van de Chicago Bulls te gaan. Montreal sloeg natuurlijk alles waarbij we je meer hebben gezien in de hottub dan er buiten, maar dat heb ik zelf volgens mij ook geëvenaard. Bedankt voor de goede gesprekken en gezelligheid, je was een fijne collega!

De Biologen **Max**, **Richard**, **Sander**, **Bas**, **Moniek**, **Eline** & **Robin.** Daar waar het studie avontuur begon en mooie vriendschappen zijn gebleven. Mede dankzij jullie heb ik al die jaren studeren vol weten te houden. Jullie vriendschap heeft mijn leven op vele manieren verrijkt en aangezien we goed contact hebben zal dat hopelijk blijven, bedankt!

De HBM crew, **Tom**, **Nick**, **Sjoerd**, **Lente**, **Roel**, **Zander**, **Jeroen**, **Miki**, **Kim**, **Anke**, **Laurance**, **Loek**, **Nadine, Floris, Teun** en **Marije**, mijn tweede familie van huis. Een plek die altijd aanvoelde als een warm bad. Fijn dat we nog altijd contact hebben, elkaar regelmatig zien en jaarlijks een weekend weg gaan, dat houden we er hopelijk in!

Bouldering buddies, **Stefan**, **Iris**, bedankt voor de leuke tijd aan de wand en vakantieavonturen. Daar waar ikzelf de ups- en downs van het PhD-leven ervaarde, konden we het leed van klimmen en afdalen bij de Piezza Salmone samen dragen. **Heleen**, **Robert**, **Floor**, **Laurien**, **Peter**, **Max** & **Anne**, bedankt voor de leuke uitjes naar Fontainebleau en overige klim en chill sessies. Het was altijd fijn om me tussen belangstellende sociale mensen als jullie te begeven. Ik wist vaak energie te putten uit jullie enthousiasme voor het boulderen en levensgenot. **Max** bedankt voor de goede gesprekken, prettige vriendschap en **Robert,** uiteraard enorm bedankt dat ik je vaak kon lastig vallen met vragen over het klussen aan een camperbus, mooi dat we hier onuitputtelijk over kunnen praten! **Bram**, bedankt voor de lessen uit onze bouldersessies. Deze lessen bleven niet alleen bij de techniek aan de wand, maar traden ook tot in detail op in de statistiek die ik moest bedrijven in hoofdstuk 2. Hartelijk dank voor je hulp, tijd en aandacht!

Sharon, **Niels**, **Jade**, **Milan** & **Loua**, bedankt voor jullie steun, support en de leuke dingen die we samen hebben gedaan om mijn altijd ratelende brein ook de ruimte en tijd voor ontspanning te geven. Het is altijd fijn om door jullie onthaald te worden met een warme knuffel en een lach. Dat we nog vele mooie herinneringen samen mogen maken!

Joyce & **Eugene**, ik wil jullie graag bedanken voor jullie vertrouwen en steun in mijn leven. Dankzij jullie goede opvoeding en raad heb ik mij kunnen ontwikkelen tot de persoon die ik nu ben. Jullie hebben mij geleerd om mijn best te doen en niet te snel op te geven. Dit heeft mij gebracht waar ik nu ben en ik ben trots op ouders als jullie, dankjewel! Ik houd van jullie pap & mam!

Lieve **Roos,** uiteraard wil ik jou ook bedanken voor je support en liefde door de jaren heen. Ik ben ongelofelijk blij met jou als mijn partner en maatje! Zonder jouw steun en vertrouwen was het afronden absoluut een veel moeilijkere opgave geweest. Ik geniet van alle avonturen die wij samen aangaan en kijk uit naar de avonturen die nog gaan komen. Ik hou van jou!

*